

Investigating the Effects of Corrosion Resistant Coating on the Ductility of Welded Wire Reinforcement

FINAL REPORT
AUGUST 2017

Submitted By:

Mohamed Shwani
Graduate Research Assistant
Utah State University

Marc Maguire
Assistant Professor
Utah State University

Utah State University
4110 Old Main Hill
Logan, UT 84332

External Project Manager
Paul Aubee
Engineering Manager
Insteel Wire Products

In cooperation with

Rutgers, The State University of New Jersey
and
U.S. Department of Transportation

Disclaimer Statement

The contents of this report reflect the views of the authors, who are responsible for the facts and the accuracy of the information presented herein. This document is disseminated under the sponsorship of the Department of Transportation, University Transportation Centers Program, in the interest of information exchange. The U.S. Government assumes no liability for the contents or use thereof.

The Center for Advanced Infrastructure and Transportation (CAIT) is a National UTC Consortium led by Rutgers, The State University. Members of the consortium are the University of Delaware, Utah State University, Columbia University, New Jersey Institute of Technology, Princeton University, University of Texas at El Paso, University of South Florida and Virginia Polytechnic Institute and the University. The Center is funded by the U.S. Department of Transportation.

1. Report No. CAIT-UTC-NC36		2. Government Accession No.		3. Recipient's Catalog No.	
4. Title and Subtitle Investigating the Effects of Corrosion Resistant Coating on the Ductility of Welded Wire Reinforcement				5. Report Date August 2017	
				6. Performing Organization Code CAIT/Utah State University	
7. Author(s) Mohamed Shwani, Marc Maguire				8. Performing Organization Report No. CAIT-UTC-NC36	
9. Performing Organization Name and Address Utah State University 4110 Old Main Hill, Logan UT 84332				10. Work Unit No.	
				11. Contract or Grant No. DTRT13-G-UTC28	
12. Sponsoring Agency Name and Address Center for Advanced Infrastructure and Transportation Rutgers, The State University of New Jersey 100 Brett Road, Piscataway, NJ 08854				13. Type of Report and Period Covered Final Report 05/01/16-08/31/17	
				14. Sponsoring Agency Code	
15. Supplementary Notes U.S. Department of Transportation/Research and Innovative Technology Administration 1200 New Jersey Avenue, SE Washington, DC 20590-0001					
16. Abstract <p>This study demonstrated that epoxy coated and galvanized WWR affects mechanical properties along with the known enhanced corrosion resistance. In this study, tensile tests were performed on a total of 108 wire samples and 18 hot rolled reinforcement samples. These samples consisted of black (non-coated), epoxy coated, and galvanized WWR. Each coating was tested on three different sized wires: D11, D20, and D31. The tensile tests showed that coating the wire had an obvious effect on some mechanical properties, but had a less pronounced effect on others. The rupture location was also found to have a significant effect. These properties were then simulated using Response 2000 to estimate their effect at the member level. Large variability (material property CVs ranged from 0.1% to 67.2% for wire) was observed in all wire samples (coated and uncoated), especially the D31 samples in all sizes' percent area reduction, as compared to a series of hot rolled reinforcement (CVs ranged from 3.3 to 5.0). Rupture location played a significant role in all material properties. Rupture at the cross weld location negatively affected all measured properties and also negatively affected the benefits observed from coating. However, the small sample sizes for the D11 and D20 wires that ruptured at a weld affects this conclusion. Additional testing is needed to confirm whether larger diameter wire is affected more by the welding process than smaller wires, but this seems to be indicated by the data. Galvanizing the wire increased the mean percent elongation from 3.7% to 6.5% and increased the standard deviation from 0.63 to 1.1. Epoxy coating the wire marginally increased the percent of elongation from 3.7% to 4.3%, but only small differences in standard deviation were observed (0.82 to 0.78). The yield stress and ultimate stress for smaller wire sizes (D11 and D20) increased when the epoxy and galvanized coating was applied. However, the coatings had the least effect on the highly variable D31 wires. Galvanizing wire resulted in a slight increasing in the elastic modulus for smaller diameter wires (D11 and D20), while galvanizing did not have any impact on the elastic modulus for D31 wires. Designers can expect an increase in deformation capacity and ductility ratio for structural members reinforced with galvanized wire, considering the average properties observed in this report: up to 11% and 25%, respectively when design for slabs and up to 76% and 55%, respectively, for beams.</p>					
17. Key Words Welded Wire Reinforcement, Engineered Steel, Mesh, Cold Worked Wire, Ductility, Epoxy Coating, Galvanized				18. Distribution Statement	
19. Security Classification (of this report) Unclassified		20. Security Classification (of this page) Unclassified		21. No. of Pages 89	22. Price

Table of Contents

Chapter 1: Introduction	5
Chapter 2: Experimental Procedures	7
WWR Coating Experiment	7
Chapter 3: Experimental Results and Discussions	11
WWR Coating Experiment	11
Rebar Results	11
Wire Results	12
Percent Elongation	17
Percent Uniform Elongation ($\% \epsilon_{su}$)	20
Elastic Modulus (E_s)	22
Yield Stress (f_y)	23
Ultimate Strength (f_u)	24
Percent Area Reduction	26
Discussion	27
Chapter 4: Conclusion	31
References	33
Appendix G	35
Stress-Strain Curves for Coating Study	35

Chapter 1: Introduction

The purpose of this investigation is to demonstrate that epoxy coating and galvanizing welded wire reinforcement (WWR) has important effects on the mechanical properties of WWR. Before these effects are addressed, a brief explanation of welded wire reinforcement, how it is made, types of coating, and tempering of wire will be discussed.

WWR is pre-manufactured reinforcing steel constructed of high-strength, cold-drawn, or cold-rolled wire that is welded together in square or rectangular grids. Each wire intersection is electrical resistance-welded by a continuous automatic welder. Pressure and heat fuse the intersecting wires into a homogeneous section and fix all wires in their proper positions. Plain wires, deformed wires, or a combination of both may be used in WWR (WRI 2006). Because of how it is manufactured, WWR has several advantages to traditional steel reinforcement, such as precise and accurate grid spacing and a higher strength. These properties can reduce the amount of steel required by as much as 25% (Maguire et al. 2012, Morcous et al. 2011, Morcous et al., 2009, Maguire 2009). Reduction of steel lessens the overall weight of WWR. Using lighter weight WWR reduces transportation costs. Precise grid spacing reduces labor and time by eliminating the need to tie individual rebar together. Precise grid spacing also eases placement.

Two types of coating, epoxy and galvanization, can be applied to welded wire reinforcement to provide better corrosion resistance. WWR is galvanized by coating bare steel with a protective layer of zinc metal. The zinc coating serves as a barrier to corrosive elements that WWR is exposed to when embedded in concrete. (Yeomans 1998).

ASTM A641 outlines the procedure and specifications for the hot-dipped galvanizing process, and ASTM A884 provides the requirements for epoxy-coated welded wire reinforcement. The epoxy coating is applied after the sheets have been welded together. Epoxy

coating is the process of applying epoxy powder to cleaned and heated steel. The powder is drawn to the bar surface by electric forces and fuses there, forming a continuous layer.

WWR is galvanized through a series of steps, starting with dipping it in a series of solutions that remove dirt, oil, oxides, and other contaminants from the surface. After it is dried, WWR is immersed in a bath of liquid zinc that is heated to 830°F (450°C). Finally, the steel is set aside to cool. The epoxy coating process for WWR also consists of a series of steps involving surface and heat treatment. First, the steel is visually inspected for oil, grease, and other contaminants. Next, the steel is transported to a blast cleaner where an abrasive steel grit strikes the steel surface at a high velocity. This step cleans and roughens the surface of the steel so the coating adheres properly. Then, the steel passes through an electric induction heater that heats the steel up to 455°F (235°C). The heated bar then passes through a powder spray booth where it is sprayed with epoxy powder. Finally, the coated steel is set aside to cool.

Past research indicates that tempering can be defined as the process of reheating steel to 1200°F (650°C). The steel, after being quenched, is cooled to about 40°C then reheated through immersion in oil or nitrate salts. Tempering also impacts the mechanical properties of steel. Some of these impacts are a significant increase of percent elongation and slight reduction of yield and ultimate strength. (Ayyub,1994; Mamlouk and Zaniewsk, 2011).

In general, epoxy and zinc coatings are applied to provide corrosion protection when concrete is exposed to de-icing, marine salts, and carbonation. Previous researchers have not discussed concerns about the effects of coating on WWR's mechanical properties in detail. This research report discusses the impact of coating on the strength and ductility of WWR found through tensile testing 108 different sized specimens of black, epoxy, and galvanized wires.

Chapter 2: Experimental Procedures

WWR Coating Experiment

A tensile test was performed by applying an axial load to the WWR specimens using a Tinius Olsen UTM machine. Figure 2.1 shows the test setup and the tensile testing machine. The Tinius Olsen UTM was connected to a computer system software that was on an Instron machine. This machine, the Instron Interface, played an important role in allowing the extensometer to interface with the software. The computer read and recorded the corresponding values of time, stress, strain, position, and load. A 2.0 in. and an 8.0 in. extensometer measured the elongation of the specimens. The goal of the tensile test was to obtain the yield strength, ultimate strength, fracture strength, percent elongation, and percent area reduction of the WWR specimens as well as obtain the general stress strain diagrams for each wire type. The tensile tests were conducted in accordance with ASTM A370 (Standard Test Methods and Definitions for Mechanical Testing of Steel Products).

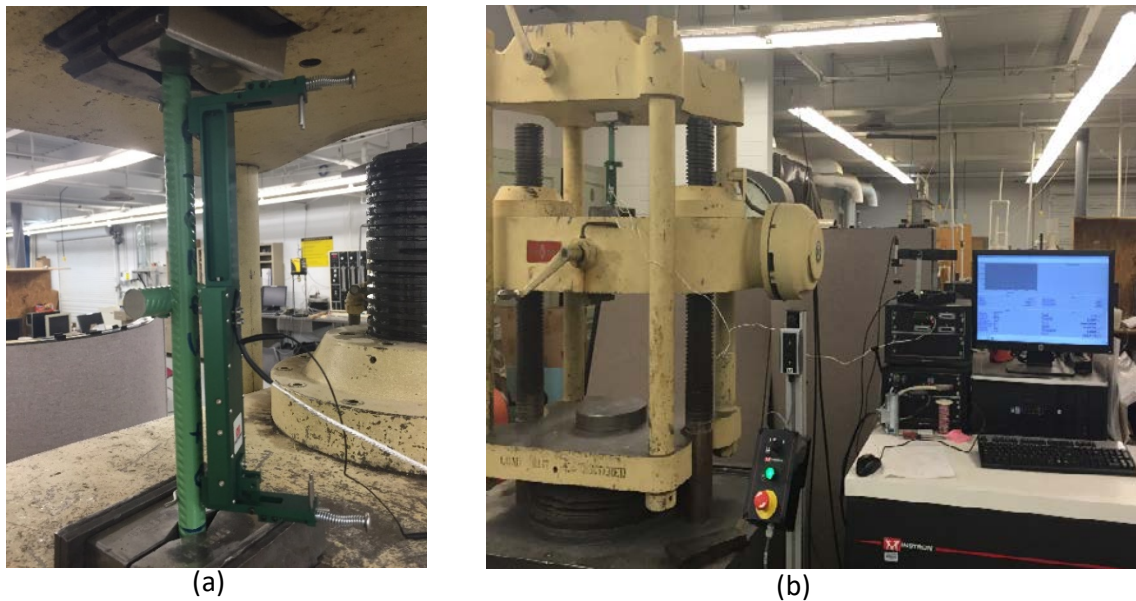


Figure 2.1 (a) Test Setup (b) Tinius Olsen UTM and Instron computer system

All WWR mats were acquired from a single manufacturer but were from different coils, one for each area of wire. For this reason, in the below analyses it is difficult to compare D11 wires to D20 and so on, but all D20 are comparable D20, etc. One third of the mats were galvanized according to ASTM A641 by a local hot dip galvanizer. A separate third of the mats were epoxy coated according to ASTM A884 by a separate certified epoxy coating company. The researchers cut all WWR specimens to 30 in. lengths, allowing for a 8 in. gage length and for 1 in. between the gage length and each of the UTM grips (7 in. long each) and a 1 in. protrusion outside of each UTM grip (ASTM A370 Section A9.3.1, see Figure 2.2). The researchers conducted the tensile tests on all 108 wire specimens and 18 rebar specimens in the structural material testing lab at Utah State University. A summary of all steel tests are presented in Table 2.1.

Table 2.1 Specimens tested in this study

<i>Designation</i>	<i>Material</i>	<i>Grade</i>	<i>Coating Type</i>	<i>Number Tested</i>
D11	Cold Worked Wire	80	None	12
D20	Cold Worked Wire	80	None	12
D31	Cold Worked Wire	80	None	12
D11	Cold Worked Wire	80	Epoxy	12
D20	Cold Worked Wire	80	Epoxy	12
D31	Cold Worked Wire	80	Epoxy	12
D11	Cold Worked Wire	80	Zinc	12
D20	Cold Worked Wire	80	Zinc	12
D31	Cold Worked Wire	80	Zinc	12
#3	Hot Rolled Rebar	60	None	6
#4	Hot Rolled Rebar	60	None	6
#5	Hot Rolled Rebar	60	None	6



Figure 2.2 Specimens after cutting to the testing length

After the bars were cut to the required length, as shown Figure 2.3, the longitudinal center of each bar was marked. The researchers then placed an additional two punches 2 in. to the right and left of the center mark to represent the gage lengths. After the gage lengths were marked, the researchers placed marks 1 in. to the right and left of the center mark. These marks were later used to mount the 2 in. extensometer.

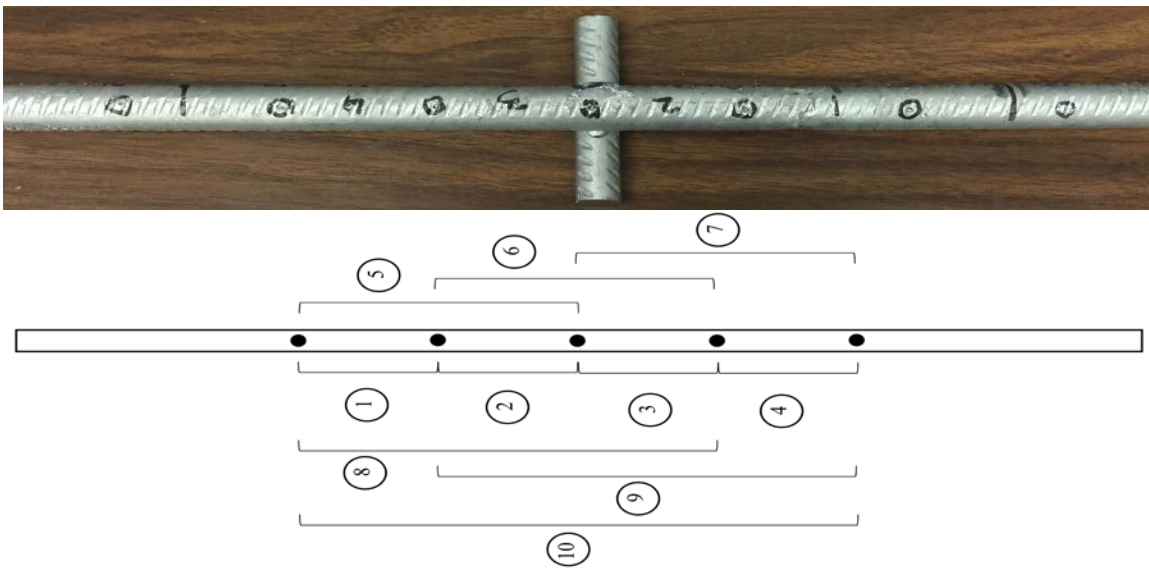


Figure 2.3 Marked gage lengths on the specimen

The researchers used a caliper to take initial and final measurements of the 10 different gage lengths created by the four 2 in. punch segments, as shown in Figure 2.3. The gage lengths included four 2 in., three 4 in., two 6 in., and one 8 in. measurement. Also, the researchers took

measurements of the largest and smallest initial diameters to determine the area of each bar before and after the test and to calculate the percent area reduction. Establishing the loading rate is required before starting the test. The researchers used displacement control in this test instead of load control since the stress-strain curve is more accurate when using displacement control. According to ASTM A370 Section 7.4, the loading rate must be less than 1/16 in. per minute per in. between the grips and greater than 1/10 of the maximum load rate. Since the distance between the grips was 10.5 in., the results showed 0.65 in. per minute as the maximum load rate and 0.065 in. per minute as the minimum load rate. To meet ASTM's requirements, the researchers used a load rate of 0.5 in. per minute.

Testing began after the researchers placed the specimen in the test apparatus and established the load rate, and the Instron system recorded the data. To avoid damages, the researchers removed the extensometer before the bar failed. This was accomplished by watching the load during the test. A drop in the load shows that the specimen is necking, which indicates that failure is about to occur. At this point, the researchers paused the test and removed the extensometer. After the extensometer was removed, the test was resumed and the bar was loaded until failure. Following failure of the bar, the researchers stopped the loading and saved the data, then reset the machine. After the bars were removed from the UTM machine, they were linked together at the fracture location to take a final measurement of the aforementioned 10 gage lengths. The researchers measured the smallest and largest diameter dimensions at the point of fracture. The elongation and area reduction percentages were calculated from the recorded data of both the initial and final measurements of the gage lengths.

Chapter 3: Experimental Results and Discussions

WWR Coating Experiment

Table 3.1 shows the average values of the various specimen strengths measured for each type of WWR used in this research project. The researchers calculated the yield strength for each WWR specimen using the 2 percent offset method and determined the ultimate strength from the largest stress obtained during the tensile test. The elastic modulus was obtained from the slope of the line in the stress-strain diagram in the elastic range.

Table 3.1 Average values of mechanical properties of tested specimens

<i>Steel Specimen</i>	<i>Number Tested</i>	<i>Elastic Modulus (GPa)</i>	<i>Yield Strength "f_y" (MPa)</i>	<i>Ultimate Strength "f_u" (MPa)</i>	<i>Elongation (%)</i>	<i>f_u/f_y</i>
D11 - Black	12	213	669	745	3.1	1.11
D20 - Black	12	213	683	765	3.4	1.12
D31 - Black	12	228	793	855	2.1	1.08
D11 - Epoxy	12	223	710	807	3.0	1.14
D20 - Epoxy	12	234	717	807	3.8	1.13
D31 - Epoxy	12	242	779	841	2.2	1.08
D11 - Galvanized	12	247	696	779	7.4	1.12
D20 - Galvanized	12	236	710	800	6.5	1.13
D31 - Galvanized	12	238	793	862	7.2	1.09
#3 – Rebar	6	207	504	792	14.4	1.57
#4 – Rebar	6	200	466	756	14.4	1.62
#5 – Rebar	6	210	510	793	15.0	1.55

Rebar Results

The rebar specimens were not the focus of this research but provide an important control sample. As will be presented in the wire testing results below, wire seems to have high material property variability. To validate the ability of the Utah State University laboratory personnel and testing protocol (ASTM A370) and equipment on traditional steel reinforcing samples, results from steel reinforcing are presented in Table 3.2.

Table 3.2 Mild Steel Rebar Material Properties

Steel Specimen	Number Tested	Number of Free Length Ruptures	Elongation (%)		Uniform Elongation ϵ_{su} (in./in.)		Area Reduction (%)		Elastic Modulus (GPa)		Yield Strength " f_y " (MPa)		Ultimate Strength " f_u " (MPa)	
			Mean	CV (%)	Mean	CV (%)	Mean	CV (%)	Mean	CV (%)	Mean	CV (%)	Mean	CV (%)
#3	6	6	14.44	1.92	11.42	2.34	57.17	3.29	207	2.82	504	0.63	792	0.50
#4	6	5	14.37	3.28	10.98	6.16	42.05	3.37	200	2.44	466	1.00	756	0.40
#5	6	5	14.95	6.08	10.39	3.96	43.06	5.01	210	3.23	510	0.65	793	0.83

Only two out of 18 total rebar specimens broke in the jaws (11%), resulting in a minimum of five successful inelastic property measurements for each of the bar sizes. Coefficients of variation are as high as 6.2% (uniform elongation, not addressed in ASTM E8 or STM A370), but typically below 3% and as low as 0.4% for the ultimate strength of the #4 rebar. Guidance in ASTM E8 indicates that a coefficient of variation for 0.02% yield stress for different steel material ranged from 1.18% to 4.97%. CV's from this study for mild steel ranged from 0.63% to 1.00% (see Table 3.2). ASTM E8 indicates that CVs for ultimate strength were from 0.25% to 2.45% and test results from this study were from 0.4% to 0.83% (see Table 3.2). Elongation CV's from ASTM E8 were 1.61% to 4.07% and from this research paper were 1.92% to 6.08% (see Table 3.2). Area reduction according to E8 was from 1.28% to 6.87% and this study was from 3.29% to 5.01% (see Table 3.2). These results indicate that the laboratory procedures are acceptable. The wire testing procedures followed the same protocols.

Wire Results

Example stress-strain curves of each bar type is compared in Figure 3.1 to Figure 3.3. Only one stress-strain curve is included for each size of WWR in Figures 3.1, 3.2, and 3.3. The results for all 108 stress-strain samples are included in Appendix G. The figures below show that the galvanized wires of all sizes (D11, D20, and D31) had the highest ductility compared with

non-coated (black) and epoxy coated wire. The epoxy coated wire had more non-significant ductility than the black wire.

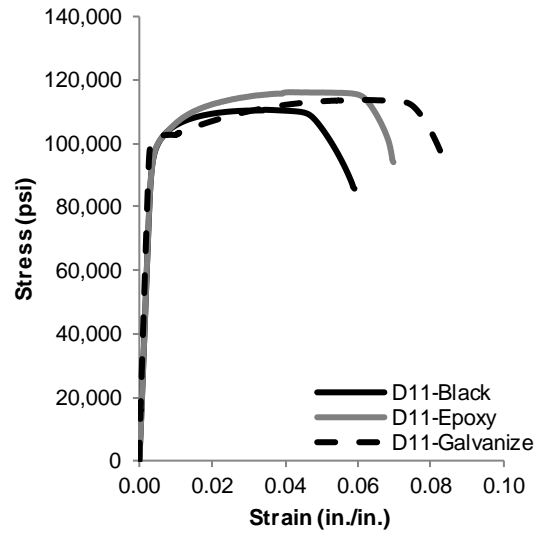


Figure 3.1 Comparison plot of D11 WWR stress-stain curves

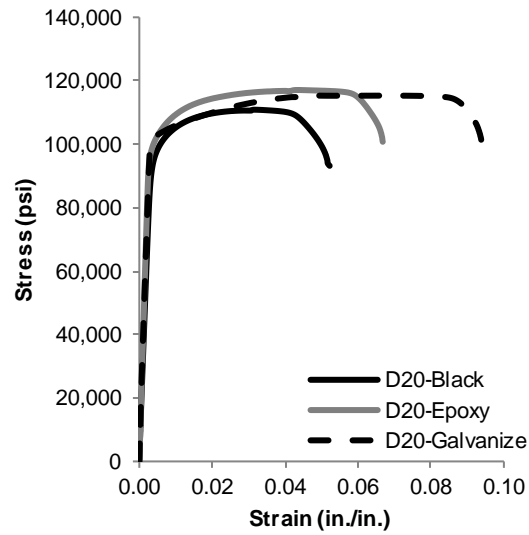


Figure 3.2 Comparison plot of D20 WWR stress-stain curves

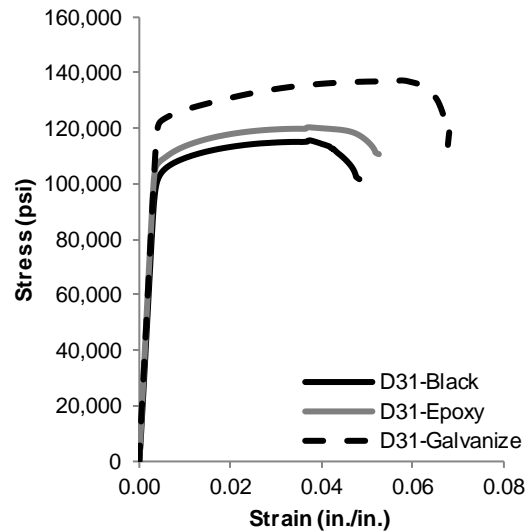


Figure 3.3 Comparison plot of D31 WWR stress-stain curves

The wire results were significantly affected by the location of the rupture. If the rupture occurred near the cross weld (within one bar diameter), the inelastic deformation properties (e.g., elongation, uniform elongation) tended to be very different. Table 3.3 presents the statistical analysis of the mechanical properties of all samples that failed at the cross weld section. The number of wires tested, wire sizes, and number of cross weld fractures are also listed in Table 3.3. Of the black specimens, 25% broke at the cross weld location compared to 28% for all D31 wires and 39% for the epoxy coated and galvanized specimens. The D31 specimens were the most likely to break at the cross weld location for all coating types. The D31 samples also had the largest variation in percent elongation (see 3.1% to 37.9% in Table 3.3), area reduction (see 4.2% to 38% in Table 43.3) and uniform elongation (2.0% to 67%), specifically for the uncoated wires. Compared to the rebar results presented in Table 3.2, there is much more variability. Reasons for this could be the manufacturing process, welding process, small number of specimens (for example, only five D11 and D20 specimens broke at the weld), and testing protocol, although the testing protocol was the same as for the rebar specimens.

Table 3.3 Statistical data for mechanical properties of tested specimens failed at cross-weld

Steel Specimen	Number Tested	Number Cross Weld Fracture	Elongation (%)		Strain @ Ultimate Strength ϵ_{su} (in./in.)		Area Reduction (%)		Elastic Modulus (ksi)		Yield Strength "f _y " (ksi)		Ultimate Strength "f _u " (ksi)	
			Mean	CV (%)	Mean	CV (%)	Mean	CV (%)	Mean	CV (%)	Mean	CV (%)	Mean	CV (%)
D11 - Black	12	0	-	-	-	-	-	-	-	-	-	-	-	-
D20 - Black	12	1	2.8	-	2.0	-	20.4	-	31,564	-	100	-	110	-
D31 - Black	12	8	2.2	37.9	1.7	54.0	9.1	38.0	32,456	9.3	111	12.3	119	11.4
D11 - Epoxy	12	0	-	-	-	-	-	-	-	-	-	-	-	-
D20 - Epoxy	12	0	-	-	-	-	-	-	-	-	-	-	-	-
D31 - Epoxy	12	10	2.6	29.8	2.2	45.1	9.0	24.4	35,582	11.1	111	11.1	120	10.3
D11 - Galvanize	12	2	7.1	3.1	6.1	2.0	24.6	4.2	33,136	19.2	98	0.8	113	0.7
D20 - Galvanize	12	2	6.2	21.2	5.8	14.3	20.4	13.9	37,690	3.3	100	0.7	113	0.1
D31 - Galvanize	12	10	3.8	30.3	3.4	67.2	6.1	32.3	34,911	3.4	115	12.4	125	10.9

Table 4-6 shows the mean value and CV for all mechanical properties of all tested samples that broke in the free wire area (away from the weld). The value of percent elongation reported here in Table 3.4 is for those samples that broke in the free wire area and inside the 8 in. gage length, whereas the rest of the data for other parameters were for all samples where rupture occurred in the free wire area inside and outside the 8 in. gage length. It was observed that in most of wires with smaller diameters (D11 and D20) fracture occurred in the free wire length, and the largest variations were observed for percent elongation (up to 70.6%, see Table 3.4), uniform elongation (8.3% to 42% in Table 3.4), and percent area reduction (9% to 55% in Table 3.4) while the smallest CVs occurred for the elastic modulus (2.0% to 10% in Table 3.4), yield strength (0.6% and 13.4% in Table 3.4) and ultimate strength (0.4% to 12.6% in Table 3.4). The largest CVs occurred in the steel specimens that had the smaller sample sizes (e.g., only two free D31 wires, epoxy and galvanized).

When rupture occurred in the cross weld, there seemed to be negligible difference in the elastic modulus but a significant difference on yield strength (compare mean of 111 ksi in Table

3.3 and 124.7 ksi in Table 3.4 for black D31) and ultimate strength (compare mean of 119 ksi in Table 3.3 and 133 ksi in Table 3.4 for black D31).

Table 3.4 Statistical data for mechanical properties of tested specimens that failed in the free wire length

Steel Specimen	Number Tested	Number Free Wire Rupture	Number Free Wire Rupture inside 8 in. gage	Elongation (%)				Strain @ Ultimate Strength ϵ_{su} (in./in.)		Area Reduction (%)		Elastic Modulus (ksi)		Yield Strength "fy" (ksi)		Ultimate Strength "fu" (Ksi)			
				Inside 8 in gage		Outside 8 in. gage		Mean	CV (%)	Mean	CV (%)	Mean	CV (%)	Mean	CV (%)	Mean	CV (%)	Mean	CV (%)
				Mean	CV (%)	Mean	CV (%)												
D11 - Black	12	12	4	4.7	4.03	3.1	39.3	3.2	5.0	28	12	30,867	6.2	96.8	3.0	107.5	2.8		
D20 - Black	12	11	4	4.8	7.96	3.4	34.8	3.1	45.9	35	9	30,794	2.0	98.7	0.6	110.5	0.4		
D31 - Black	12	4	0	-	-	2.1	20.1	2.3	22.4	31	9	34,138	8.6	124.7	10.2	133.2	8.8		
D11 - Epoxy	12	12	1	5.4	-	3.0	30.6	3.7	42.0	30	18	30,755	8.9	103.5	1.8	116.5	0.8		
D20 - Epoxy	12	12	5	4.9	5.07	3.8	27.5	3.6	40.6	20	11	33,959	5.0	103.8	1.4	116.5	1.2		
D31 - Epoxy	12	2	0	-	-	2.2	70.6	2.9	34.1	30	55	32,868	2.0	123.3	13.0	132.1	12.6		
D11 - Galvanize	12	10	5	8.2	7.12	7.4	31.3	7.5	38.8	23	13	36,337	10.0	101.0	1.8	113.0	1.2		
D20 - Galvanize	12	10	5	7.7	3.22	6.5	20.3	5.7	39.3	14.7	15	33,526	5.4	103.7	6.8	116.6	5.7		
D31 - Galvanize	12	2	2	7.2	3.16	7.2	3.2	8.0	39.3	14.7	23.1	32,227	4.7	113.2	13.4	127	11.3		

Galvanized coating had the largest increase in mean elongation when compared to the black wires (compare largest difference in D31 mean elongation: 7.2% for epoxy coated and 2.1% for black in Table 3.4), but epoxy coating provided no significant difference (compare largest difference in mean D20 elongations 3.8% for epoxy and 3.4% for black in Table 3.4). However, only marginal differences were observed in the cross weld rupture specimens, where D31, the most statistically relevant weld rupture specimens, exhibited an increase in elongations of 2.2% to 2.6% for epoxy coating and 2.2% to 3.8% for galvanized coating.

For the elastic modulus, the differences between elastic moduli was different for the coated wire; however, the trend was not consistent. For example, for the D11 wire, galvanizing increased the elastic modulus by 5,511 ksi, whereas for D31 wire, galvanizing decreased the elastic modulus by 1,885 ksi. Yield strength and ultimate strength exhibited similar trends for

epoxy and galvanized coating, where mean strengths increased for the D11 and D20 wires (up to 8.4%), but decreased marginally (up to 9.3%) for the D31 wires.

Percent Elongation

Figure 3.4 shows the percent elongation cumulative histograms using a 2 in. gage length for all three coating types and three different sizes in normal probability scale. The average mean values for black, epoxy, and galvanized wire were 3.79%, 4.21%, and 6.51%, respectively. These results show that galvanizing the wire increases its percent elongation significantly. The average standard deviation for black, epoxy, and galvanized wire was 0.63%, 0.40%, and 1.10%, respectively. If the rupture occurs close to the cross weld, as was observed in this study, the percent elongation and percent area reduction will be small compared to when rupture occurs in the free wire area. Figures 3.5 and 3.6 show both the brittle and ductile failure models. The standard deviation values for both black and epoxy coated wire were smaller than the standard deviation of galvanized wires.

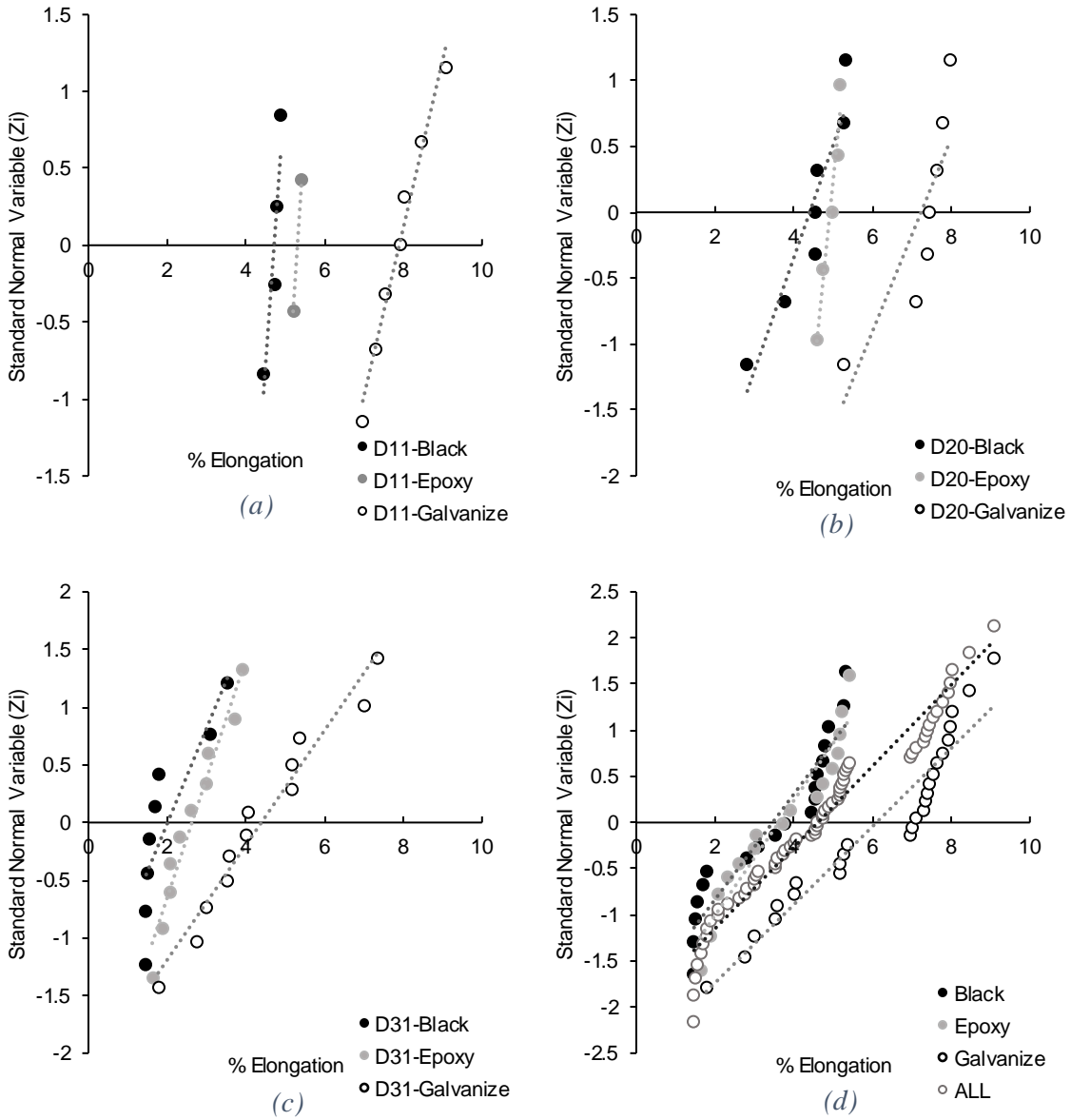


Figure 3.4 Percent elongation test results for 8 in. gauge for WWR (a) D11, (b) D20, (c) D31, (d) All black and epoxy and galvanized together



Figure 3.5 Brittle failure at cross weld in epoxy coated wire



Figure 3.6 Ductile failure mode in free wire of Black (none-coated) wire

Figure 3.4 shows that percent elongation of galvanized wire is greater than that of epoxy coated and black wire, on average. However, many lower elongation galvanized samples were of similar elongation to the black or epoxy samples. A similar observation could be made for epoxy wire.

Percent Uniform Elongation ($\% \epsilon_{su}$)

The percent uniform elongation is defined as the strain at maximum stress sustained by the WWR sample during a tensile test just before necking or fracture (ASTM E8/E8M, 2010).

Figure 3.7 (a) illustrates the typical stress-strain curve for a WWR sample and the difference between uniform and total elongation.

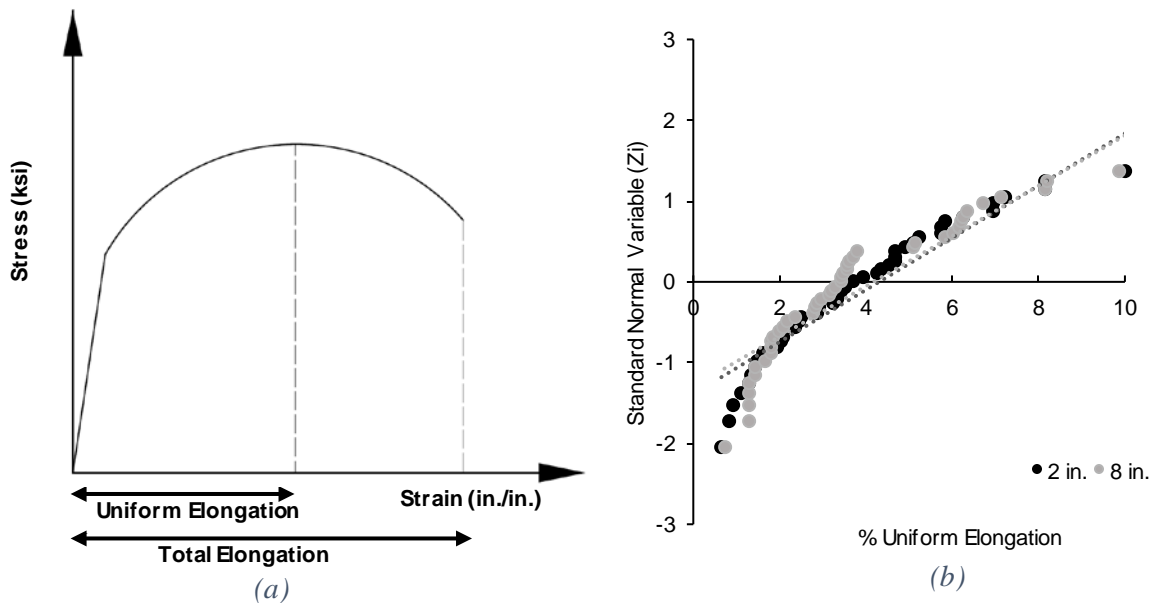


Figure 3.7 (a) Typical Stress-Strain Curve for WWR, (b) Comparing the Uniform elongation form both 2 in. and 8 in. extensometers of the all WWR tested samples

Figure 3.7 (b) compares the uniform elongation for all WWR samples tested using both the 2 in. and 8 in. extensometer. It was observed that the two values obtained from both extensometers were similar: the mean values were 4.3% and 4.2% for the 2 in. and 8 in. extensometer, respectively, and the same standard deviation was 2.8% for both. This validates the use of a 2 in. or 8 in. extensometer for measuring the uniform elongation and implies that any gauge length extensometer can provide an adequate uniform elongation measurement.

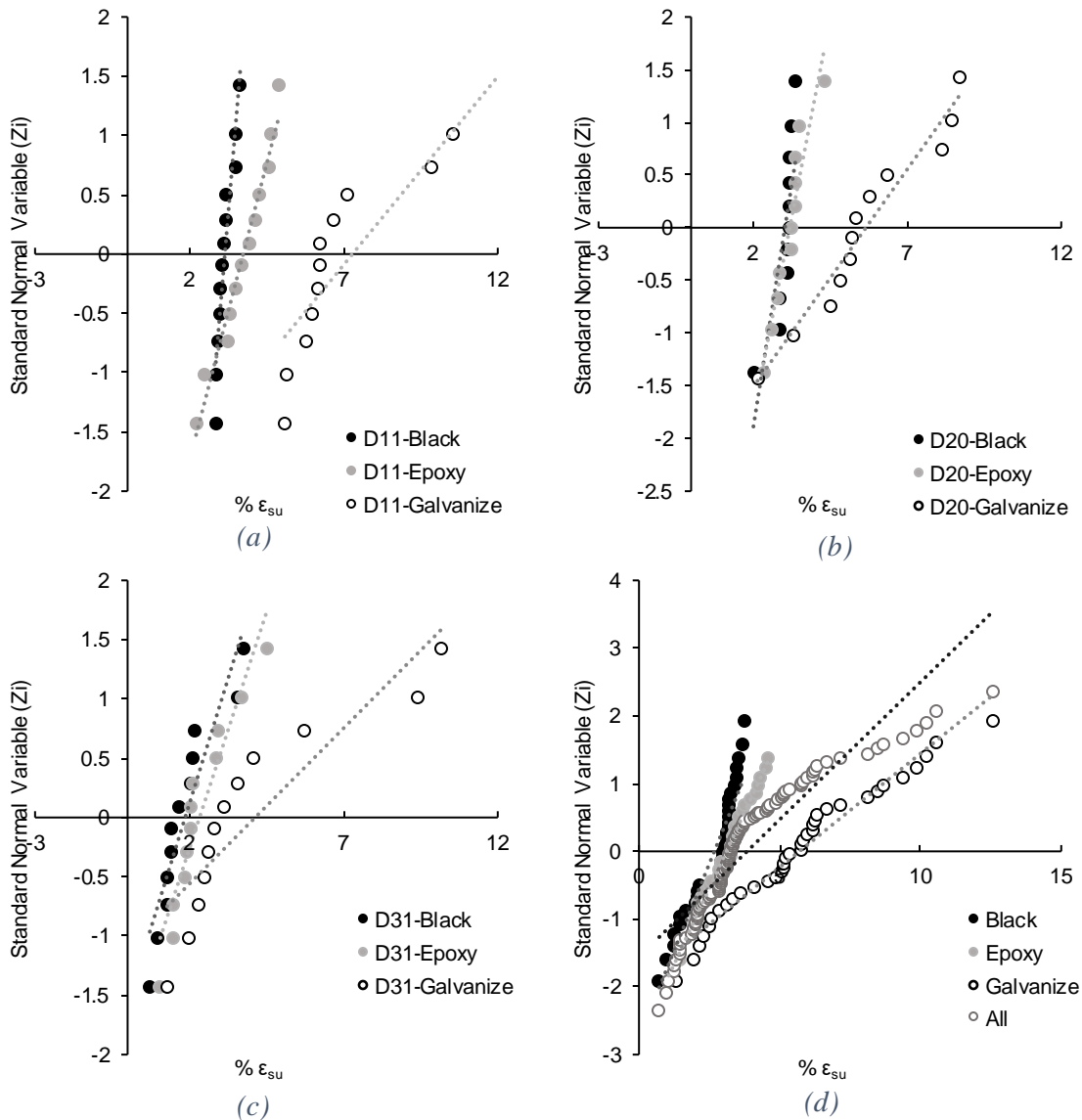


Figure 3.8 Percent elongation test results for 8 in. gauge for WWR (a) D11, (b) D20, (c) D31, (d) All black and epoxy and galvanized together

Figure 3.8 shows the percent uniform elongation cumulative histograms using an 8 in. gauge length for all three coating types and all three sizes in normal probability scale. The average mean values for black, epoxy, and galvanized wire were 2.69%, 3.09%, and 6.48%, respectively. These results show that galvanizing wire increases their percent uniform elongation significantly. The standard deviation for black, epoxy, and galvanized wire was 0.53%, 0.79%, and 2.42%,

respectively. The standard deviation values for both black and epoxy coated wire were smaller than the standard deviation of the galvanized wires.

Elastic Modulus (E_s)

Figure 3.9 shows the normal probability plot for D11, D20, and D31 WWR. Overall, the galvanized wires had a higher modulus of elasticity than the epoxy and non-coated wires, but the difference was not significant. In many instances, there was a significant overlap between the specimens at the tails of the distributions. The results showed that coating the wires with epoxy, galvanizing the wires, and the wire size does not significantly increase or decrease the value of the elastic modulus.

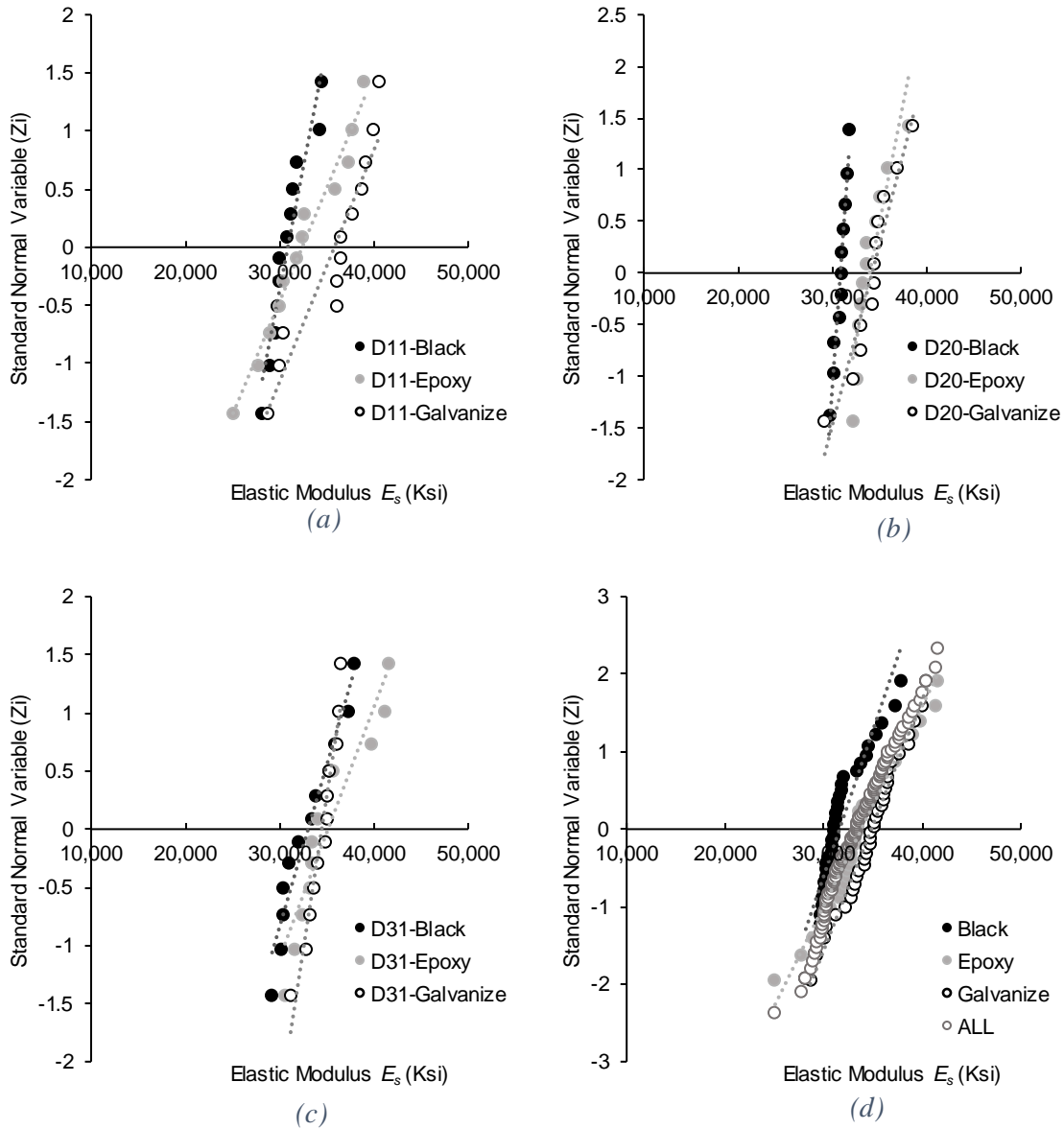


Figure 3.9 Elastic Modulus test results for 8 in. gauge for WWR (a) D11, (b) D20, (c) D31, (d) All black and epoxy and galvanized together

Yield Stress (f_y)

Figure 3.10 shows the yield strength probability plots for the wire specimens. The researchers observed marginally greater yield stress value for wires coated with epoxy than those coated with zinc or black wires. However, the small differences in mean and the high variability indicates that any change is marginal. Significant bi-linearity in the probability plots, most

apparent in Figure 3.10c and Figure 3.10d, show the differences between wires that rupture at the cross wire and those that rupture at the free wire. The D31 samples had the highest variability.

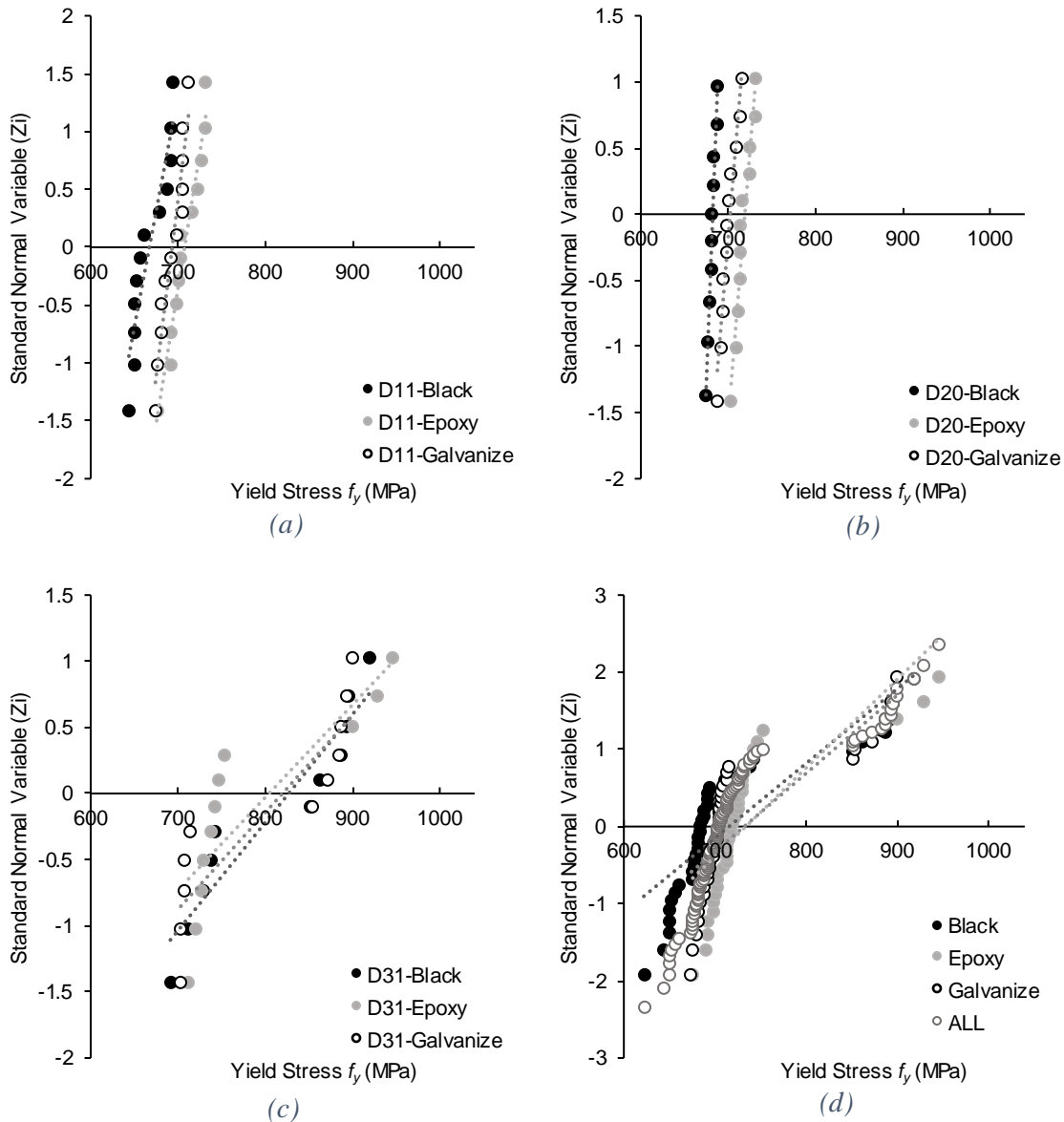


Figure 3.10 Yield stress test results for 8 in. gauge for WWR (a) D11, (b) D20, (c) D31, (d) All black and epoxy and galvanized together

Ultimate Strength (f_u)

Figure 3.11 shows the ultimate strength probability plots for the wire specimens for D11 (Figure 3.11a), D20 (Figure 3.11b), and D31 (Figure 3.11c) wires and all wires together (Figure

3.11d). The researchers observed slightly greater ultimate stress values for wires coated with epoxy than those coated with zinc or black wires. However, the small differences in mean and the high variability indicates that any change is marginal and there is an overlap between the strengths of each, similar to those observed for yield strength (see Figure 3.10). Significant bilinearity in the probability plots, most apparent in Figure 3.11c and Figure 3.11d, shows the differences between wires that rupture at the cross wire and those that rupture at the free wire. D31 samples had the highest variability.

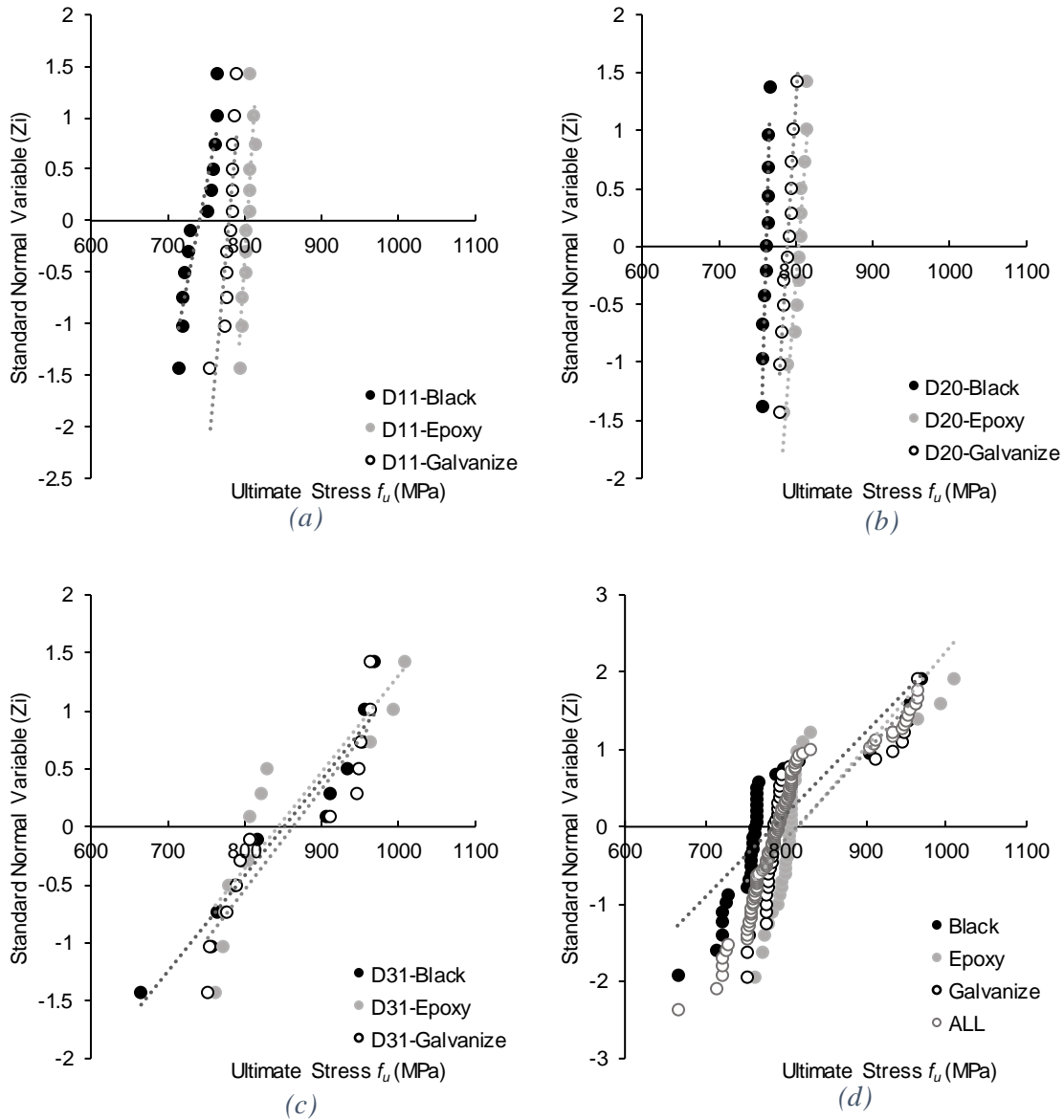


Figure 3.11 Ultimate strength test results for 8 in. gauge for WWR (a) D11, (b) D20, (c) D31, (d) All black and epoxy and galvanized together

Percent Area Reduction

Figure 3.12 shows the area reduction probability plots for the wire specimens for D11 (Figure 3.12a), D20 (Figure 3.12b), and D31 (Figure 3.12c) wires and all wires together (Figure

3.12d). Smaller wire sizes (D11 and D20) had a smaller variation than the larger wire sizes, while a larger variation was observed in D31 wires for all three types of wire.

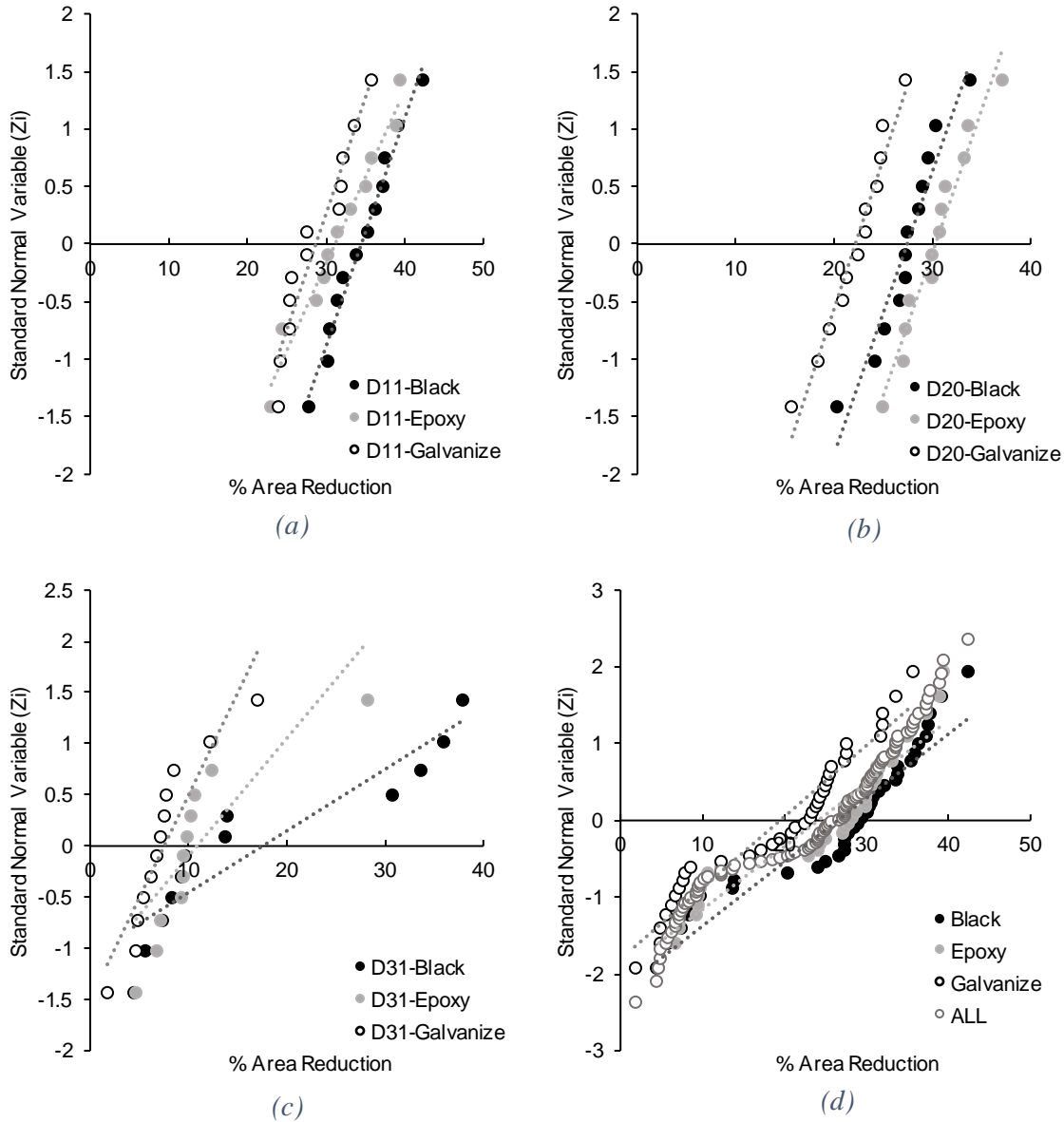


Figure 3.12 Area reduction test results for 8 in. gauge for WWR (a) D11, (b) D20, (c) D31, (d) All black and epoxy and galvanized together

Discussion

Epoxy coating and galvanizing were found to produce favorable results in all cases, with the exception of percent area reduction, which decreased. This is counter intuitive as higher area

reduction is typically associated with larger elongations (ASTM E8, 2010). Percent elongations resulted in the largest increase from galvanized coating, but was also subject to higher variability. The D31 wires were found to be highly variable, mostly due to their high frequency of weld rupture.

Engineers rely on adequate ductility to handle support settlement and overloads by redistributing loads into adjacent members to obtain reliable and redundant structural systems. Member ductility is not explicitly addressed in ACI 318 (2014) and it is not trivial to estimate member deformation. Deflection and ductility ratio will be used in the following analysis to quantify ductility of members reinforced with coated WWR. The ductility factor is the ratio of deflection at peak load to deflection at yielding point, or the ratio of work done from the original point to the peak load to the work done to the yielding point.

In order to quantify the impact of the wire testing results for reinforced concrete design engineers, a moment curvature analysis was performed using the program Response 2000 (Bentz 2000). For this analysis, a simple supported span, one-way slab, and T-beam were assumed to be used, the slab and the beam were reinforced with the minimum and maximum reinforcement ratio. The slab was then reinforced with a minimum reinforcing ratio of 0.2% and maximum reinforcement ratio of 0.32%. The average measured properties for D31 wire (black and galvanized) presented in the previous sections were assigned to the reinforcement. For the beam, the minimum reinforcement ratio of 0.38% and maximum reinforcing ratio of 0.6% were assumed. A uniform load was used and load-deflection curves were created for each slab. Figure 3.13 presents the load versus mid-span deflection curves for D31 black and galvanized wires.

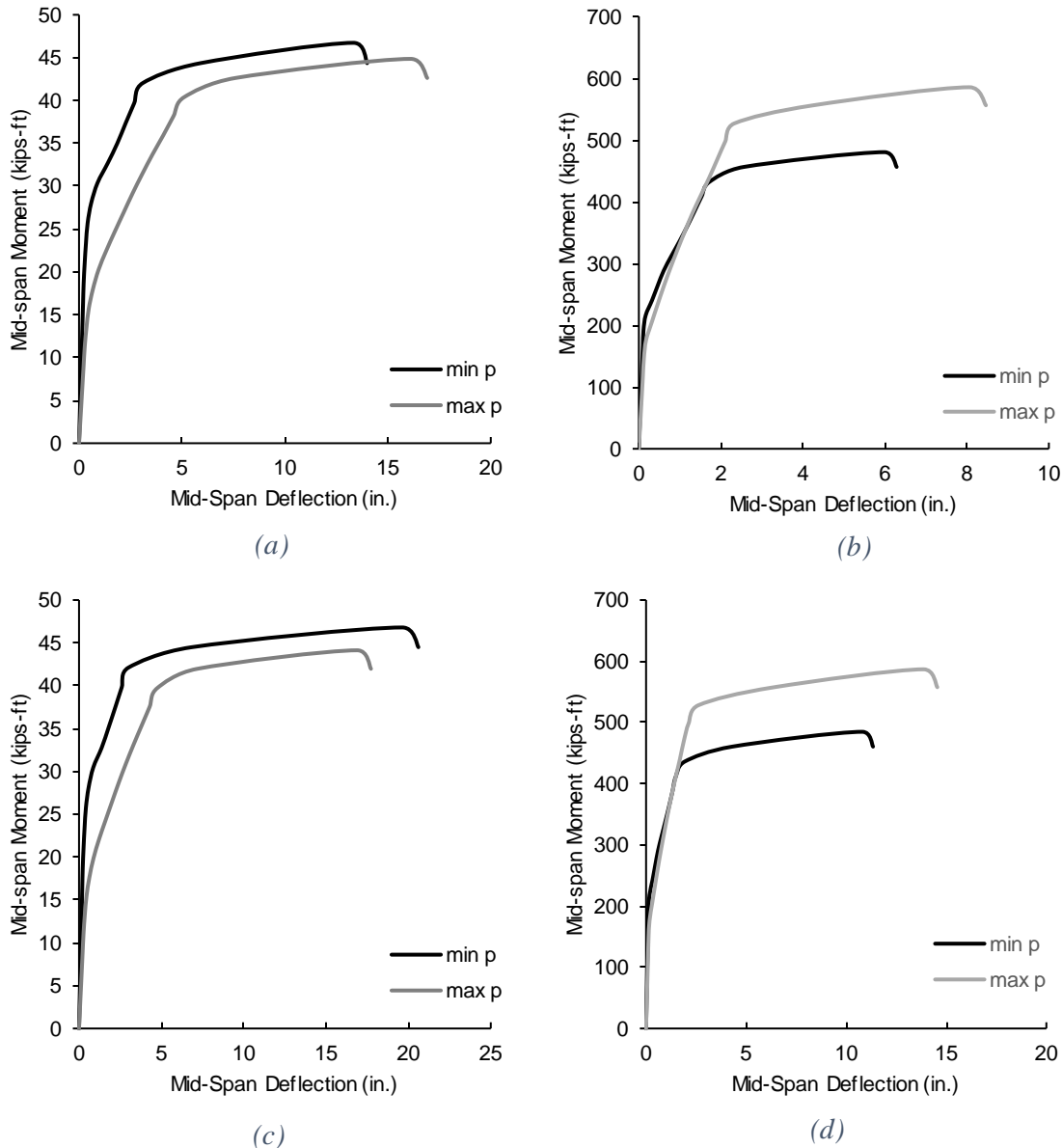


Figure 3.13 Load- Deflection curves for min. and max reinforcement ratios (a) One-way slab D31 Black, (b) Beam D31 Black, (c) One-way slab D31 Galvanized, (d) Beam D31 Galvanized

Table 3.5 presents the maximum deflections and ductility ratios the simulated slabs and beams. No significant benefit was observed for epoxy coated wire over the uncoated wire (only 15% deflection increase and 12% ductility ratio increase per Table 3.5). However, the addition of galvanized coating increases member deformation by 26% for slabs and 76% for beams and increases the ductility ratio by 25% for slabs and 55% for beams.

Table 3.5 Maximum deflection and ductility factor for simulated beams and slabs

<i>Wire Coating type</i>	<i>Slab Reinforcement Ratio ρ (%)</i>				<i>Beam Reinforcement Ratio ρ (%)</i>			
	<i>min = 0.2</i>		<i>max =0.32</i>		<i>min = 0.38</i>		<i>max =0.6</i>	
	<i>max. mid-span deflection (in.)</i>	<i>Ductility Factor μ</i>	<i>max. mid-span deflection (in.)</i>	<i>Ductility Factor μ</i>	<i>max. mid-span deflection (in.)</i>	<i>Ductility Factor μ</i>	<i>max. mid-span deflection (in.)</i>	<i>Ductility Factor μ</i>
Black (None-Coated)	14.0	2.52	16.9	1.90	6.30	2.60	8.50	2.20
Galvanized	20.6	3.66	17.7	1.97	11.3	3.91	14.6	3.52

Chapter 4: Conclusion

This study demonstrated that epoxy coated and galvanized WWR affects mechanical properties along with the known enhanced corrosion resistance. In this study, tensile tests were performed on a total of 108 wire samples and 18 hot rolled reinforcement samples. These samples consisted of black (non-coated), epoxy coated, and galvanized WWR. Each coating was tested on three different sized wires: D11, D20, and D31. The tensile tests showed that coating the wire had an obvious effect on some mechanical properties, but had a less pronounced effect on others. The rupture location was also found to have a significant effect. These properties were then simulated using Response 2000 to estimate their effect at the member level. The following conclusions can be made from the above experimental study:

- Large variability (material property CVs ranged from 0.1% to 67.2% for wire) was observed in all wire samples (coated and uncoated), especially the D31 samples in all sizes' percent area reduction, as compared to a series of hot rolled reinforcement (CVs ranged from 3.3 to 5.0).
- Rupture location played a significant role in all material properties. Rupture at the cross weld location negatively affected all measured properties and also negatively affected the benefits observed from coating. However, the small sample sizes for the D11 and D20 wires that ruptured at a weld affects this conclusion. Additional testing is needed to confirm whether larger diameter wire is affected more by the welding process than smaller wires, but this seems to be indicated by the data.
- Uniform elongation can be measured using a 2 in. or 8 in. extensometer, the latter of which recommended by ASTM A370, to obtain similar results.

- Galvanizing the wire increased the mean, 8 in. gage length, percent elongation from 3.7% to 6.5% and increased the standard deviation from 0.63 to 1.1.
- Epoxy coating the wire marginally increased the percent of elongation from 3.7% to 4.3%, but only small differences in standard deviation were observed (0.82 to 0.78).
- Epoxy and galvanized coatings increased the elastic modulus marginally (7.1% and 10.3% on average).
- Coatings decreased the percent of area reduction (9.1% and 26.1% on average).
- The yield stress and ultimate stress for smaller wire sizes (D11 and D20) increased when the epoxy and galvanized coating was applied. However, the coatings had the least effect on the highly variable D31 wires.
- Galvanizing wire resulted in a slight increasing in the elastic modulus for smaller diameter wires (D11 and D20), while galvanizing did not have any impact on the elastic modulus for D31 wires.
- Designers can expect an increase in deformation capacity and ductility ratio for structural members reinforced with galvanized wire, considering the average properties observed in this report. Up to 11% and 25%, respectively when design for slabs and up to 76% and 55%, respectively, for beams. While this parametric study was highly limited, it does show the potential for enhanced member performance.

References

American Concrete Institute. (2014). "Building code requirements for structural concrete and commentary." ACI 318-14, Farmington Hills, MI.

ASTM (2017). "Standard test methods and definitions for mechanical testing of steel products." A370, West Conshohocken, PA.

ASTM (2014). "Standard Specification for Zinc-Coated (Galvanized) Carbon Steel Wire" A641, West Conshohocken, PA.

ASTM (2014). "Standard Specification for Epoxy-Coated Steel Wire and Welded Wire Reinforcement" A884, West Conshohocken, PA.

ASTM (2016). "Standard Test Methods for Tension Testing of Metallic Materials" E8, West Conshohocken, PA.

Ayyub, B., M., Chang, P., Al-Mutairi, N., (1994) "Welded Wire Fabric for Bridges: I: Ultimate Strength and Ductility" J. Struct. Engrg., ASCE.

Bentz, E.C. "Sectional Analysis of Reinforced Concrete Members," PhD Thesis, Department of Civil Engineering, University of Toronto, 2000, 310 pp.

Maguire, M., "Impact of 0.7 inch diameter prestressing strands in bridge girders" *Master's Thesis*, University of Nebraska-Lincoln, Lincoln, NE.

Maguire, M., Morcous, G., Tadros, M. K. (2012) "Structural performance of precast/prestressed bridge double-tee girders made of high-strength concrete, welded wire reinforcement, and 18-mm-diameter strands." ASCE Journal of Bridge Engineering, 18(10), 1053-1061.

Morcous G., Hatami, A., Maguire, M., Hanna, K., Tadros, M. K. (2011) "Mechanical and bond properties of 18-mm-(0.7-in.-) diameter prestressing strands" *ASCE Journal of Materials in Civil Engineering*, 24(6), 735-744.

Morcous G., Maguire, M., Tadros, M. K. (2011) "Welded-wire reinforcement versus random steel fibers in precast, prestressed concrete bridge girders." *PCI Journal*. 56(2). 113-120.

Morcous, G., Maguire, M., Tadros, M. K. (2009) "Shear Capacity of Ultra-High-Performance Concrete I-Girders with Orthogonal Welded Wire Reinforcement." *American Concrete Institute Special Publication 265*, 511-532.

Sarver, B. (2010). "Mechanical and Geometric Properties of Corrosion Resistant Reinforcing Steel in Concrete" Master Thesis, Blacksburg, Virginia 2010.

Wire Reinforcement Institute. (2016) "Manual of Standard practice, Structural Welded Wire Reinforcement." *WWR-500*. 9th Edition.

Yeomans, S. R. (1998) "Corrosion of the Zinc Alloy Coating in Galvanized Reinforced Concrete" *National Association of Corrosion Engineers International Corrosion 98 Conference*. San Diego, CA.

Appendix G.

Stress-Strain Curves for Coating Study

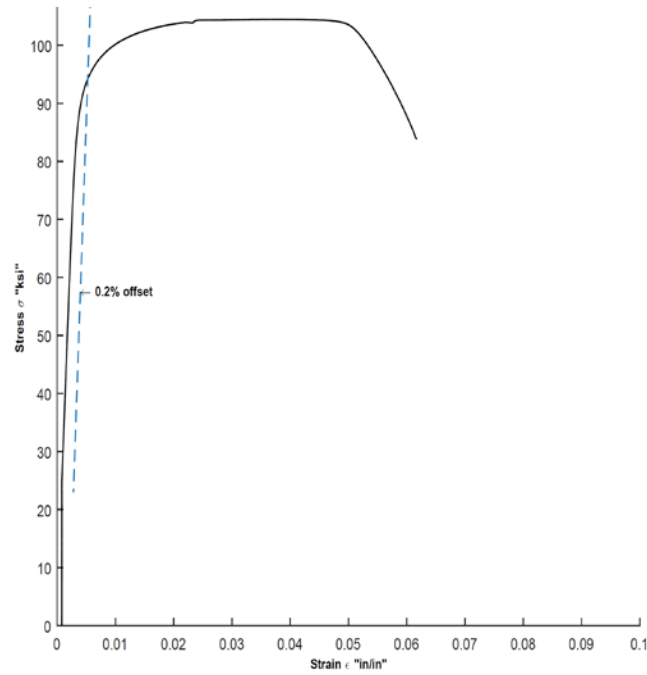


Figure G-1 Stress-Strain Curve for D11 Black WWR Sample 1

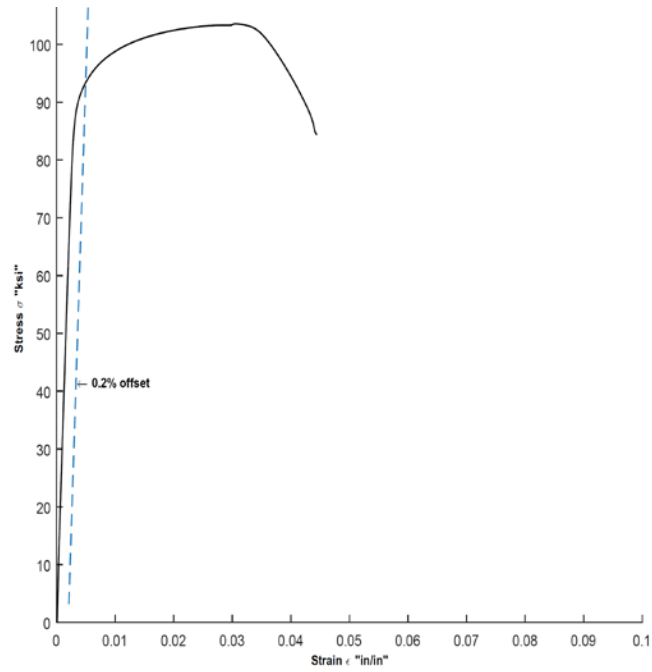


Figure G-2 Stress-Strain Curve for D11 Black WWR Sample 2

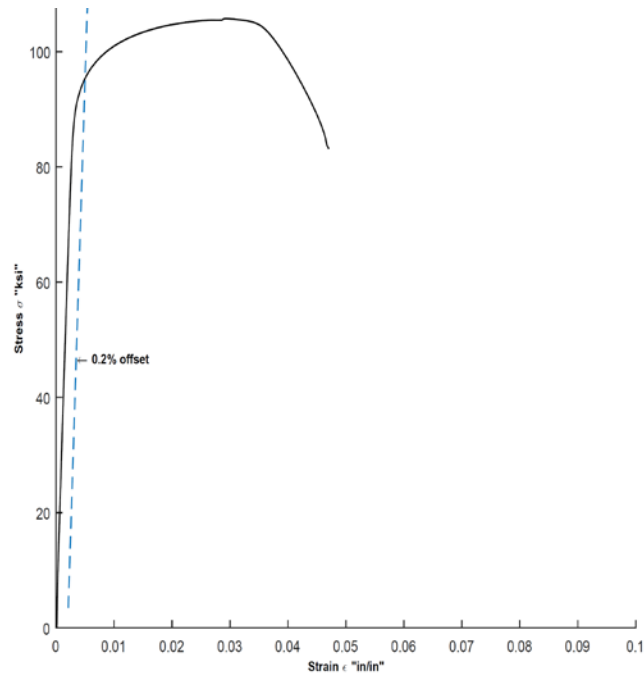


Figure G-3 Stress-Strain Curve for D11 Black WWR Sample 3

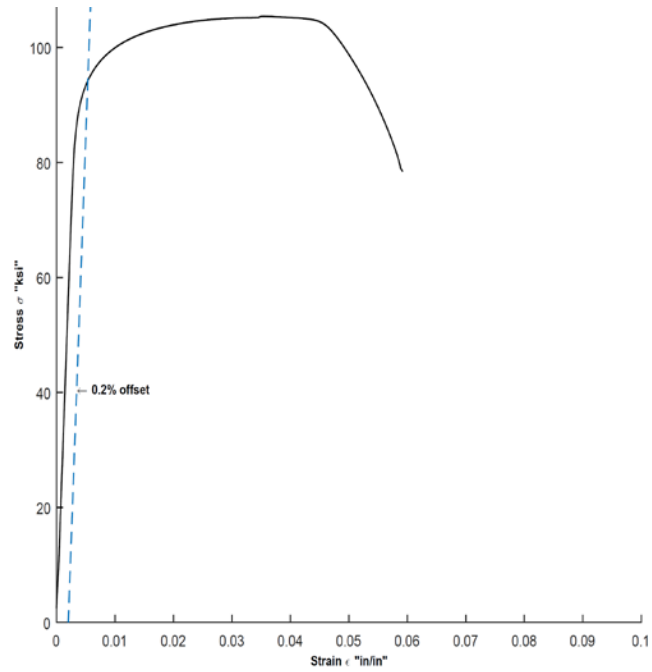


Figure G-4 Stress-Strain Curve for D11 Black WWR Sample 4

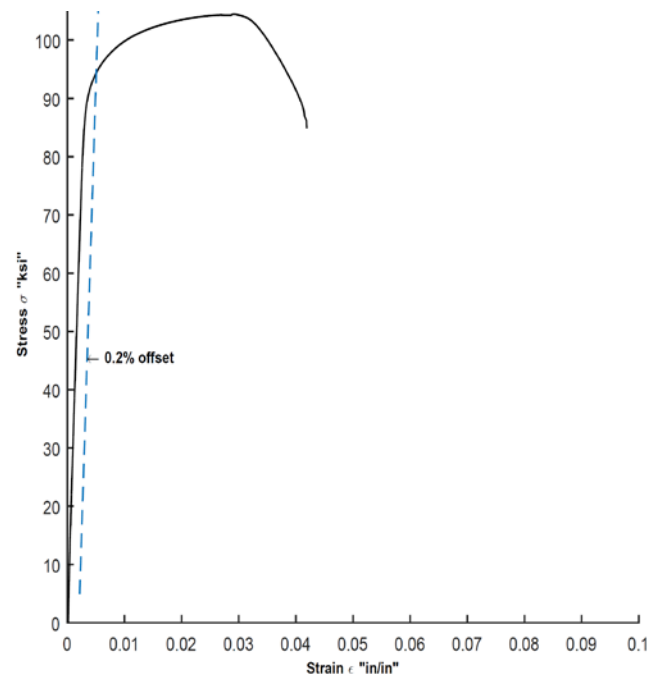


Figure G-5 Stress-Strain Curve for D11 Black WWR Sample 5

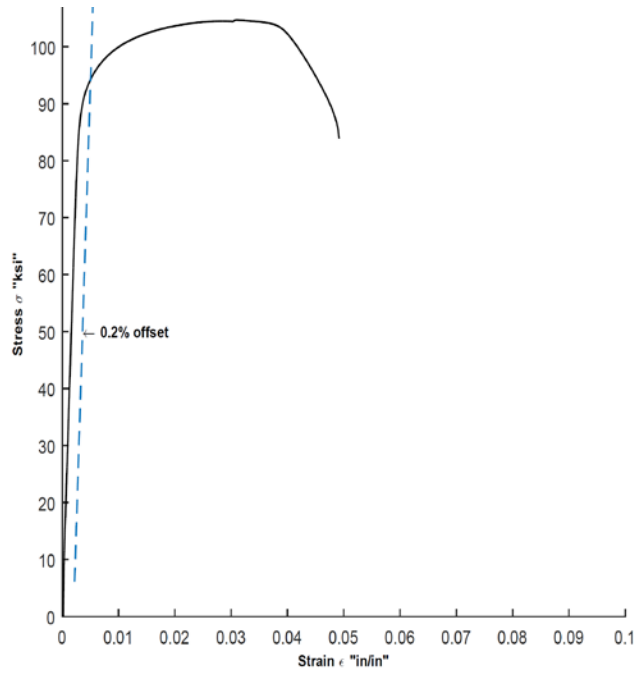


Figure G-6 Stress-Strain Curve for D11 Black WWR Sample 6

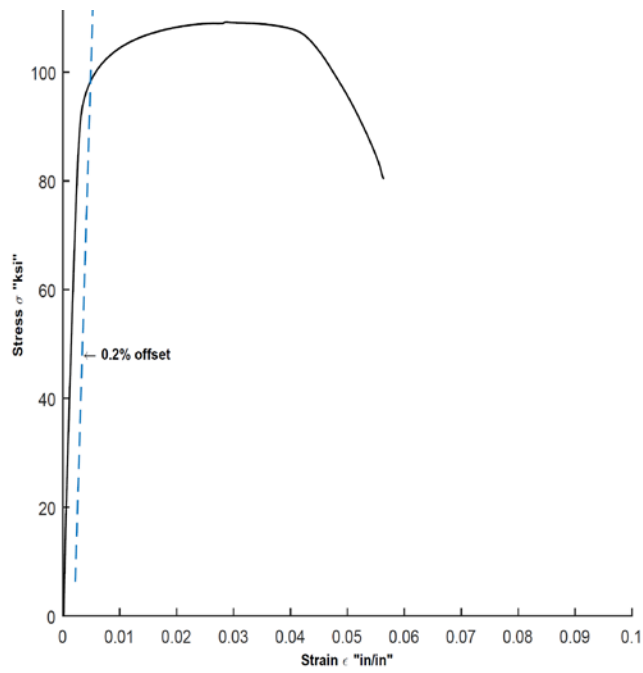


Figure G-7 Stress-Strain Curve for D11 Black WWR Sample 7

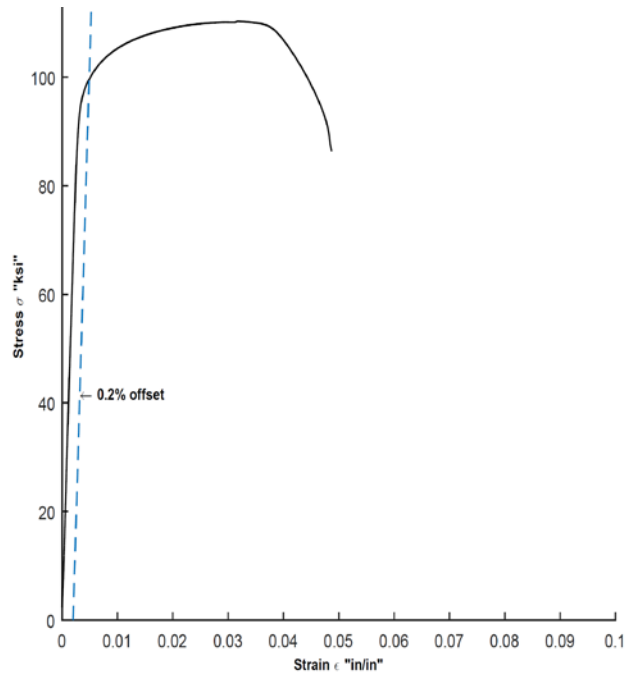


Figure G-8 Stress-Strain Curve for D11 Black WWR Sample 8

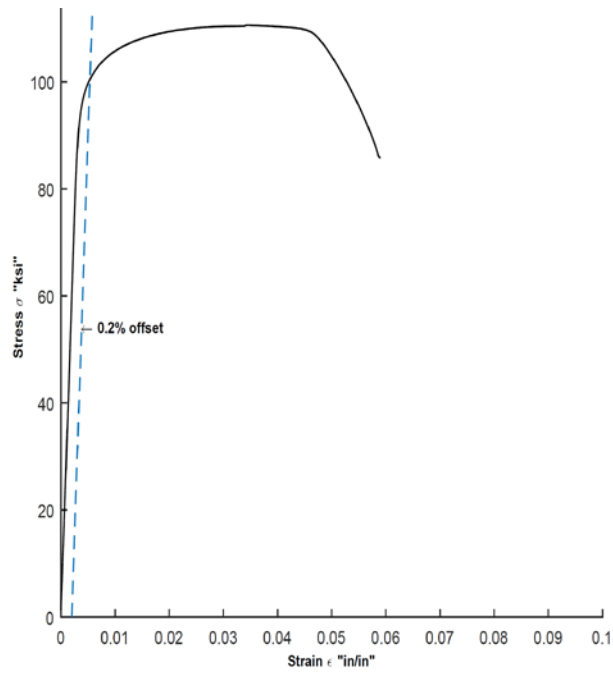


Figure G-9 Stress-Strain Curve for D11 Black WWR Sample 9

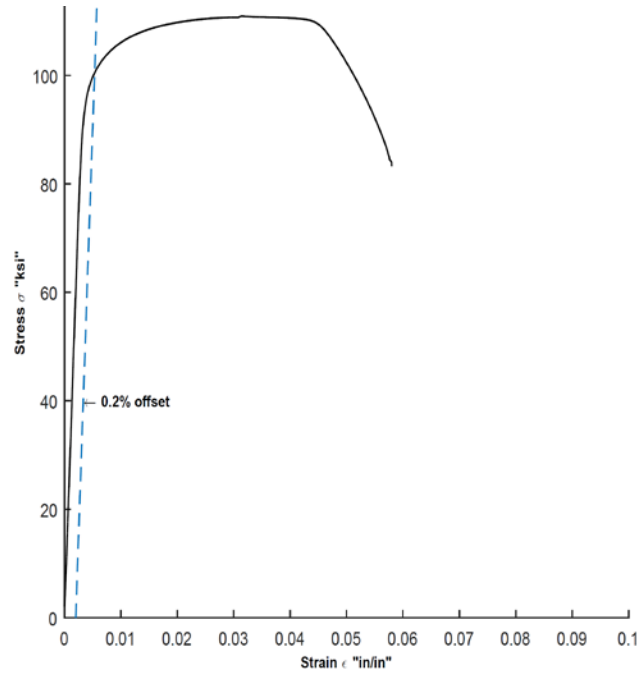


Figure G-10 Stress-Strain Curve for D11 Black WWR Sample 10

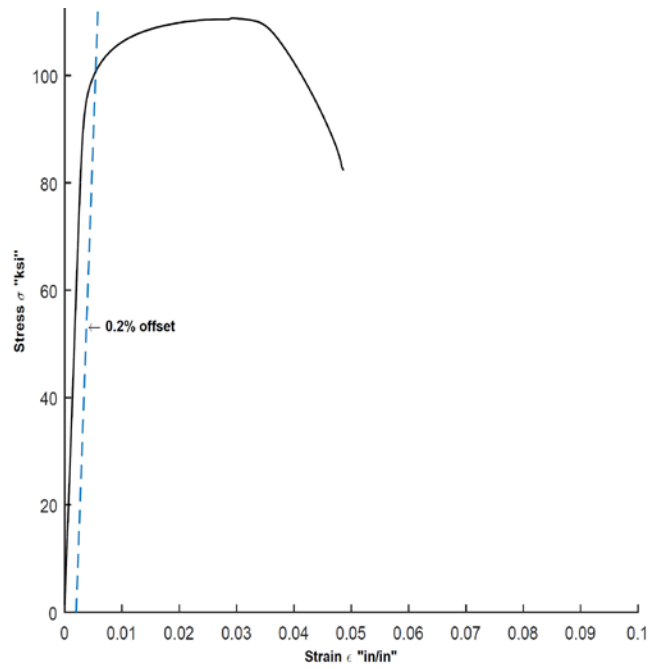


Figure G-11 Stress-Strain Curve for D11 Black WWR Sample 11

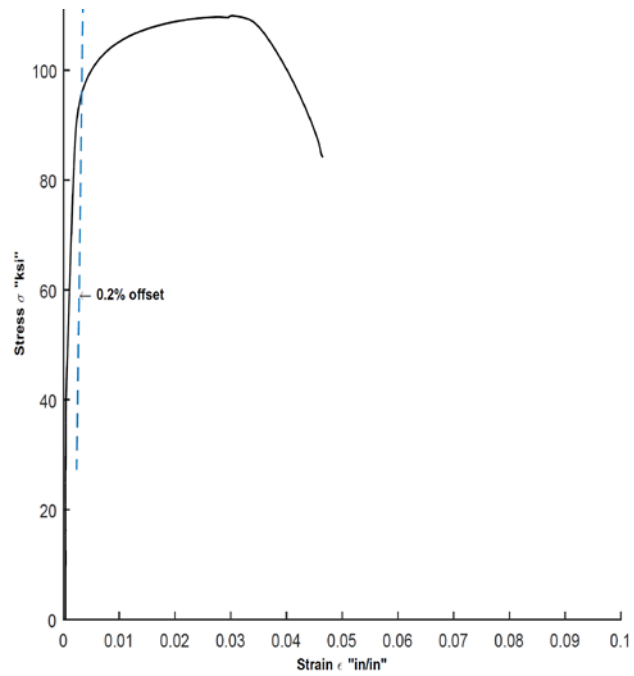


Figure G-12 Stress-Strain Curve for D11 Black WWR Sample 12

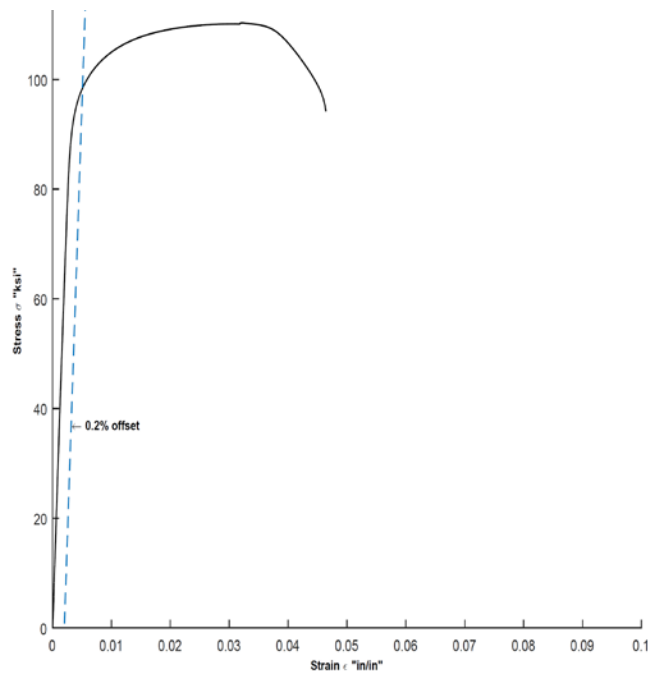


Figure G-13 Stress-Strain Curve for D20 Black WWR Sample 1

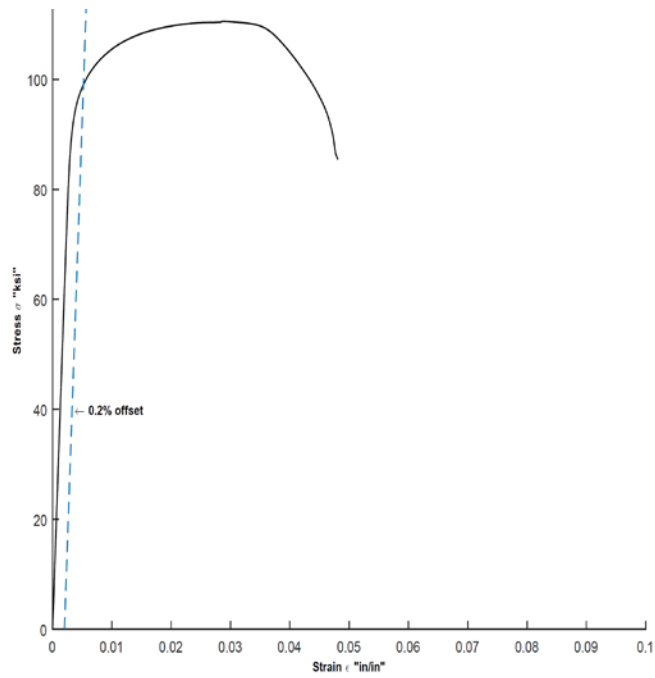


Figure G- 14 Stress-Strain Curve for D20 Black WWR Sample 2

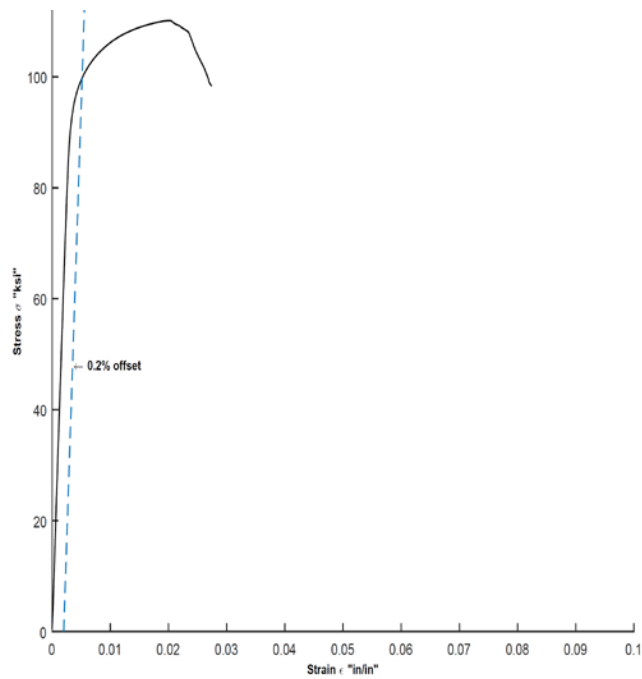


Figure G- 15 Stress-Strain Curve for D20 Black WWR Sample 3

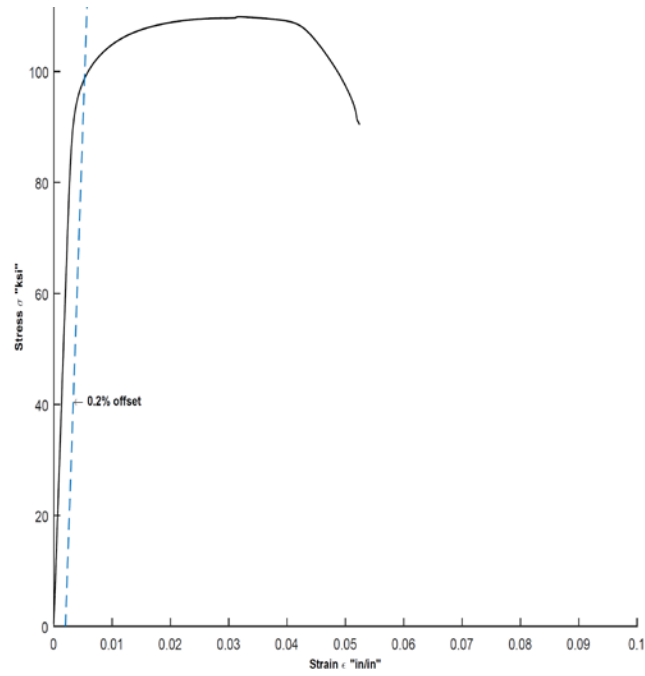


Figure G- 16 Stress-Strain Curve for D20 Black WWR Sample 4

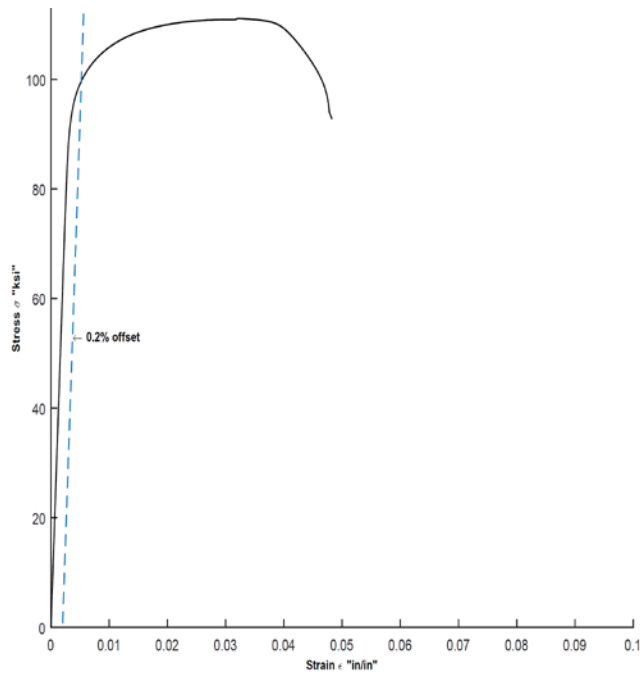


Figure G- 17 Stress-Strain Curve for D20 Black WWR Sample 5

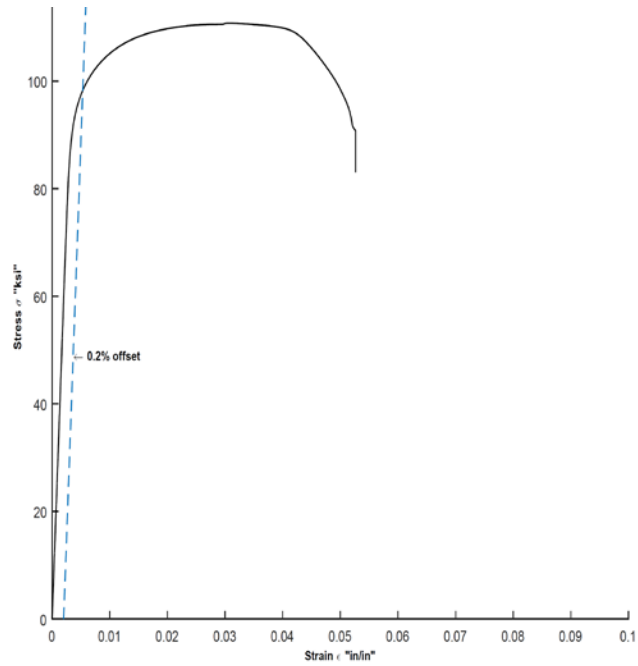


Figure G- 18 Stress-Strain Curve for D20 Black WWR Sample 6

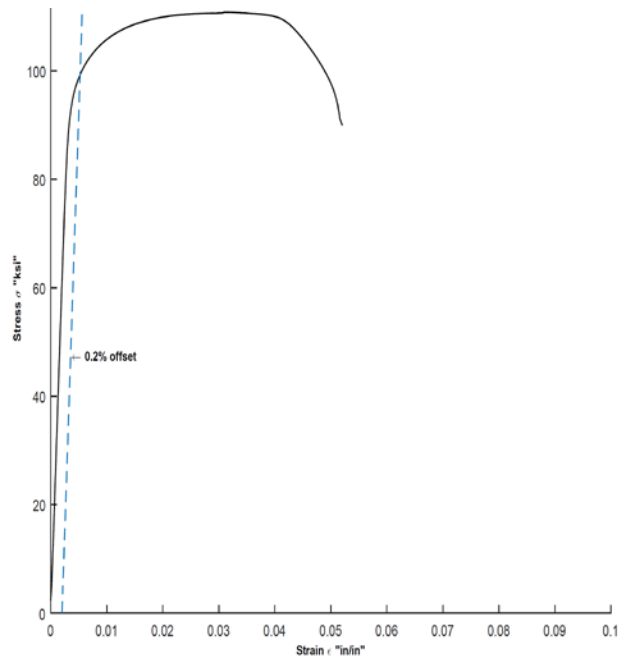


Figure G- 19 Stress-Strain Curve for D20 Black WWR Sample 7

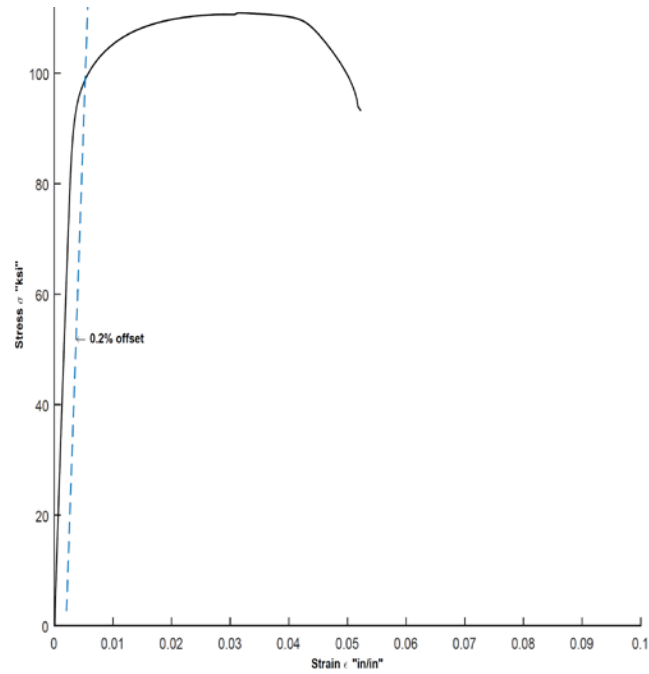


Figure G- 20 Stress-Strain Curve for D20 Black WWR Sample 8

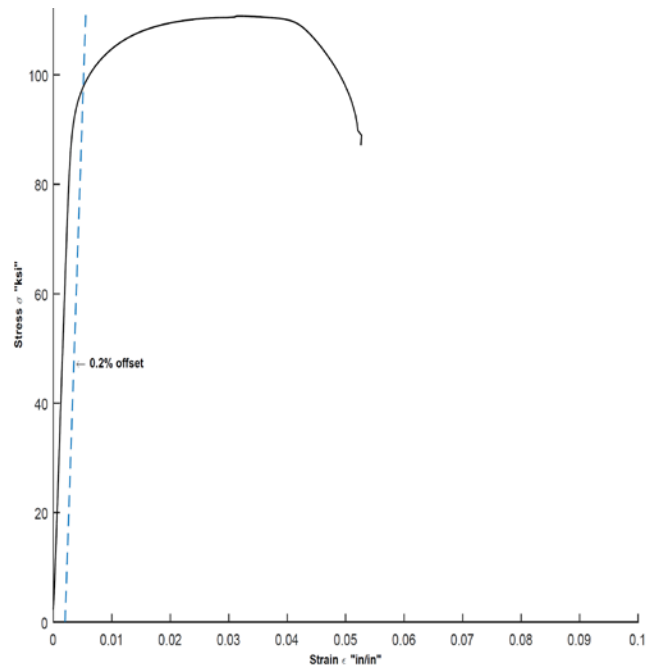


Figure G- 21 Stress-Strain Curve for D20 Black WWR Sample 9

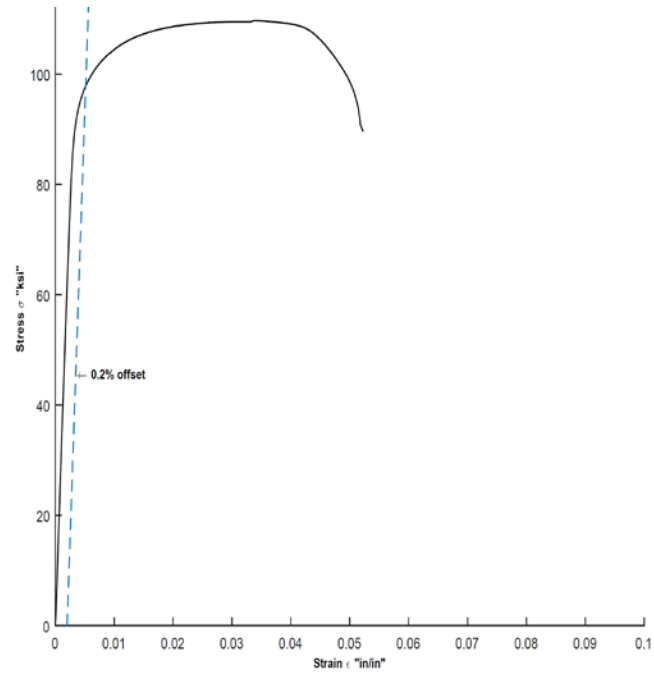


Figure G- 22 Stress-Strain Curve for D20 Black WWR Sample 10

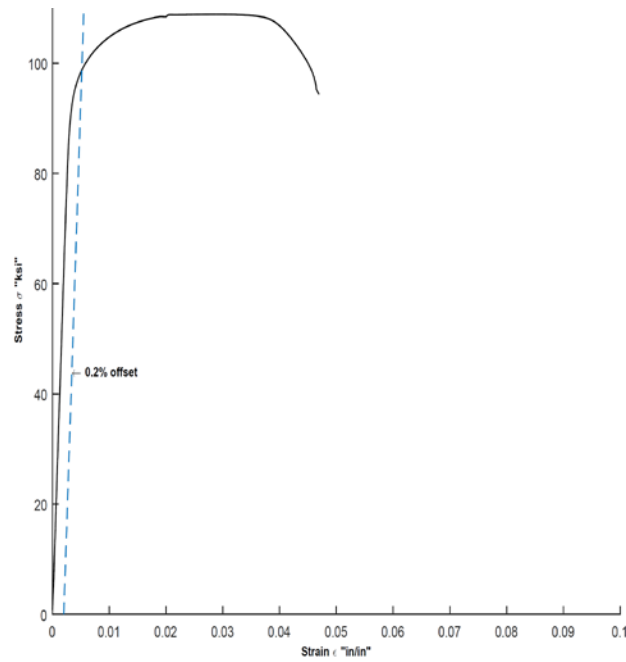


Figure G- 23 Stress-Strain Curve for D20 Black WWR Sample 11

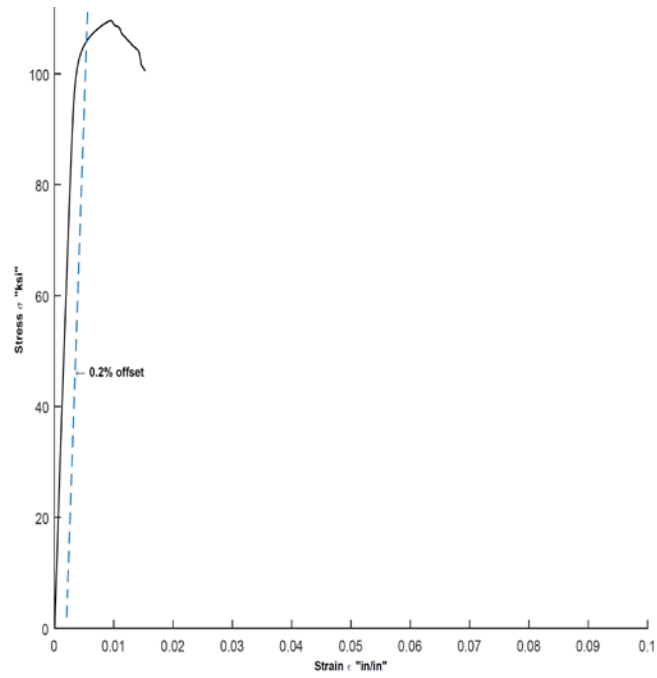


Figure G- 24 Stress-Strain Curve for D31 Black WWR Sample 1

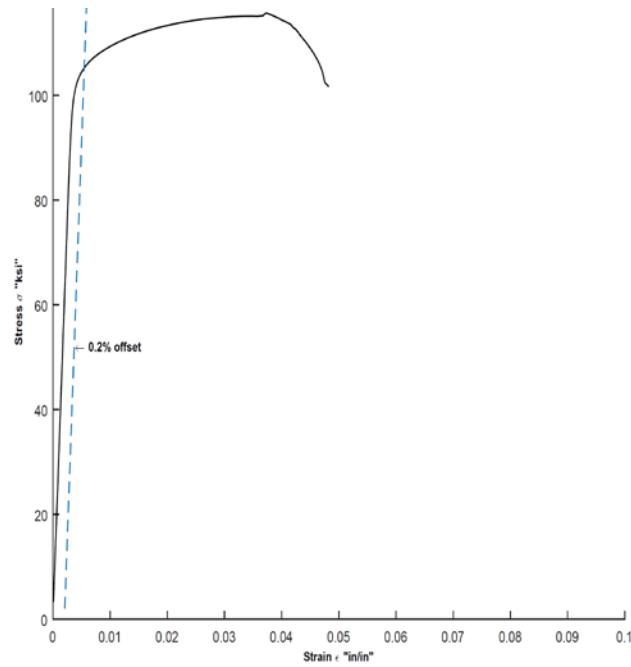


Figure G- 25 Stress-Strain Curve for D31 Black WWR Sample 2

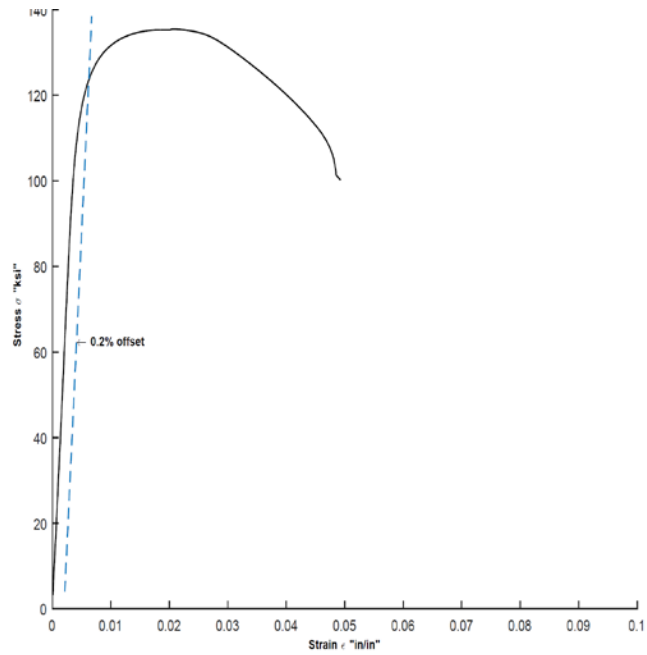


Figure G-26 Stress-Strain Curve for D31 Black WWR Sample 3

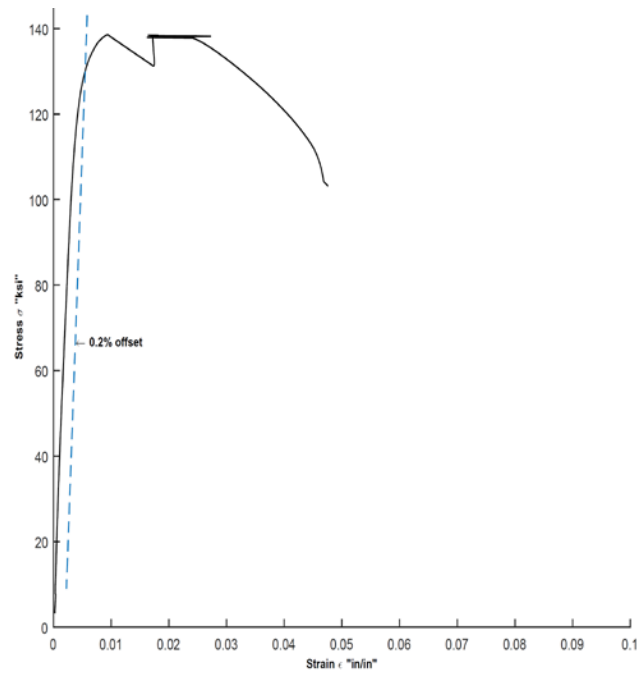


Figure G-27 Stress-Strain Curve for D31 Black WWR Sample 4

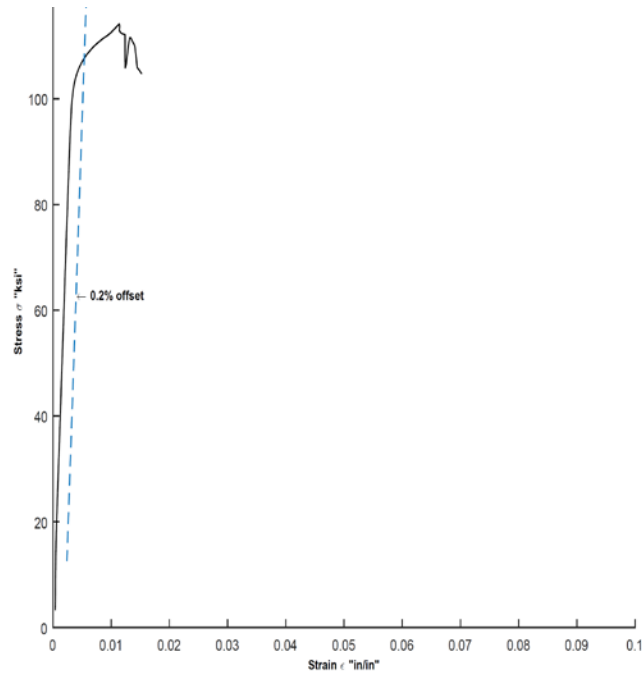


Figure G- 28 Stress-Strain Curve for D31 Black WWR Sample 5

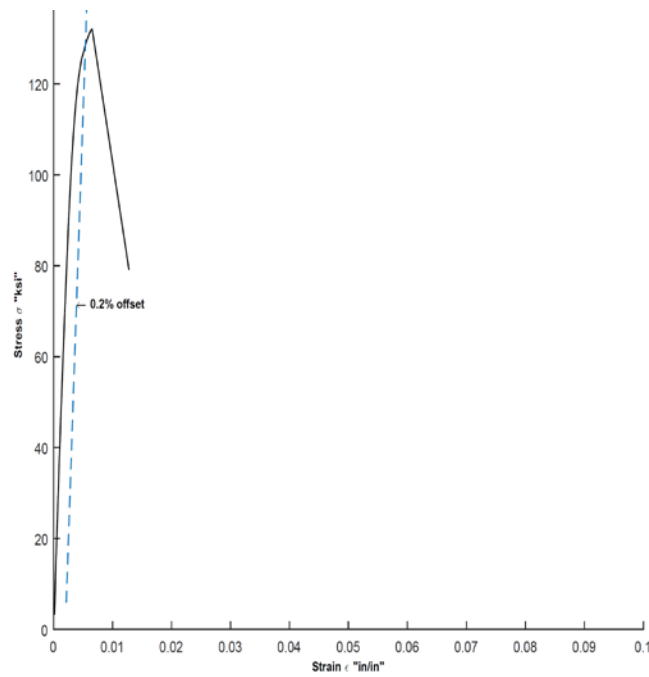


Figure G- 29 Stress-Strain Curve for D31 Black WWR Sample 6

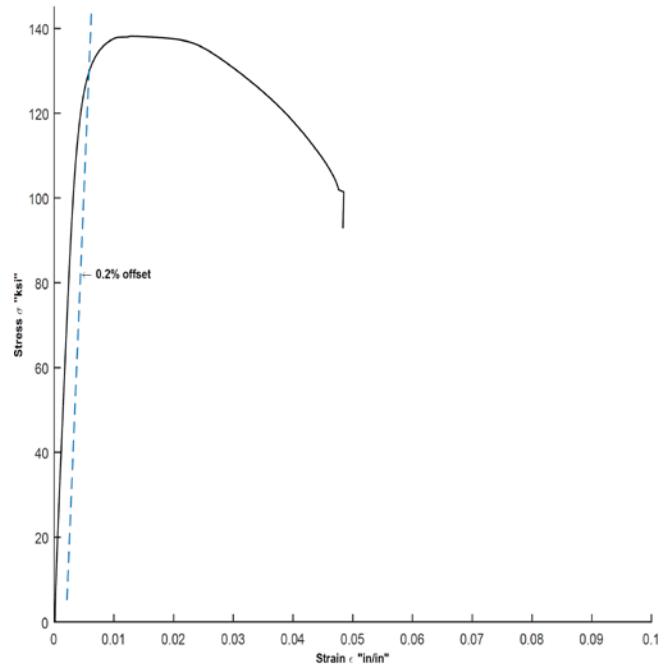


Figure G- 30 Stress-Strain Curve for D31 Black WWR Sample 7

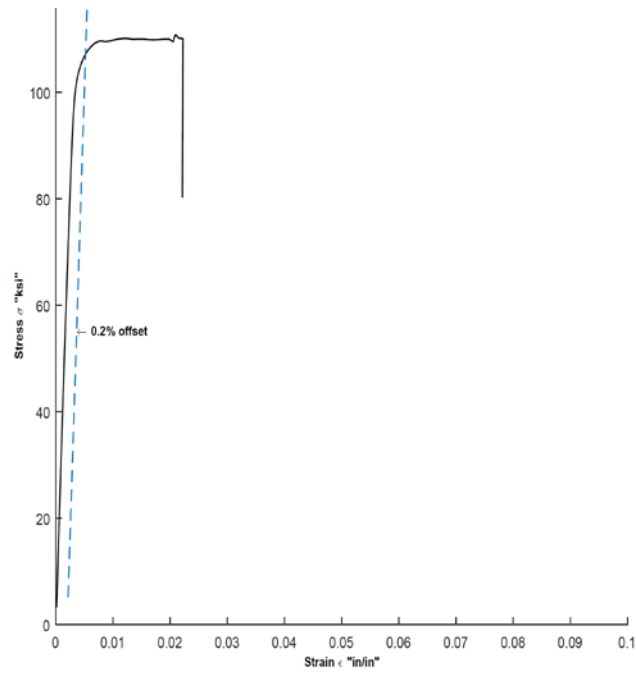


Figure G- 31 Stress-Strain Curve for D31 Black WWR Sample 8

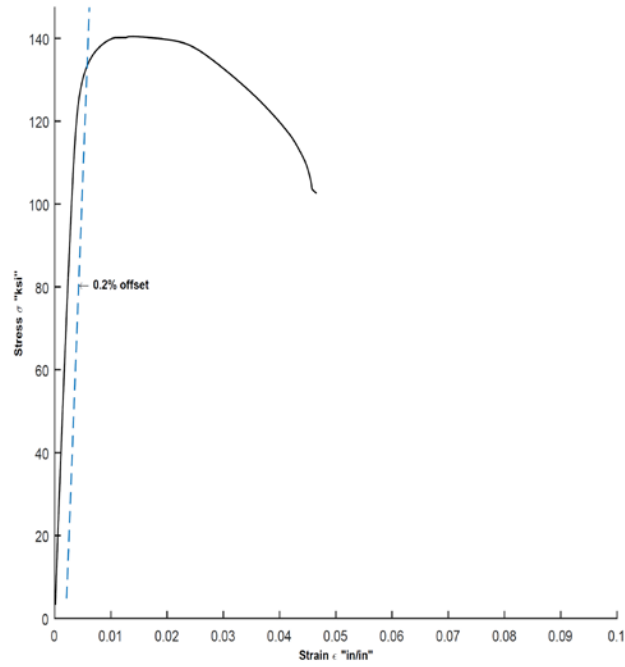


Figure G- 32 Stress-Strain Curve for D31 Black WWR Sample 9

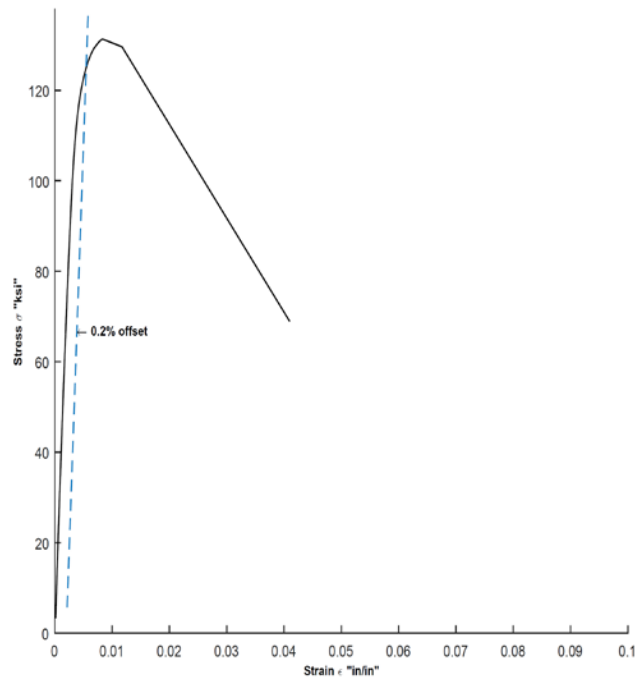


Figure G- 33 Stress-Strain Curve for D31 Black WWR Sample 10

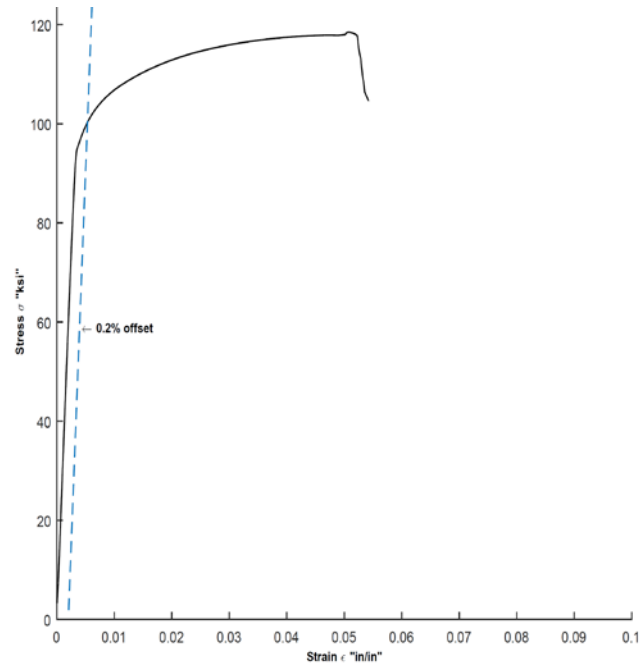


Figure G- 34 Stress-Strain Curve for D31 Black WWR Sample 11

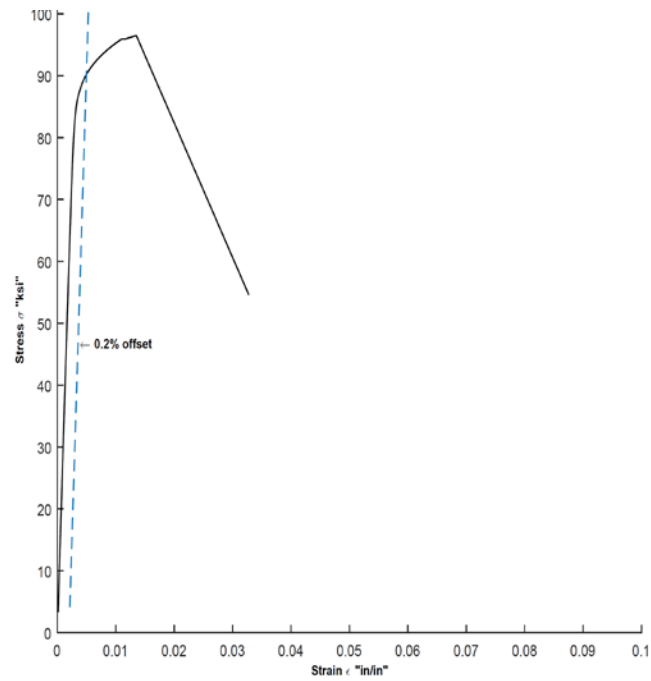


Figure G- 35 Stress-Strain Curve for D31 Black WWR Sample 12

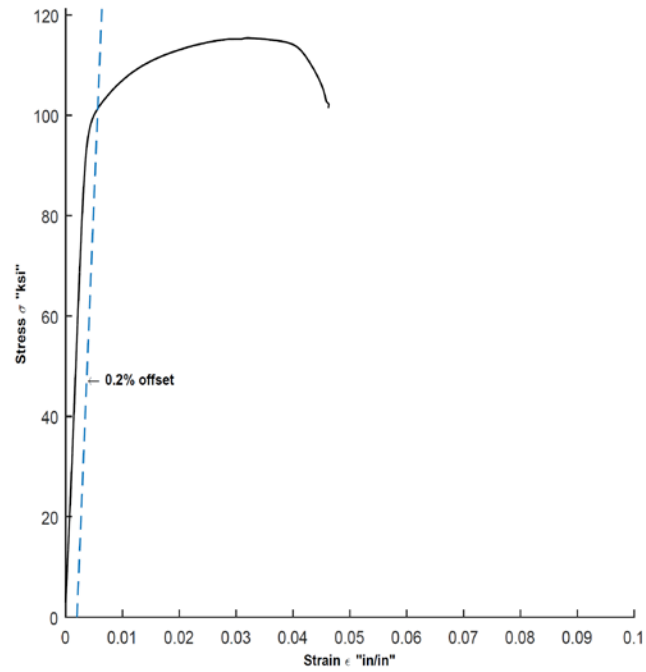


Figure G-36 Stress-Strain Curve for D11 Epoxy WWR Sample 1

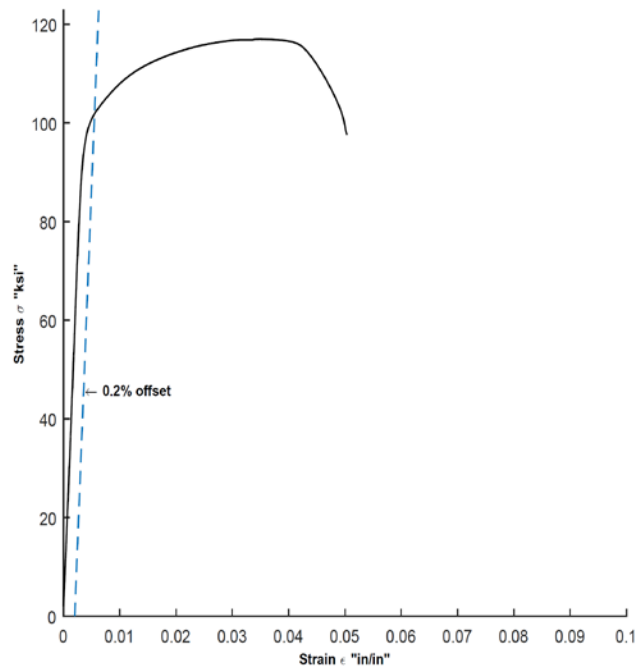


Figure G-37 Stress-Strain Curve for D11 Epoxy WWR Sample 2

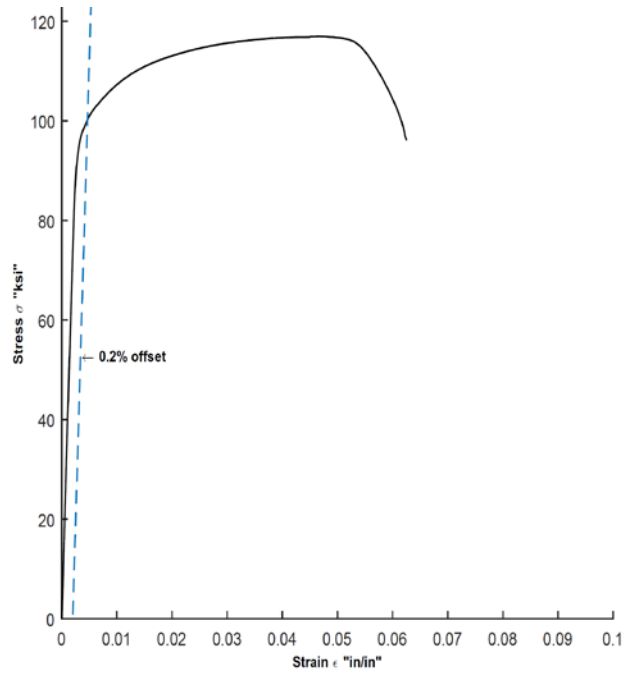


Figure G-38 Stress-Strain Curve for D11 Epoxy WWR Sample 3

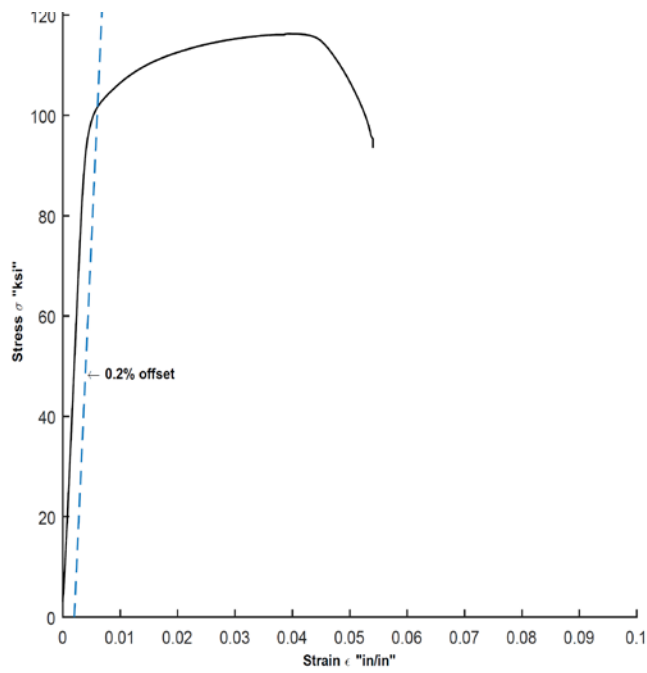


Figure G-39 Stress-Strain Curve for D11 Epoxy WWR Sample 4

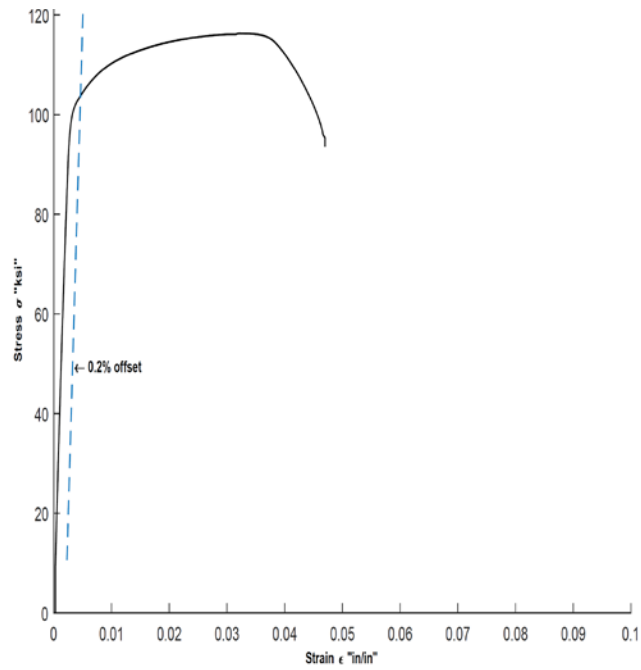


Figure G-40 Stress-Strain Curve for D11 Epoxy WWR Sample 5

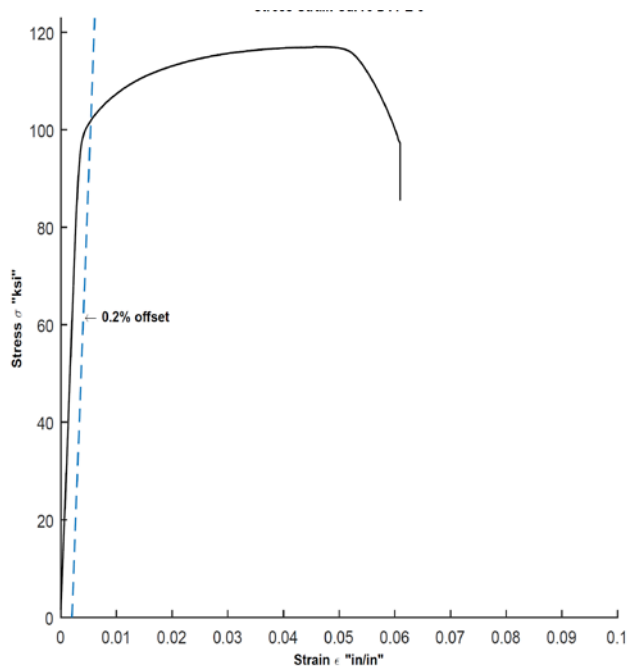


Figure G-41 Stress-Strain Curve for D11 Epoxy WWR Sample 6

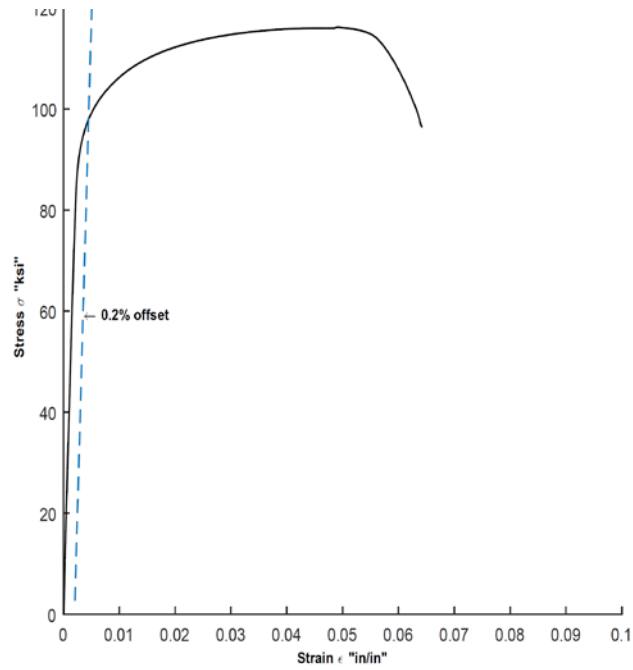


Figure G-42 Stress-Strain Curve for D11 Epoxy WWR Sample 7

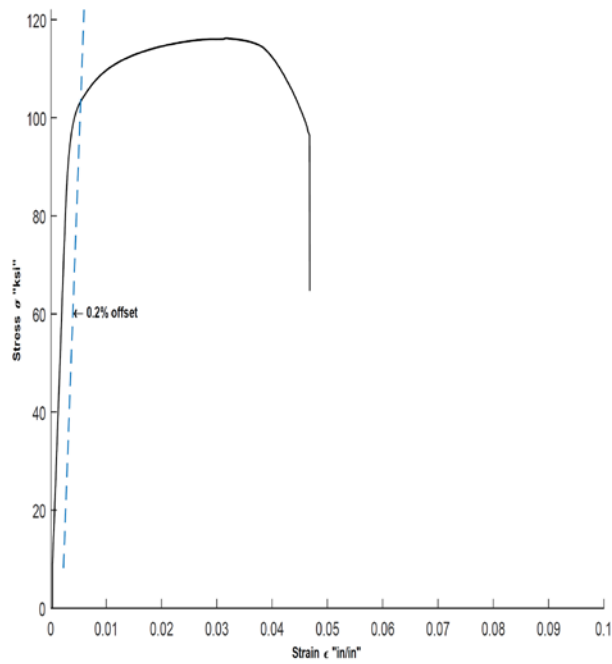


Figure G-43 Stress-Strain Curve for D11 Epoxy WWR Sample 8

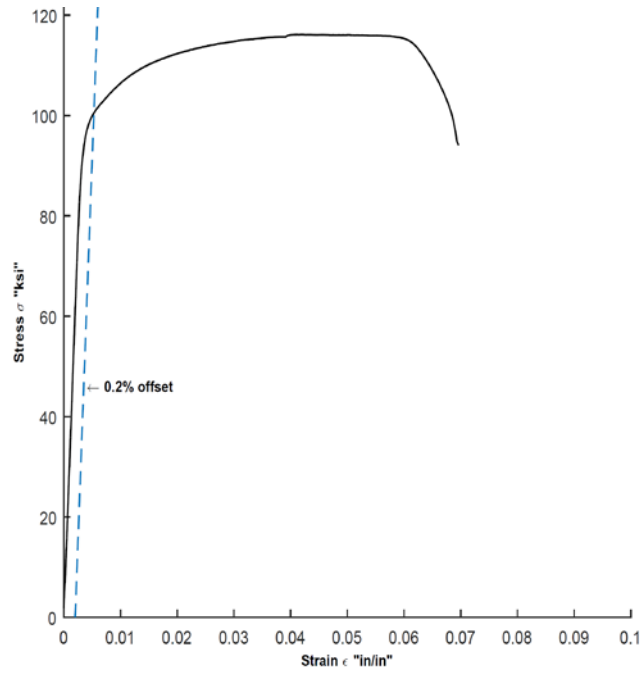


Figure G-44 Stress-Strain Curve for D11 Epoxy WWR Sample 9

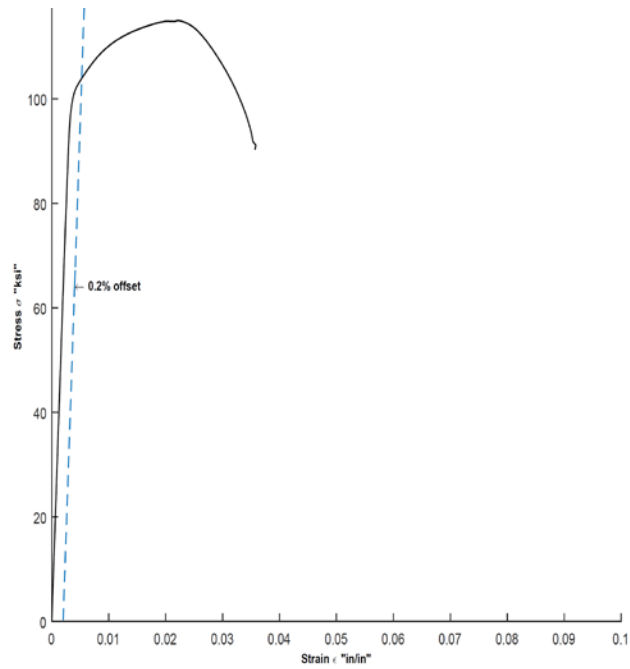


Figure G-45 Stress-Strain Curve for D11 Epoxy WWR Sample 10

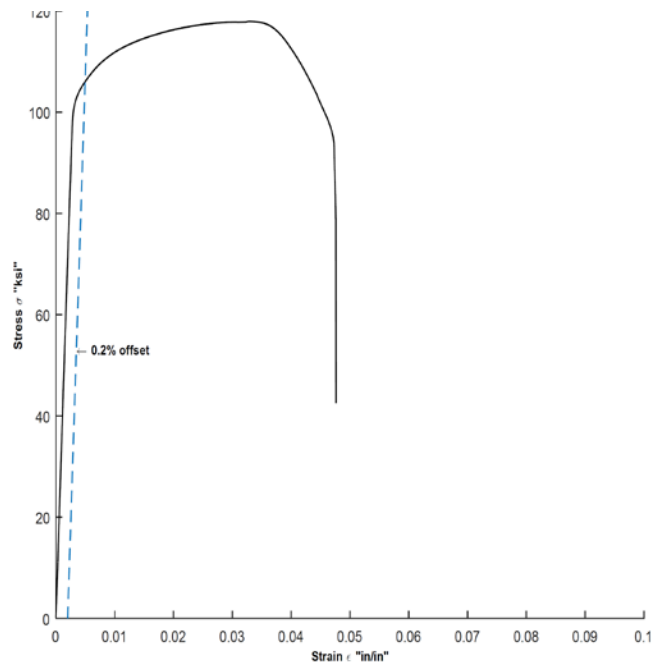


Figure G-46 Stress-Strain Curve for D11 Epoxy WWR Sample 11

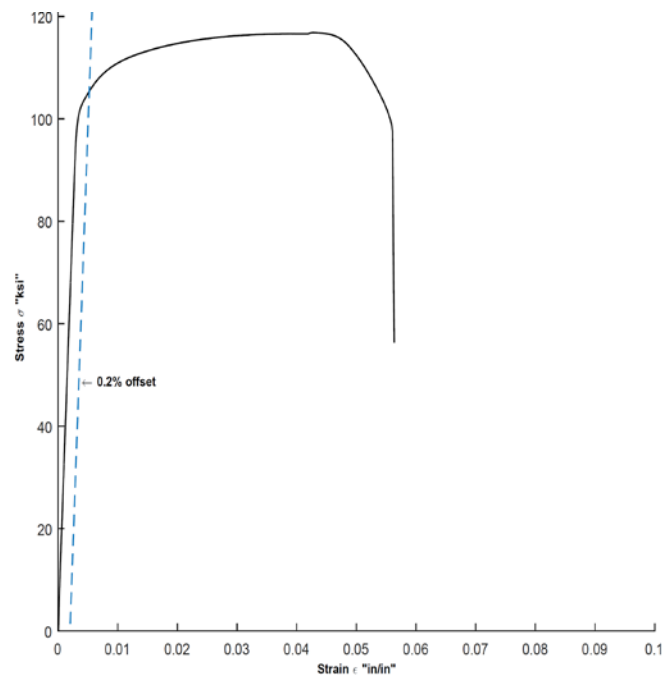


Figure G-47 Stress-Strain Curve for D11 Epoxy WWR Sample 12

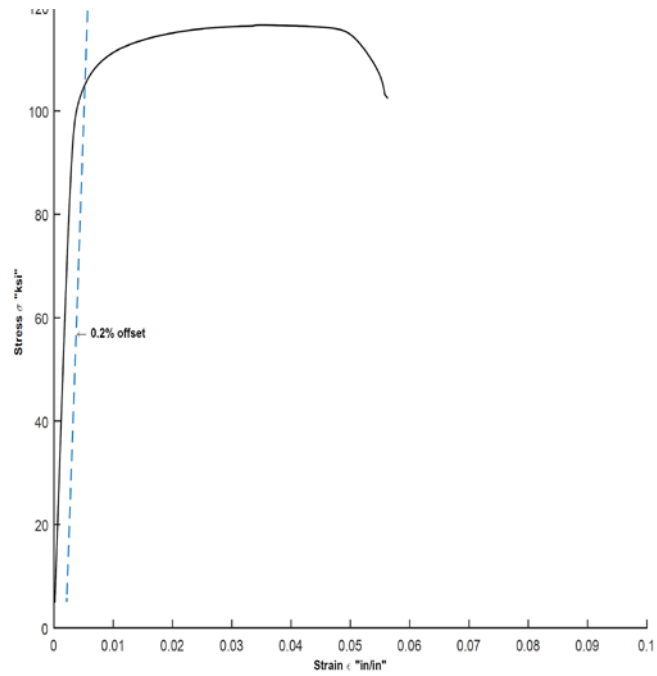


Figure G-48 Stress-Strain Curve for D20 Epoxy WWR Sample 1

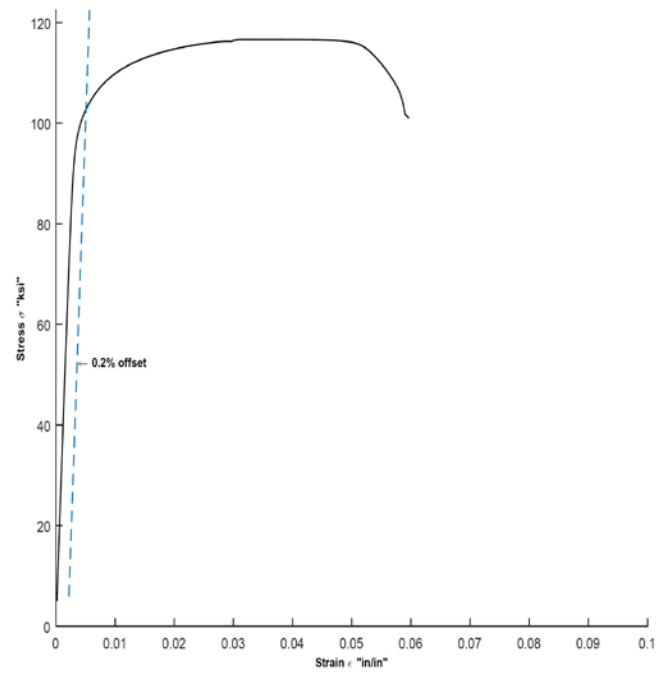


Figure G-49 Stress-Strain Curve for D20 Epoxy WWR Sample 2

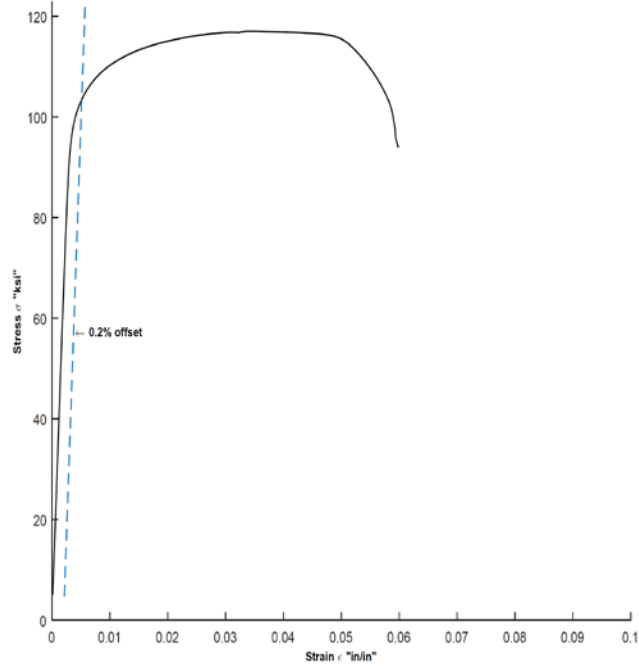


Figure G- 50 Stress-Strain Curve for D20 Epoxy WWR Sample 3

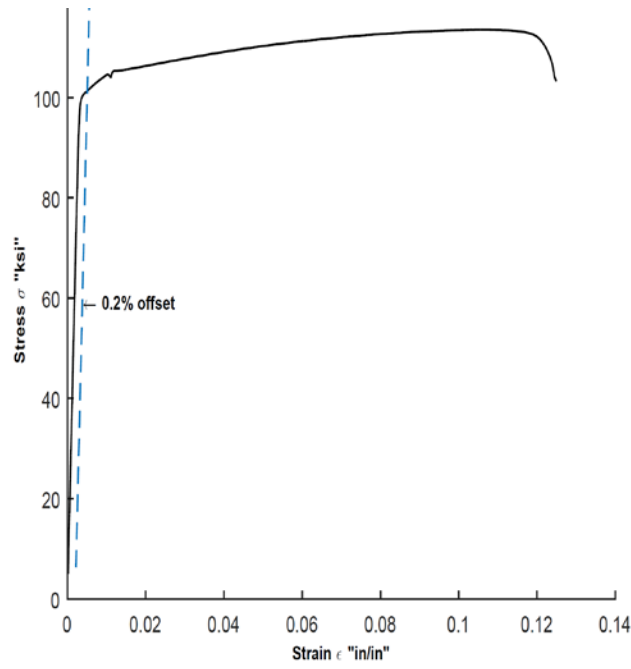


Figure G- 51 Stress-Strain Curve for D20 Epoxy WWR Sample 4

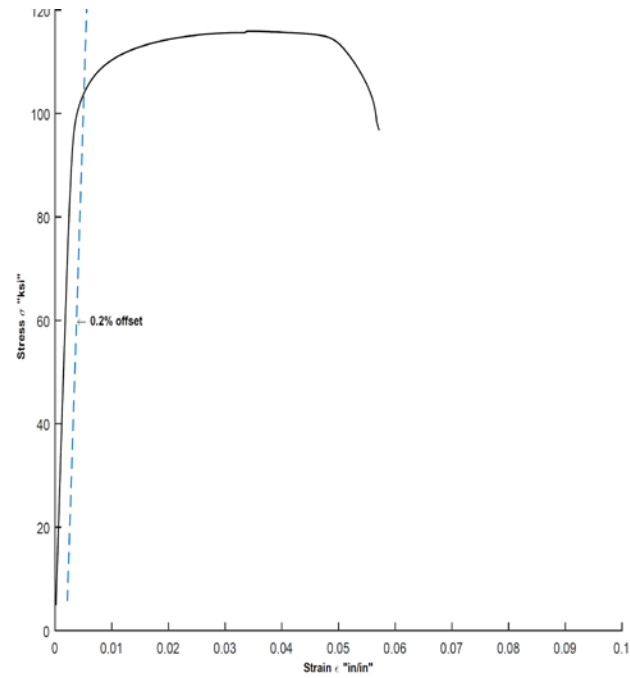


Figure G- 52 Stress-Strain Curve for D20 Epoxy WWR Sample 5

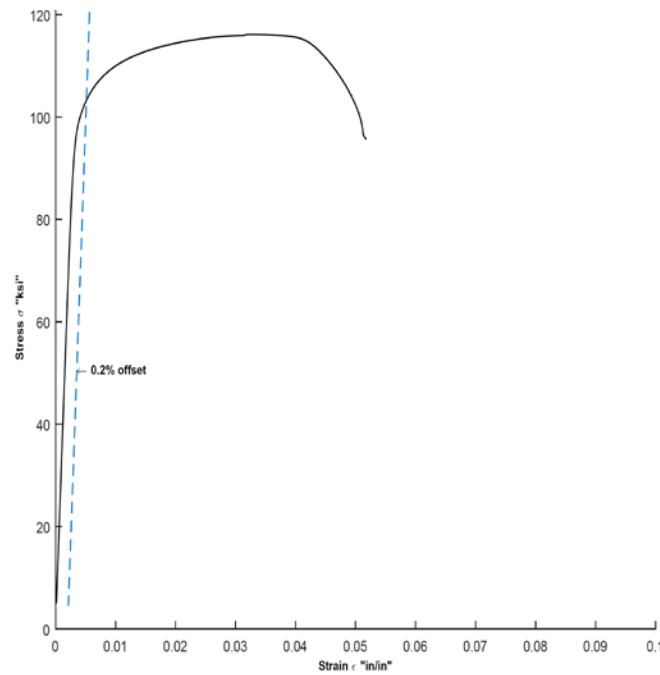


Figure G- 53 Stress-Strain Curve for D20 Epoxy WWR Sample 6

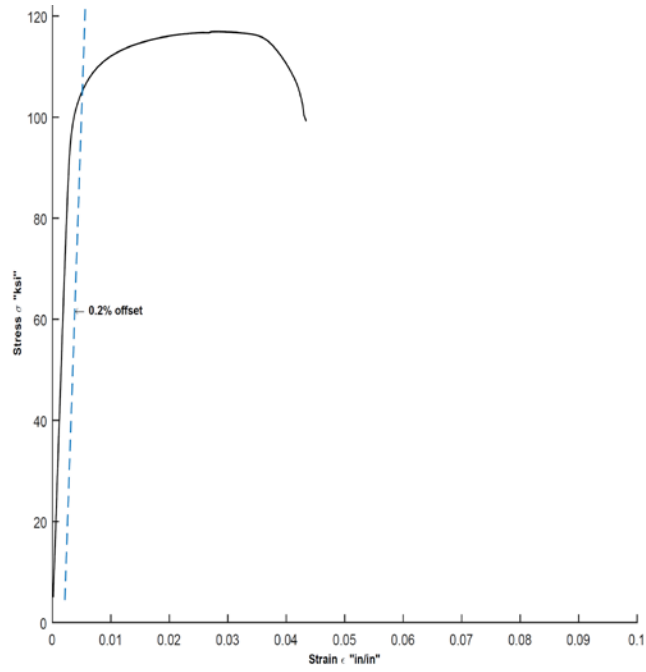


Figure G- 54 Stress-Strain Curve for D20 Epoxy WWR Sample 7

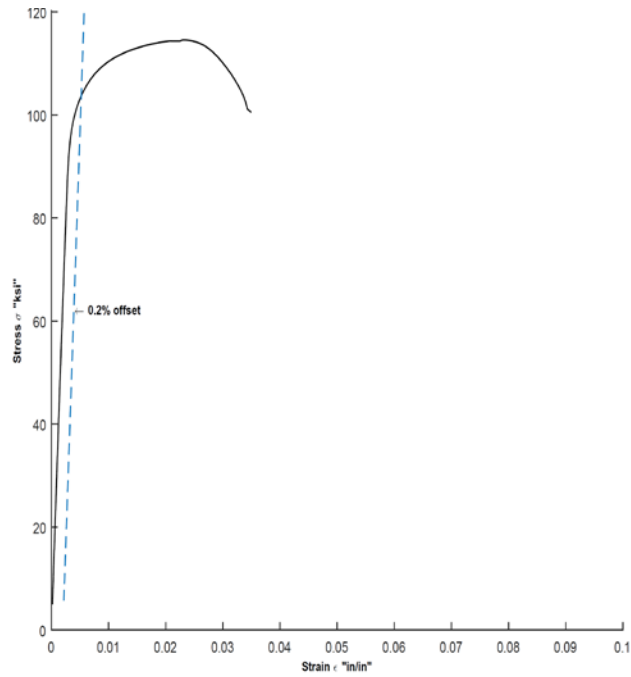


Figure G- 55 Stress-Strain Curve for D20 Epoxy WWR Sample 8

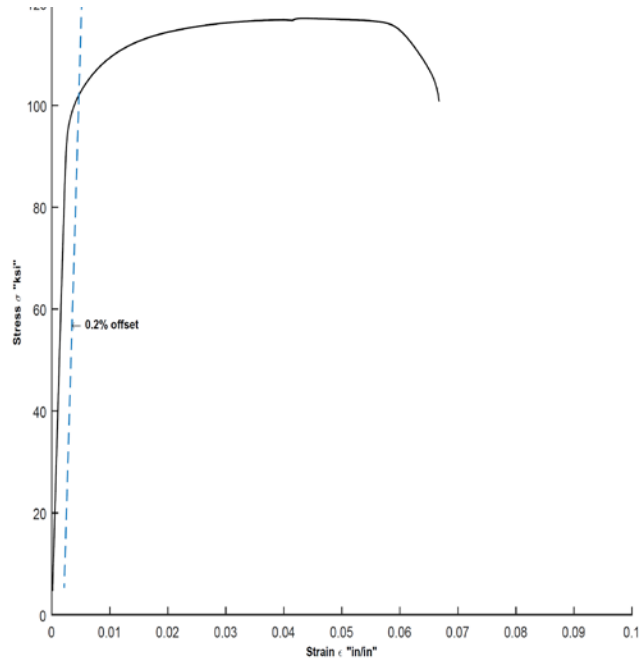


Figure G- 56 Stress-Strain Curve for D20 Epoxy WWR Sample 9

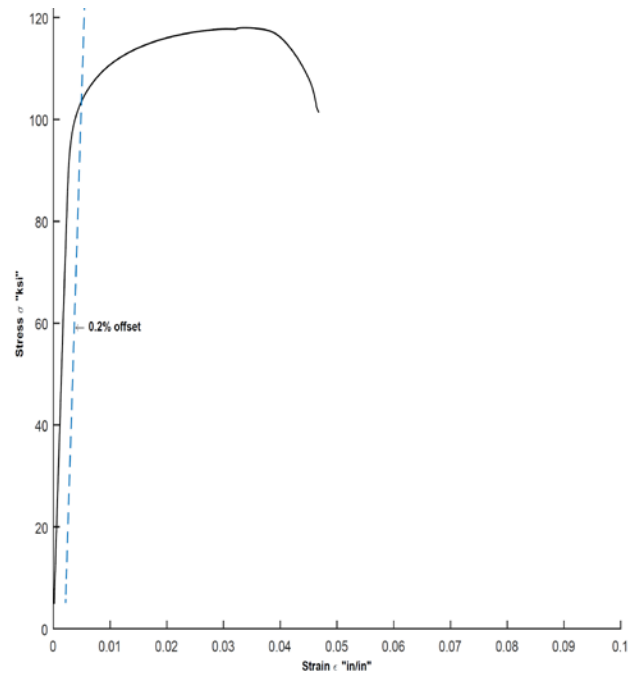


Figure G- 57 Stress-Strain Curve for D20 Epoxy WWR Sample 10

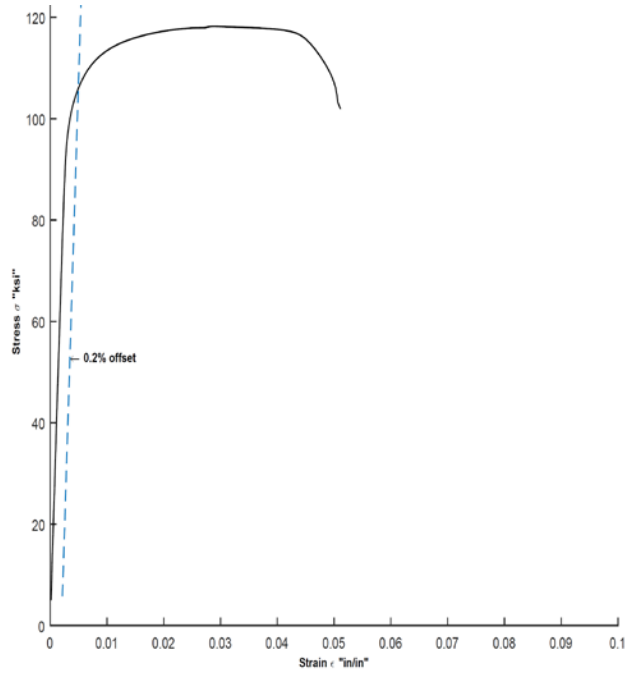


Figure G- 58 Stress-Strain Curve for D20 Epoxy WWR Sample 11

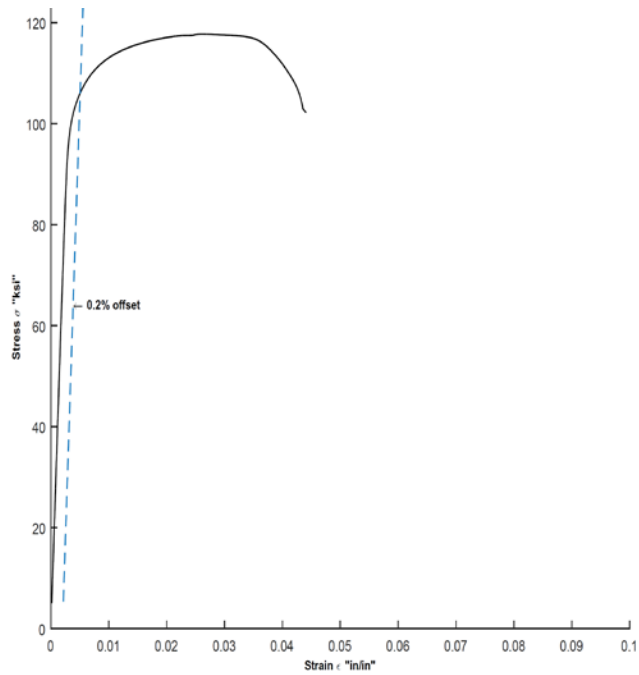


Figure G- 59 Stress-Strain Curve for D20 Epoxy WWR Sample 12

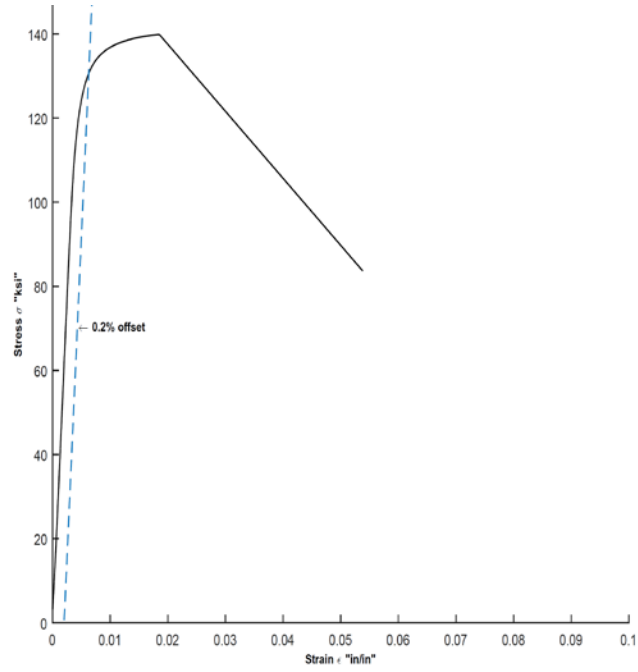


Figure G-60 Stress-Strain Curve for D31 Epoxy WWR Sample 1

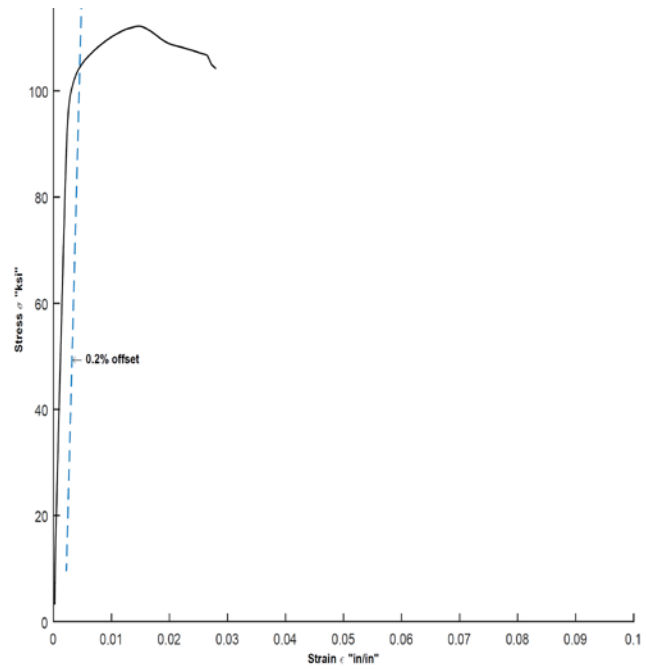


Figure G-61 Stress-Strain Curve for D31 Epoxy WWR Sample 2

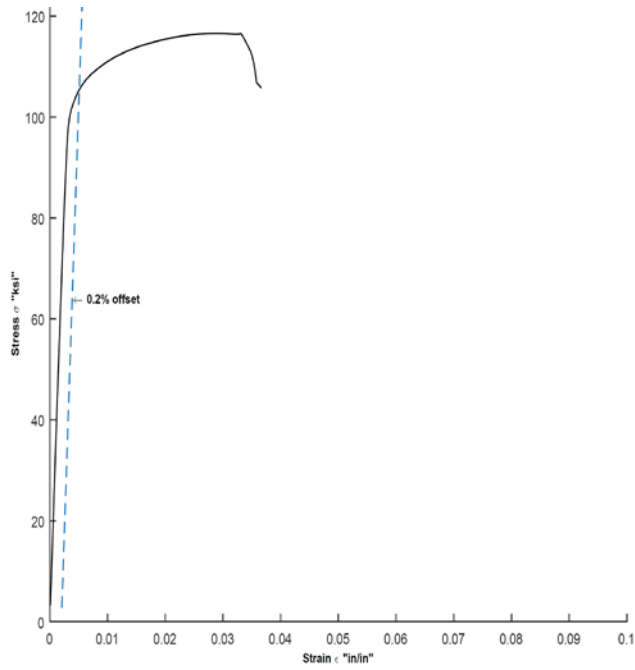


Figure G-62 Stress-Strain Curve for D31 Epoxy WWR Sample 3

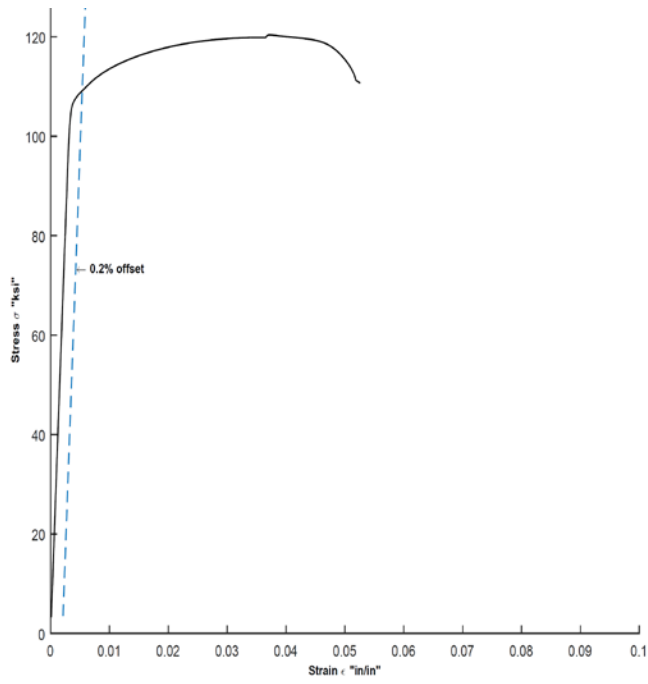


Figure G-63 Stress-Strain Curve for D31 Epoxy WWR Sample 4

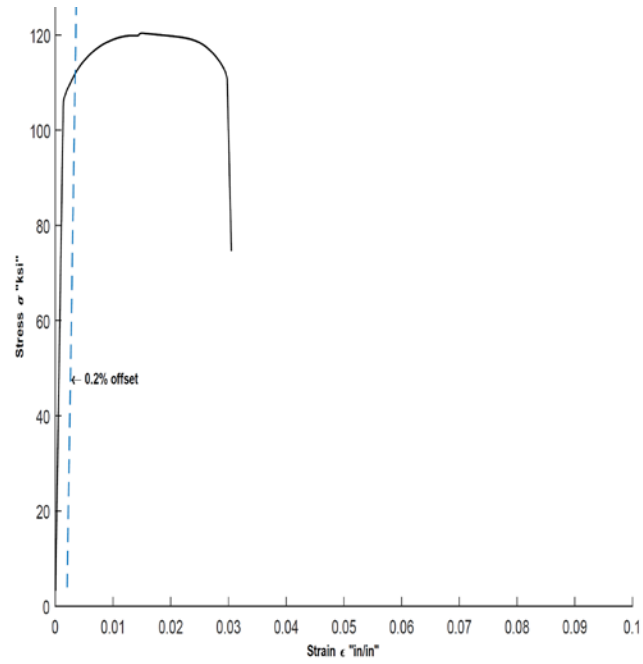


Figure G-64 Stress-Strain Curve for D31 Epoxy WWR Sample 5

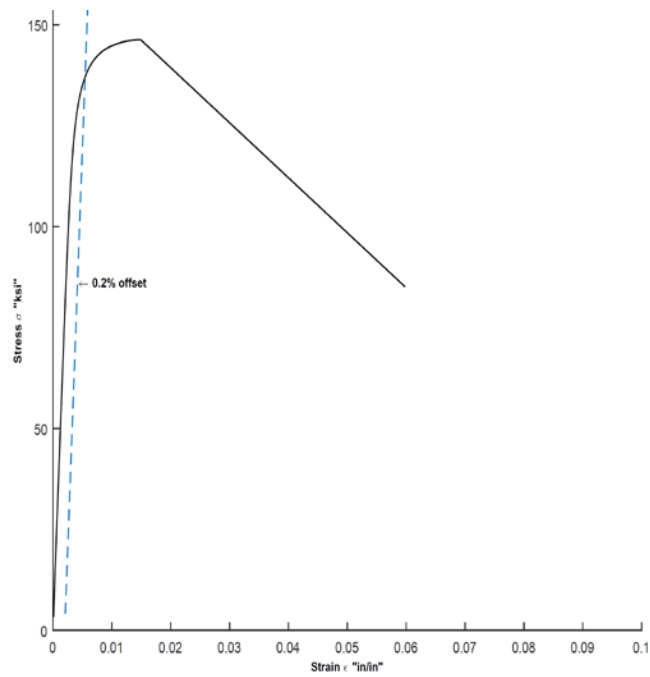


Figure G-65 Stress-Strain Curve for D31 Epoxy WWR Sample 6

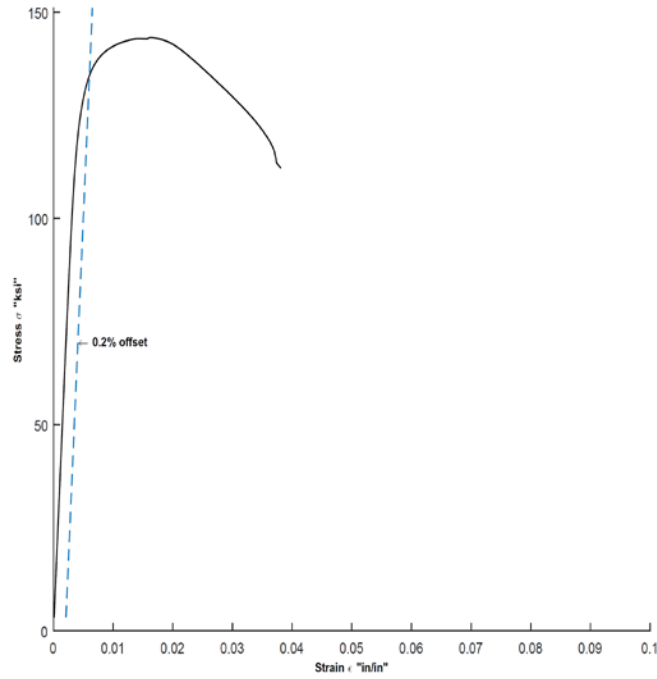


Figure G-66 Stress-Strain Curve for D31 Epoxy WWR Sample 7

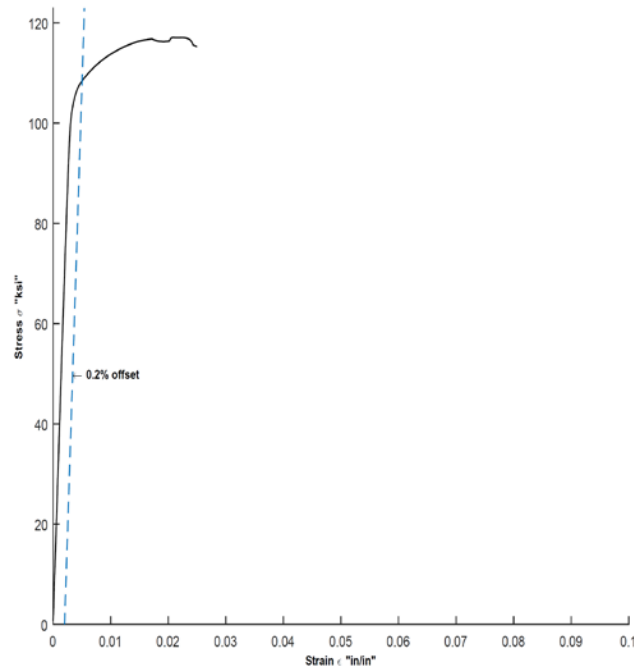


Figure G-67 Stress-Strain Curve for D31 Epoxy WWR Sample 8

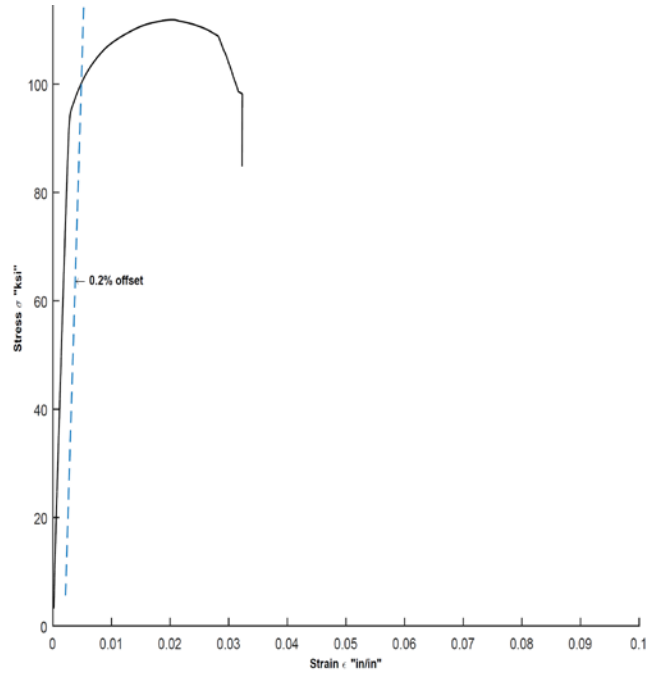


Figure G-68 Stress-Strain Curve for D31 Epoxy WWR Sample 9

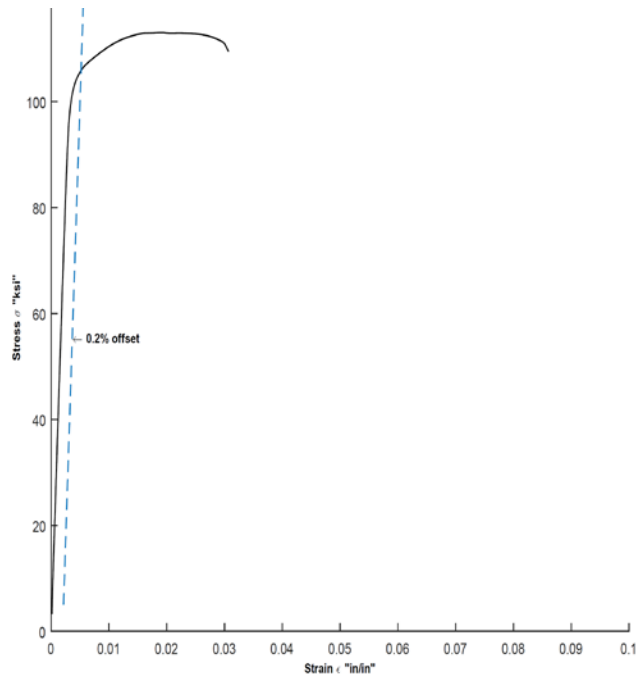


Figure G-69 Stress-Strain Curve for D31 Epoxy WWR Sample 10

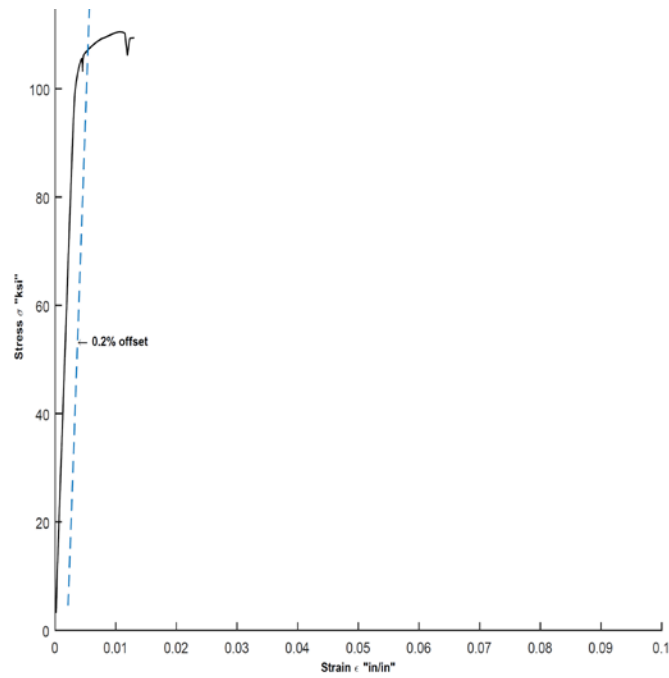


Figure G- 70 Stress-Strain Curve for D31 Epoxy WWR Sample 11

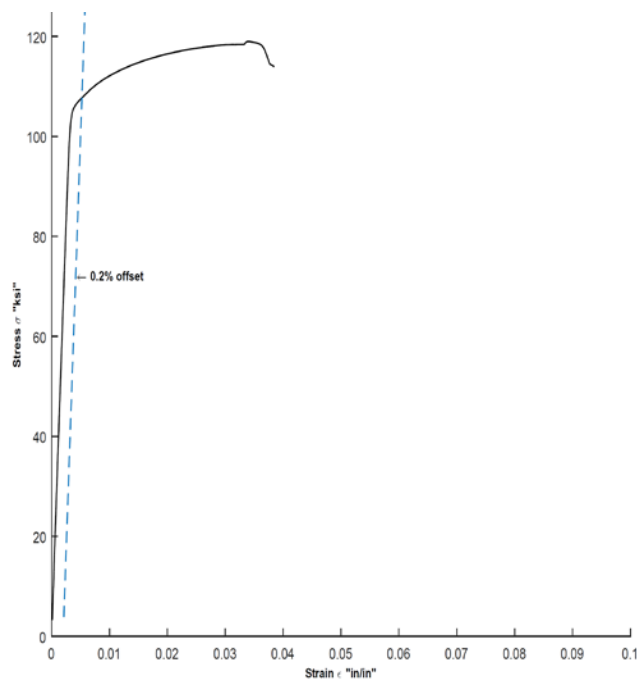


Figure G- 71 Stress-Strain Curve for D31 Epoxy WWR Sample 12

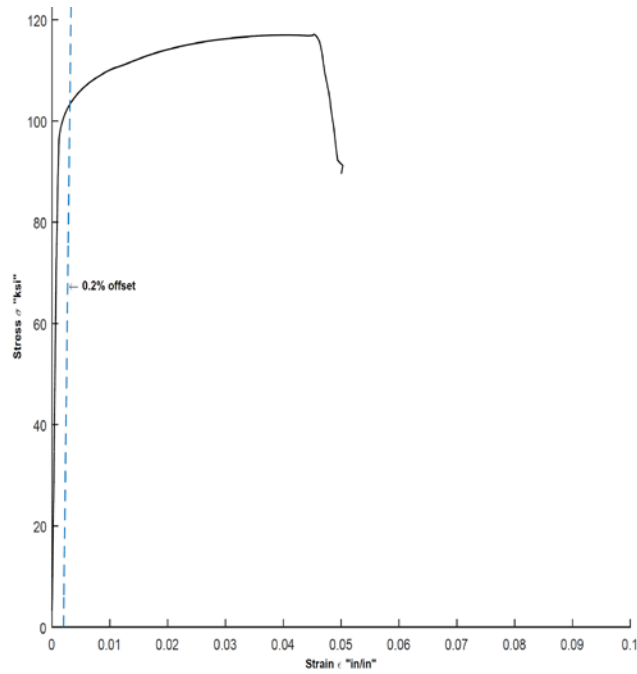


Figure G-72 Stress-Strain Curve for D31 Epoxy WWR Sample 13

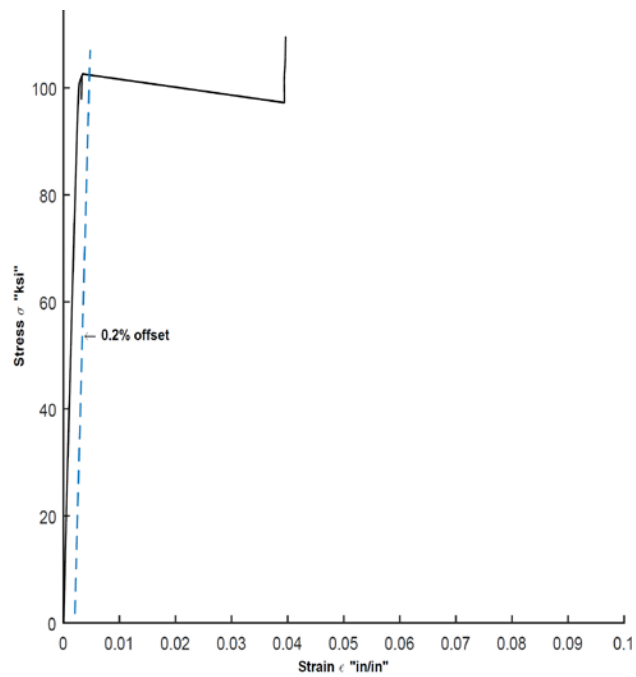


Figure G-73 Stress-Strain Curve for D11 Galvanize WWR Sample 1

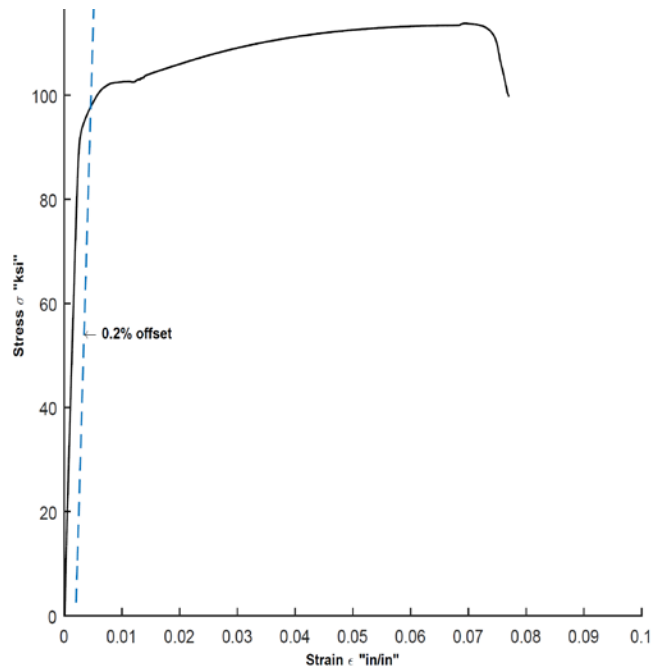


Figure G- 74 Stress-Strain Curve for D11 Galvanize WWR Sample 2

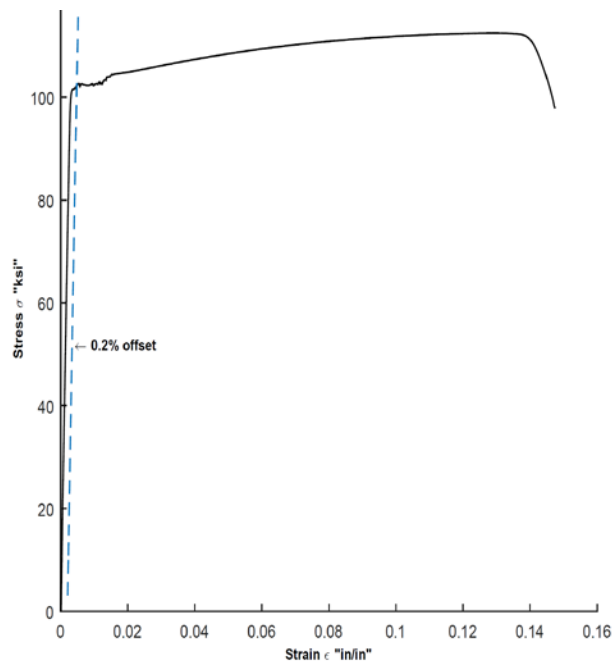


Figure G- 75 Stress-Strain Curve for D11 Galvanize WWR Sample 3

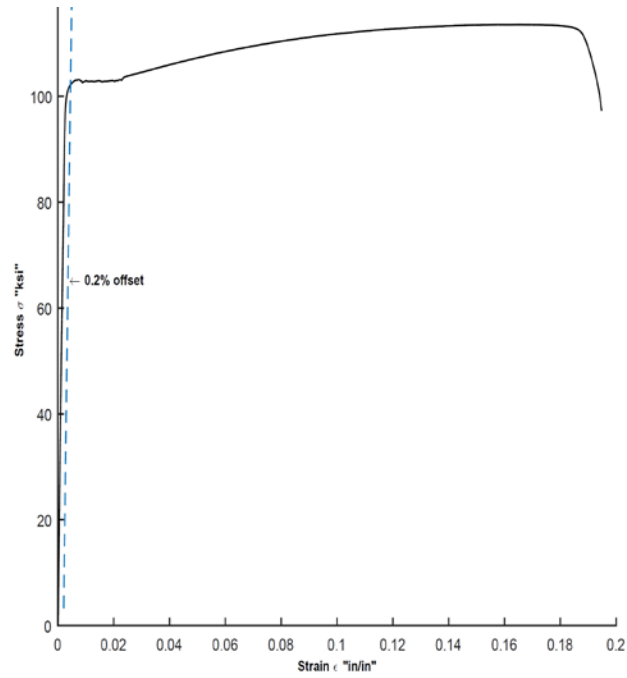


Figure G- 76 Stress-Strain Curve for D11 Galvanize WWR Sample 4

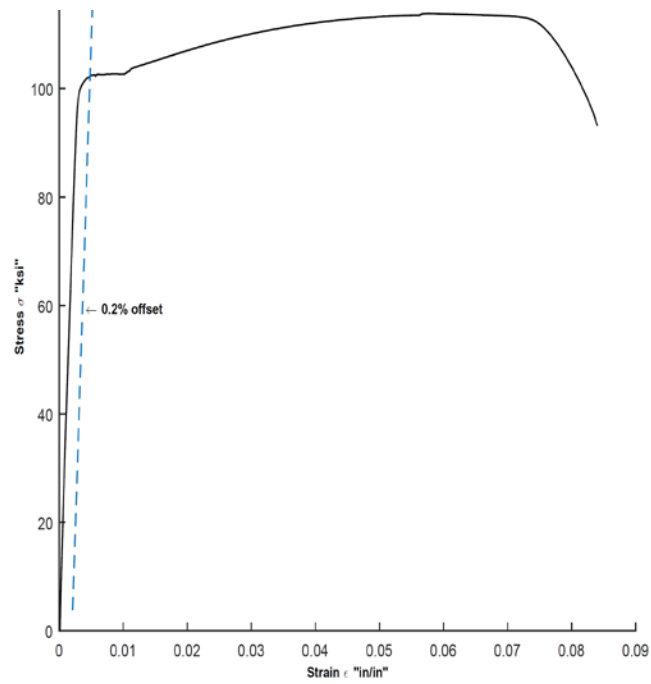


Figure G- 77 Stress-Strain Curve for 11 Galvanize WWR Sample 5

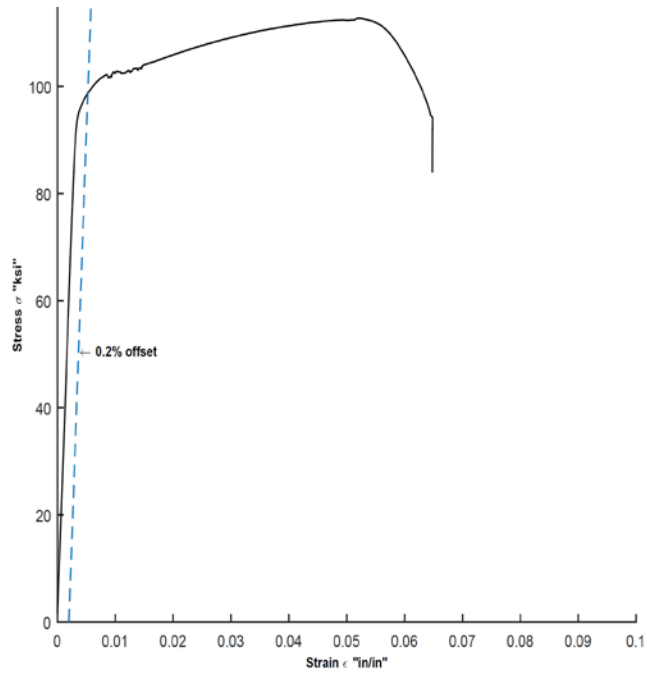


Figure G- 78 Stress-Strain Curve for D11 Galvanize WWR Sample 6

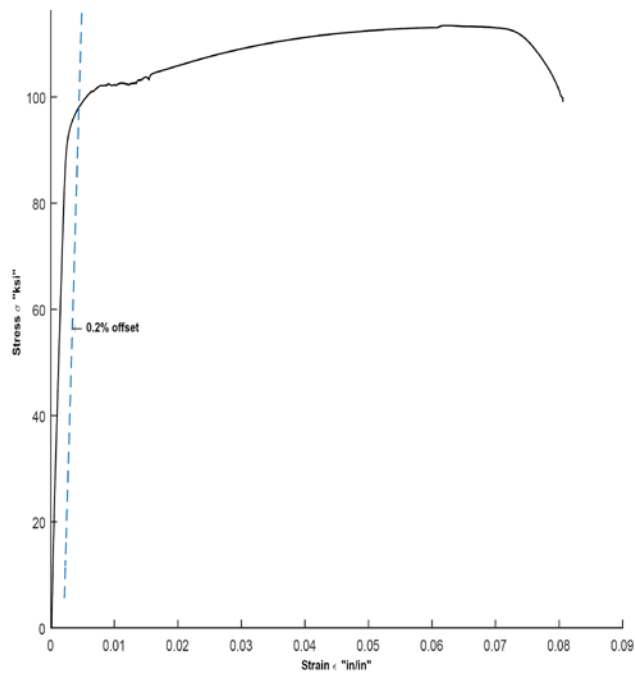


Figure G- 79 Stress-Strain Curve for D11 Galvanize WWR Sample 7

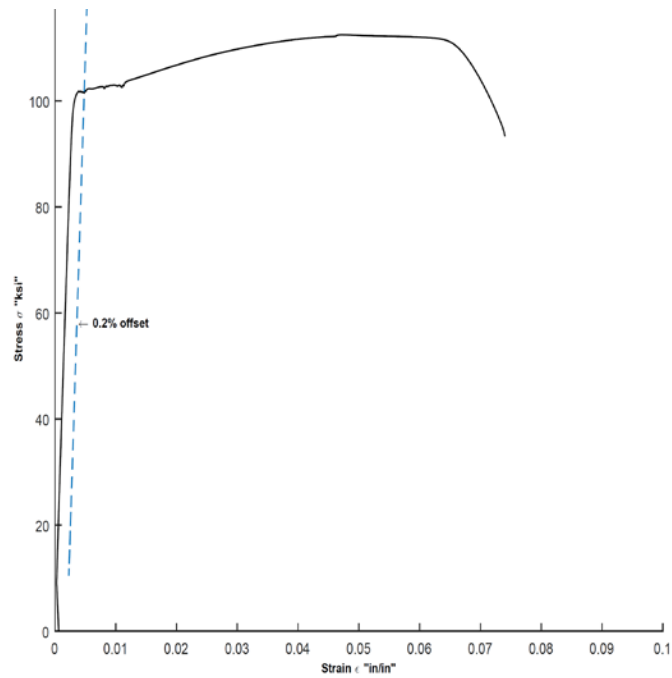


Figure G- 80 Stress-Strain Curve for D11 Galvanize WWR Sample 8

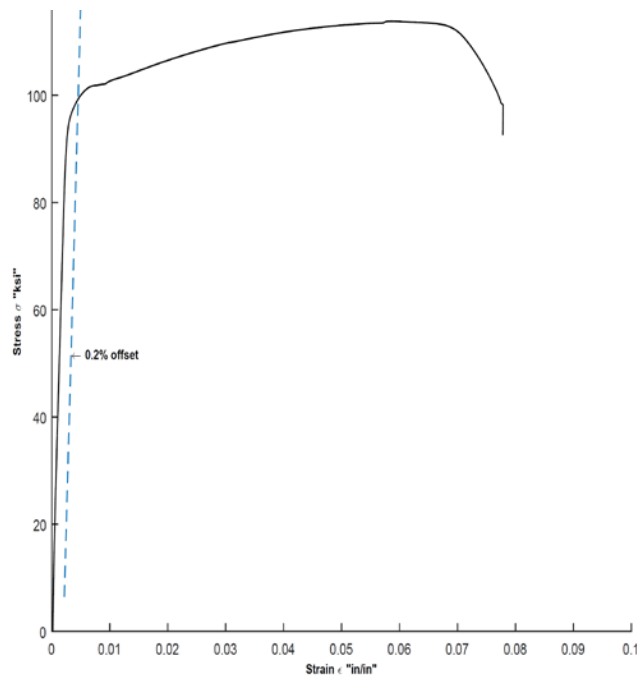


Figure G- 81 Stress-Strain Curve for D11 Galvanize WWR Sample 9

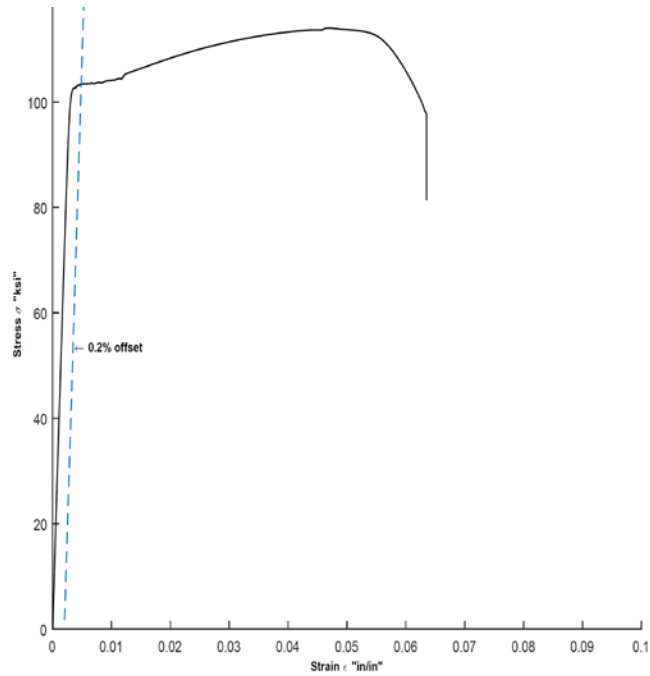


Figure G- 82 Stress-Strain Curve for D11 Galvanize WWR Sample 10

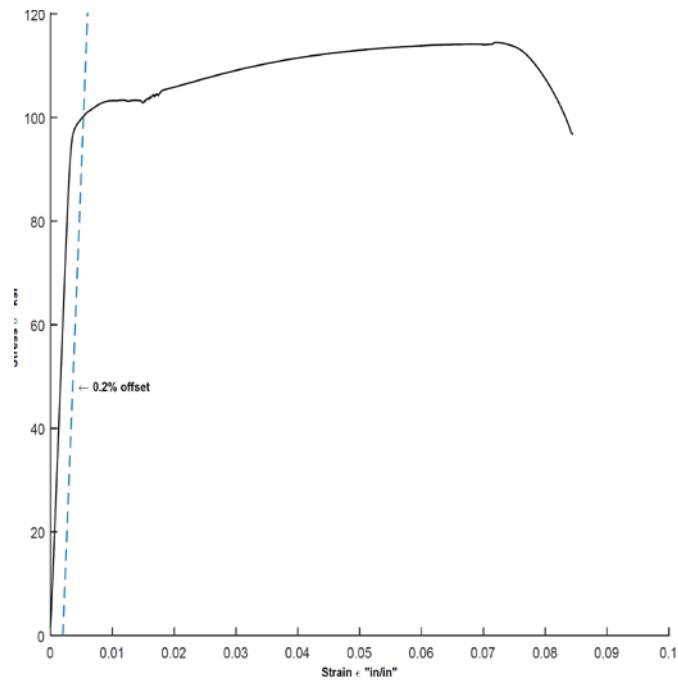


Figure G- 83 Stress-Strain Curve for D11 Galvanize WWR Sample 11

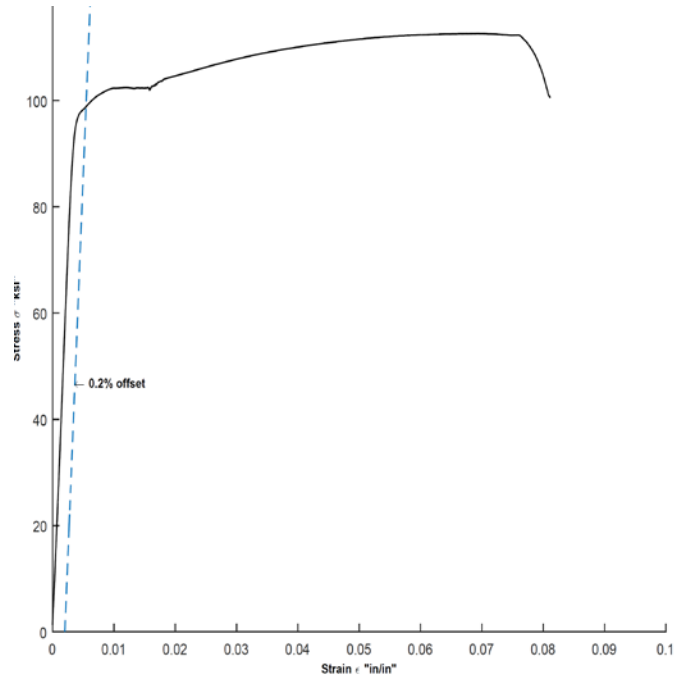


Figure G- 84 Stress-Strain Curve for D11 Galvanize WWR Sample 12

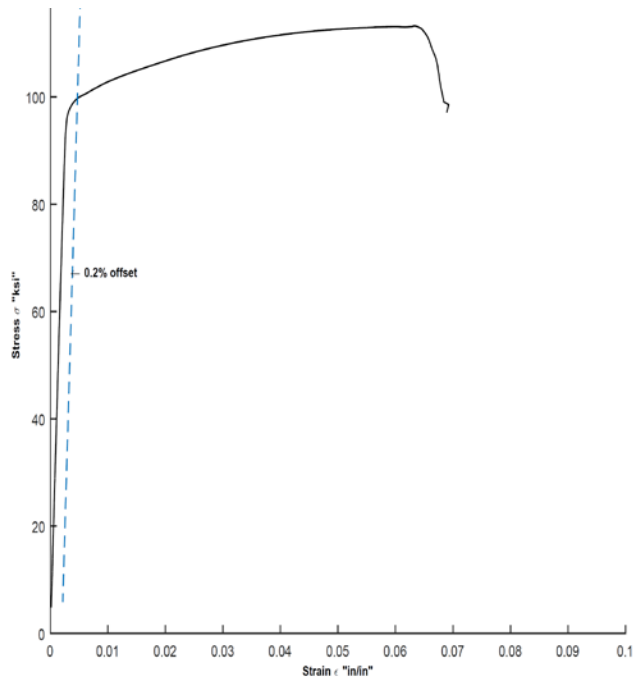


Figure G- 85 Stress-Strain Curve for D20 Galvanize WWR Sample 1

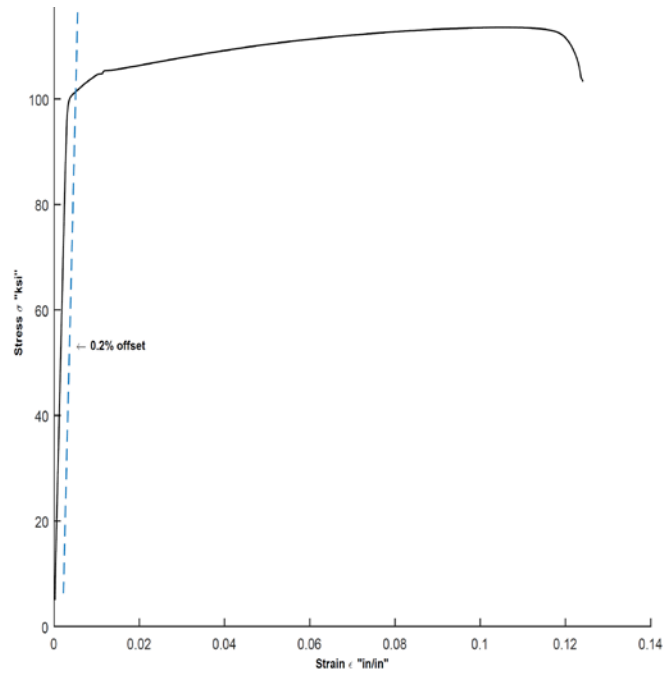


Figure G- 86 Stress-Strain Curve for D20 Galvanize WWR Sample 2

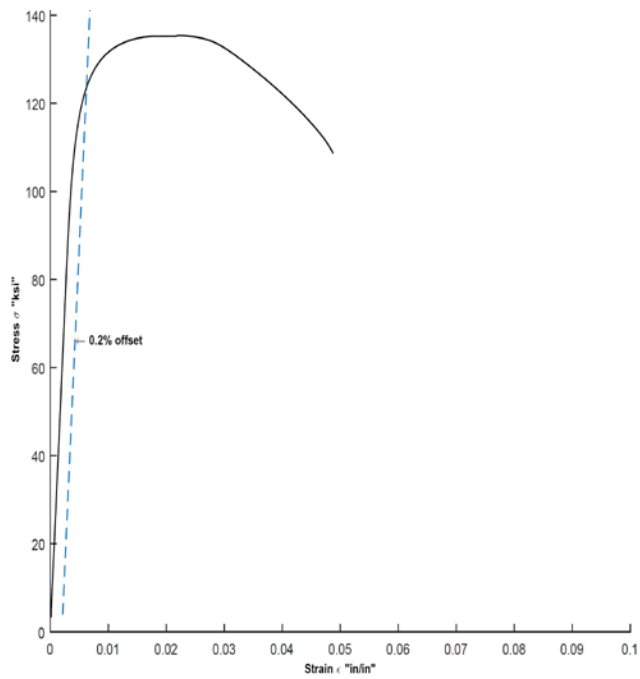


Figure G- 87 Stress-Strain Curve for D20 Galvanize WWR Sample 3

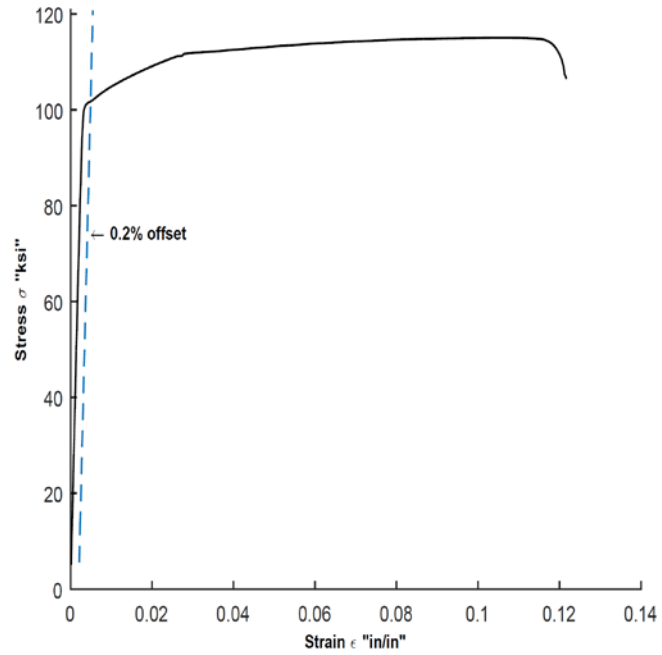


Figure G- 88 Stress-Strain Curve for D20 Galvanize WWR Sample 4

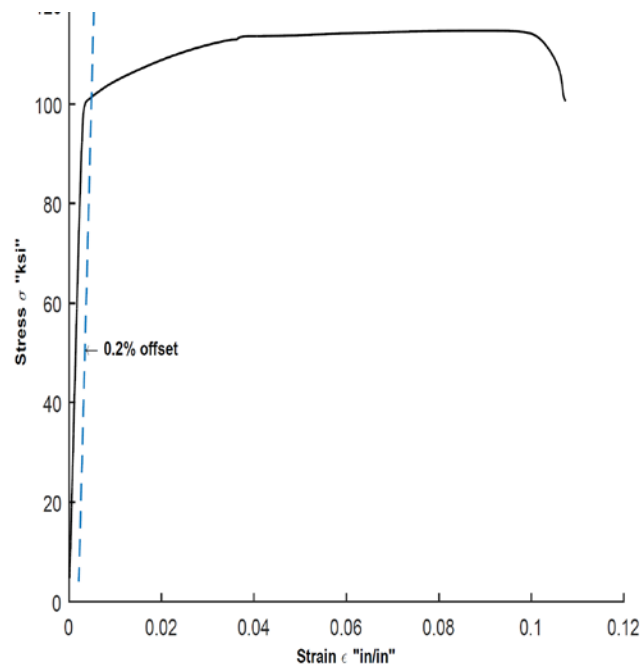


Figure G- 89 Stress-Strain Curve for D20 Galvanize WWR Sample 5

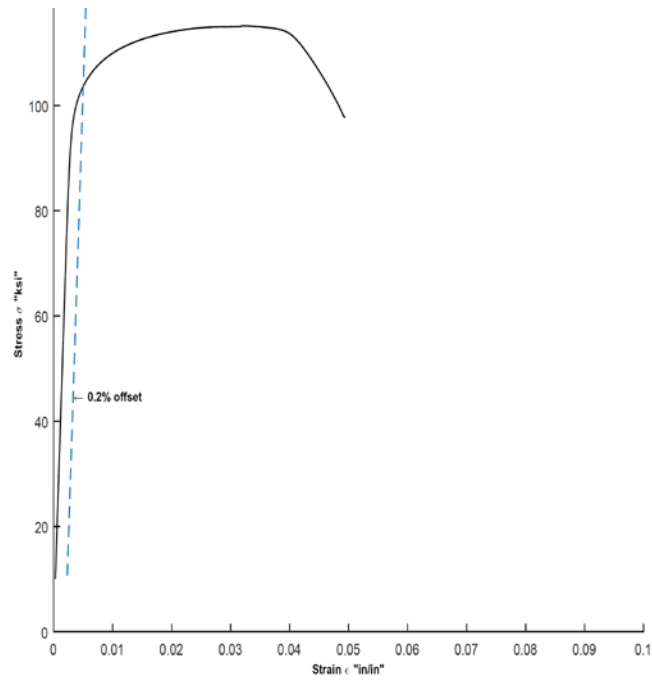


Figure G- 90 Stress-Strain Curve for D20 Galvanize WWR Sample 6

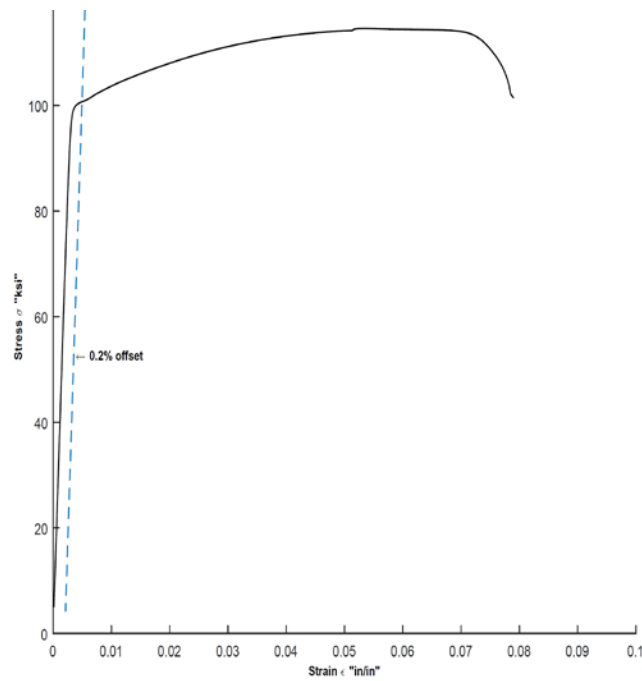


Figure G- 91 Stress-Strain Curve for D20 Galvanize WWR Sample 7

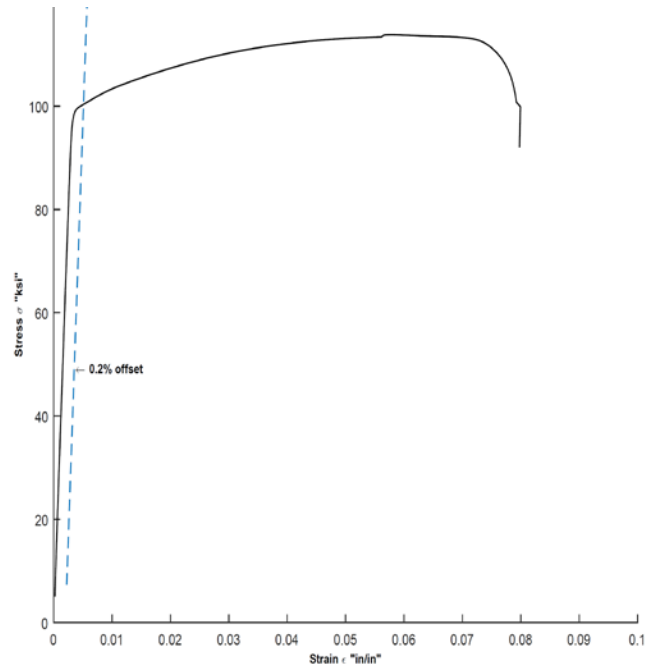


Figure G- 92 Stress-Strain Curve for D20 Galvanize WWR Sample 8

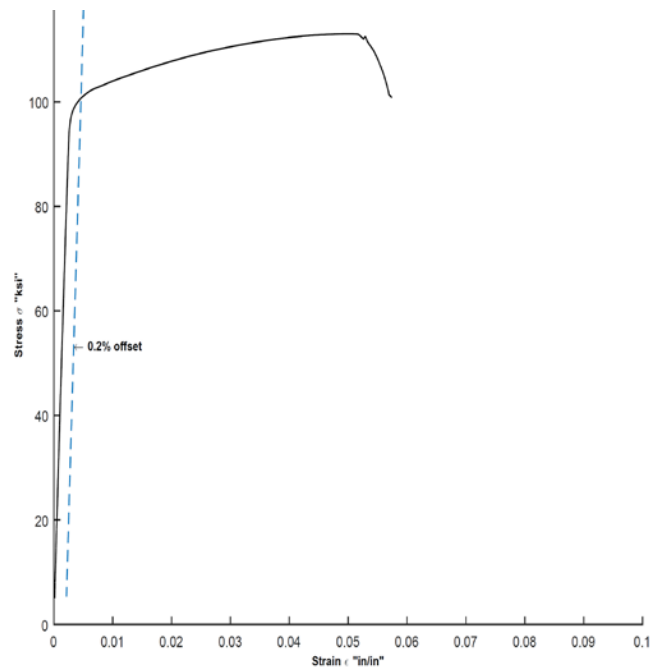


Figure G- 93 Stress-Strain Curve for D20 Galvanize WWR Sample 9

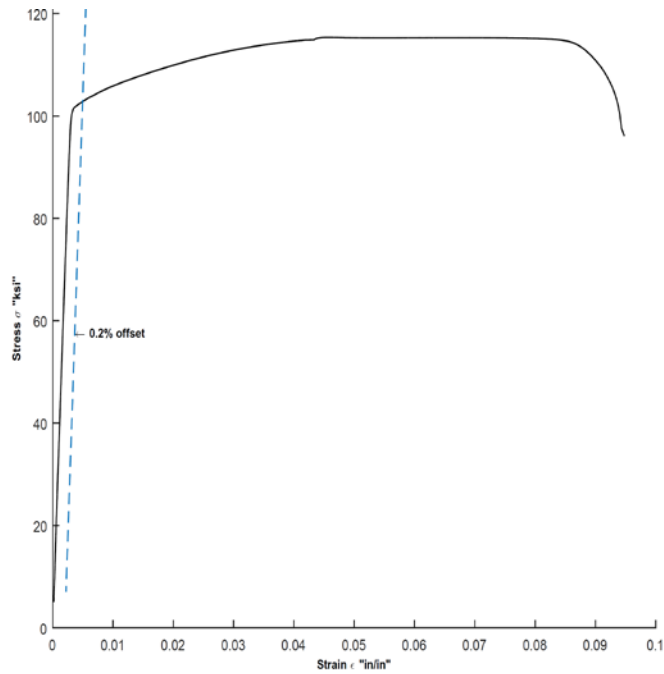


Figure G-94 Stress-Strain Curve for D20 Galvanize WWR Sample 10

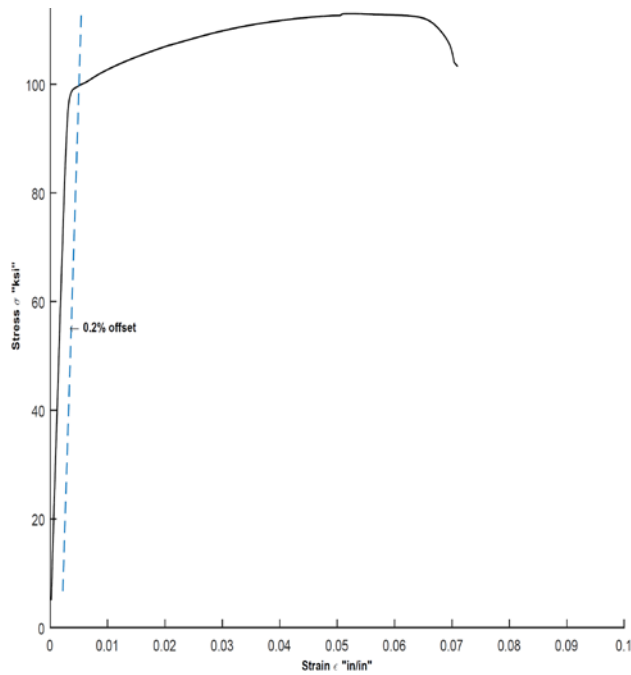


Figure G-95 Stress-Strain Curve for D20 Galvanize WWR Sample 11

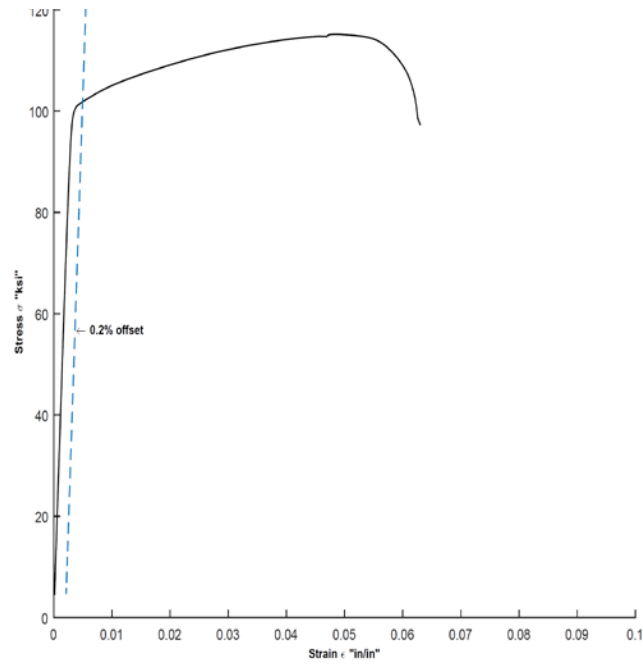


Figure G- 96 Stress-Strain Curve for D20 Galvanize WWR Sample 12

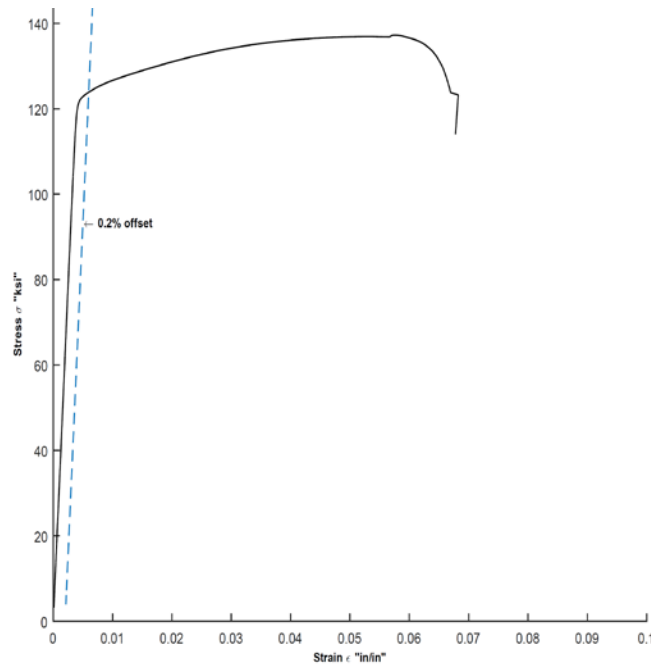


Figure G- 97 Stress-Strain Curve for D31 Galvanize WWR Sample 1

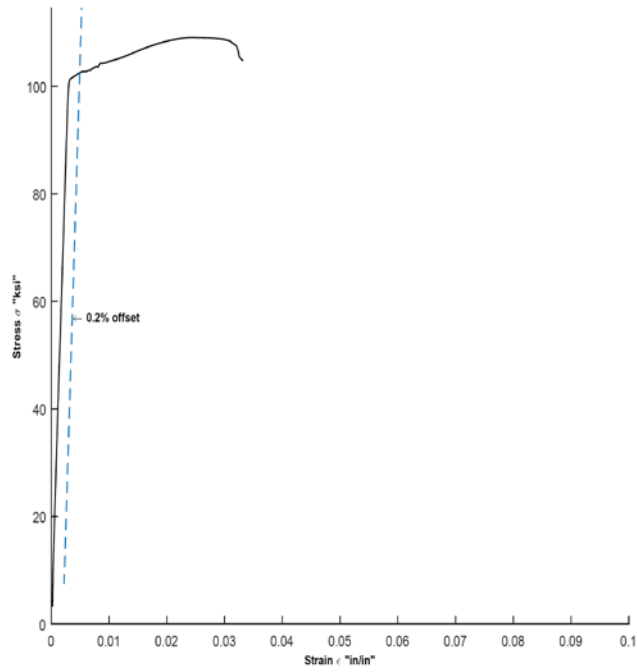


Figure G- 98 Stress-Strain Curve for D31 Galvanize WWR Sample 2

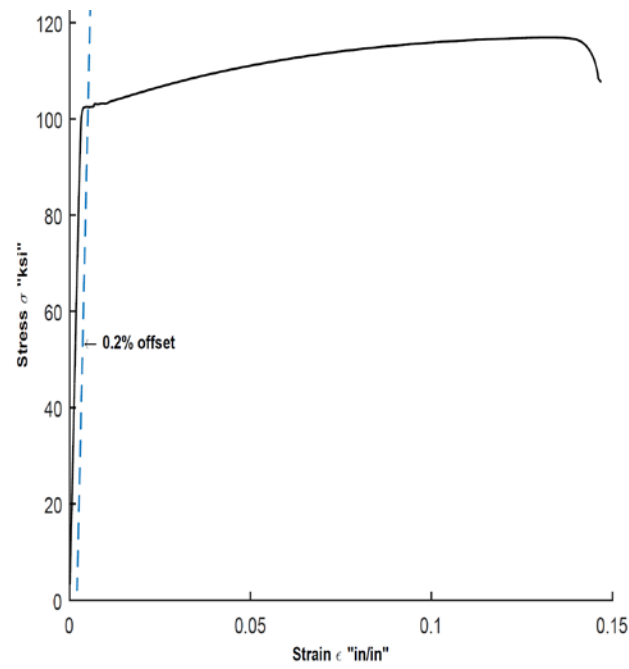


Figure G- 99 Stress-Strain Curve for D31 Galvanize WWR Sample 3

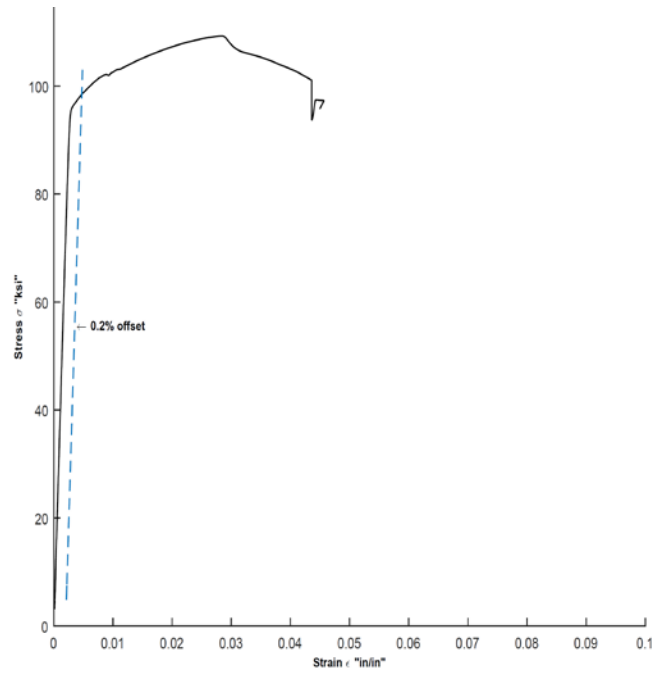


Figure G-100 Stress-Strain Curve for D31 Galvanize WWR Sample 4

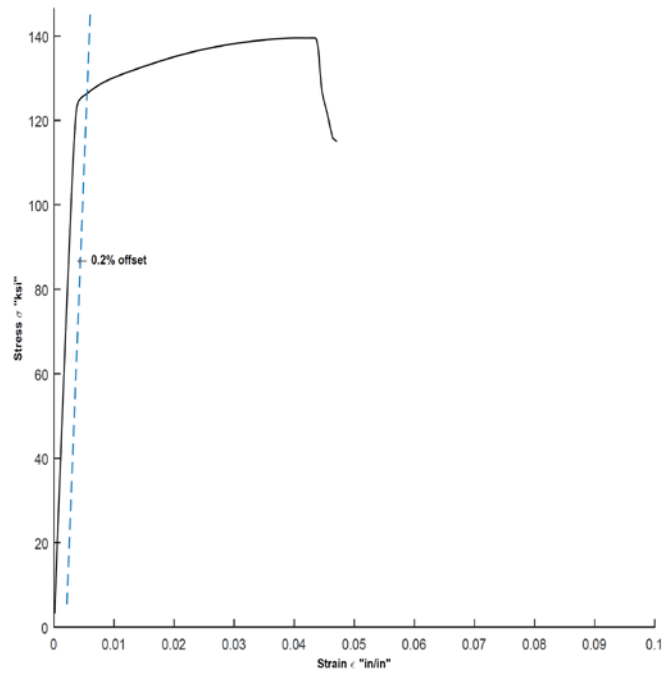


Figure G-101 Stress-Strain Curve for D31 Galvanize WWR Sample 5

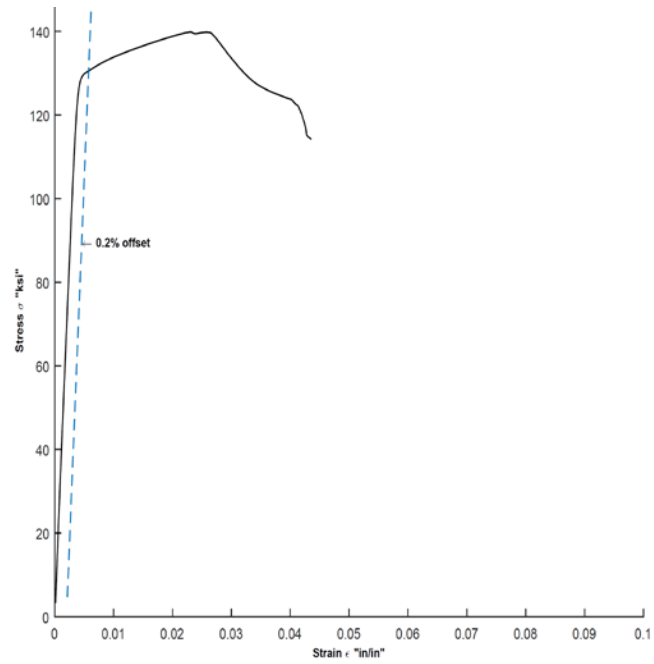


Figure G-102 Stress-Strain Curve for D31 Galvanize WWR Sample 6

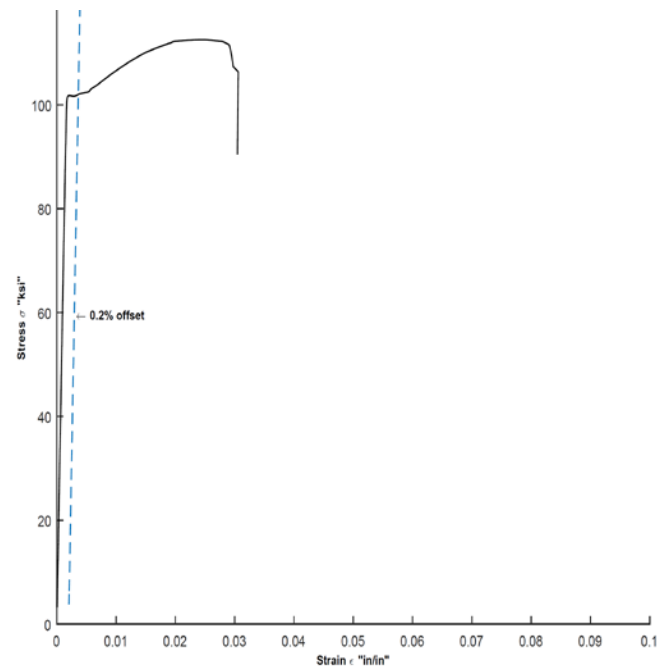


Figure G-103 Stress-Strain Curve for D31 Galvanize WWR Sample 7

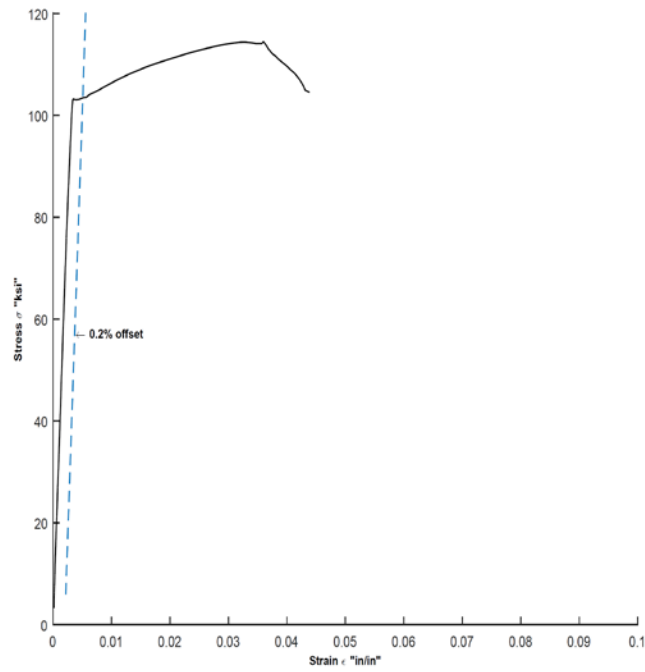


Figure G-104 Stress-Strain Curve for D31 Galvanize WWR Sample 8

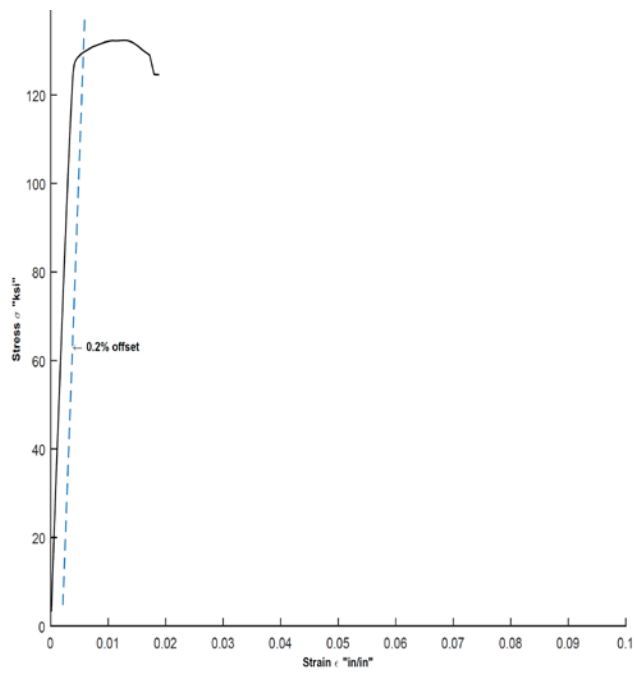


Figure G-105 Stress-Strain Curve for D31 Galvanize WWR Sample 9

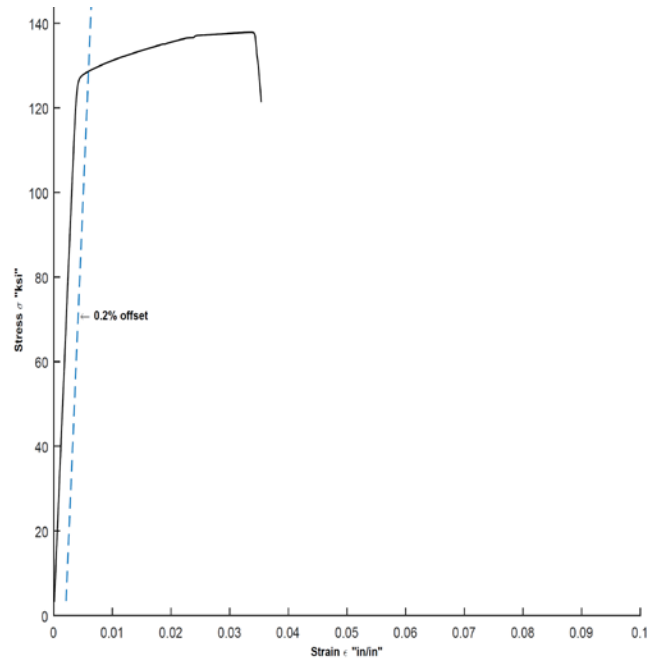


Figure G-106 Stress-Strain Curve for D31 Galvanize WWR Sample 10

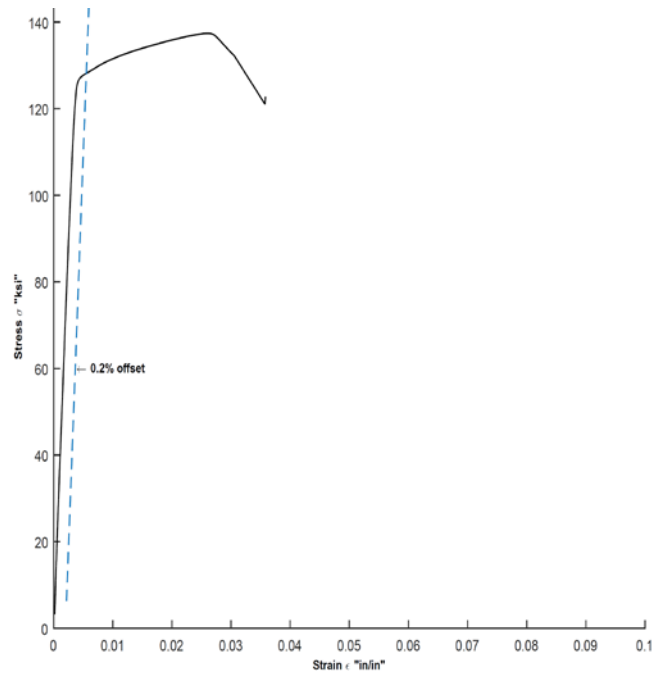


Figure G-107 Stress-Strain Curve for D31 Galvanize WWR Sample 11

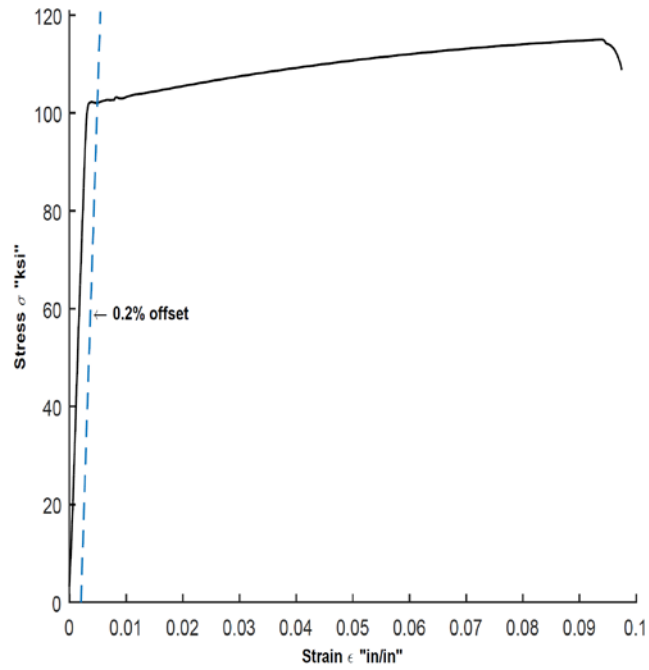


Figure G-108 Stress-Strain Curve for D31 Galvanize WWR Sample 12